UTS UNIVERSITY OF TECHNOLOGY SYDNEY

MSF Brine Reject Dilution in the Forward Osmosis Process: Performance Analysis

by Daoud Khanafer

Thesis submitted in fulfilment of the requirements for the degree of

Doctor of Philosophy

under the supervision of Dr Ali Altaee and Professor John L. Zhou

University of Technology Sydney
Faculty of Engineering and Information Technology

December 2022

Certificate of Original Authorship

I, Daoud, declare that this thesis is submitted in fulfilment of the requirements for the award of the Doctor of Philosophy in the Faculty of Engineering and Information Technology at the University of Technology Sydney.

This thesis is wholly my own work unless otherwise referenced or acknowledged. In addition, I certify that all information sources and literature used are indicated in the thesis.

This document has not been submitted for qualifications at any other academic institution.

This research is supported by the Australian Government Research Training Program.

Signature of student

Production Note:
Signature removed prior to publication.

Date: December,2022

Acknowledgments

I would like to acknowledge and give my warmest thanks to my supervisor Dr Ali Altaee. The completion of this project could not have been possible without his continuous support and guidance.

Thank you also to the co-supervisor Professor John L. Zhou for his cooperation.

I would like to thank all those whose assistance proved to help in accomplish my work.

I cannot forget to acknowledge the Qatar Foundation for funding this project.

List of Publications

Khanafer, D., Yadav, S., Ganbat, N., Altaee, A., Zhou, J. and Hawari, A.H. 2021b. Performance of the Pressure Assisted Forward Osmosis-MSF Hybrid Desalination Plant. Water 13(9), 1245.

Khanafer, D., Ibrahim, I., Yadav, S., Altaee, A., Hawari, A. and Zhou, J. 2021a. Brine reject dilution with treated wastewater for indirect desalination. Journal of Cleaner Production, 129129.

Ibrar, I., Altaee, A., Zhou, J.L., Naji, O. and **Khanafer, D**. 2020. Challenges and potentials of forward osmosis process in the treatment of wastewater. Critical Reviews in Environmental Science and Technology 50(13), 1339-1383.

Yadav, S., Ibrar, I., Bakly, S., **Khanafer, D**., Altaee, A., Padmanaban, V., Samal, A.K. and Hawari, A.H. 2020. Organic fouling in forward osmosis: A comprehensive review. Water 12(5), 1505.

SOLAR CO-GENERATION OF ELECTRICITY AND WATER, LARGE SCALE PHOTOVOLTAIC SYSTEMS - Desalination By Forward Osmosis: Failure, Success, and Future Expectations - Ibrar Ibrar, **Daoud Khanafer**, Sudesh Yadav, Salam Bakly, Jamshed Ali Khan, and Ali Altaee.

Patent Application: Ali Altaee, **Daoud Khanafer**, Alaa Hawari, A METHOD FOR SEAWATER SOFTENING WITH A COMMERCIAL ANOFILTRATION MEMBRANE IN THE FORWARD OSMOSIS. Application NO 63242097, 09-SEP-2021.

Table of Contents

List of figures

List of tables

Abbreviations

A	Pure water permeability
AL	Active layer
B	Solute permeability
CP	Concentration polarization
CTA	Cellulose triacetate
DI	Deionized
DS	Draw solution
EDS	Energy Dispersive X-ray Spectroscopy
FO	Forward Osmosis
FS	Feed solution
FTIR	Fourier transform infrared
GCC	Gulf Cooperation Council
ICP	Internal Concentration polarization
J_w	Water flux
MSF	Multi-Stage Flashing
NF	Nanofiltration
PAFO	Pressure-assisted forward osmosis
RO	Reverse Osmosis
S	Structural parameter
SEM	Scanning electron microscopy
SL	Support layer
TBT	Top brine temperature
TDS	Total dissolved solids
TFC	Thin Film Composite
TSE	Tertiary sewage effluen

Abstract

One of the largest global risks is freshwater scarcity. In countries with limited natural water resources, water reclamation and desalination have become a strategic source of clean and usable water. Specifically, seawater desalination is a sustainable flow of fresh water in the Gulf Cooperation Council (GCC) countries located in the driest part of the world. Multi-Stage Flashing (MSF) desalination has been proved to be the most reliable thermal desalination technology in the GCC countries, mainly considering Qatar's MSF plants. Despite its efficiency and high-quality water production, MSF technology suffers major drawbacks affecting its performance. Scale formation, specifically the non-alkaline scale, has been a serious issue from thermodynamic and economic perspectives. Pretreatment of the feed solution to the MSF plants was proposed and investigated in the literature to tackle the scale issue. The current project's novelty is to design and test the FO-MSF hybrid system for seawater pretreatment by the FO process for the MSF desalination plant. Several commercial FO and NF membranes were applied for recycling the MSF brine reject within the FO system using the brine as a draw solution.

Selecting the appropriate membrane and the ideal draw solution is essential for an efficient FO process. Since the brine reject solution is the only DS used in all the experiments conducted in this study, the variables included the membrane and the feed solution. TFC and CTA FO membranes with fresh sweater feed solution were used in the FO system for the MSF plant. Pressure-assisted FO (PAFO) process was introduced, and experimental results showed 50% more permeation flux by increasing the feed pressure from 1 to 4 bar. When tertiary sewage effluent (TSE) was proposed as a feed solution using TFC membranes, a considerably high water flux of 35 L/m²h was achieved. Under the same operating conditions in the FO mode using fresh seawater on the feed side, commercial NF membranes were tested for the first time in the FO system. A more feasible membrane selection can be the NF membranes as they demonstrated better results than FO membranes. However, higher performance was achieved when TSE and NF were combined in the FO process.

Experimentally, this combination recorded a maximum water flux of 39.5 L/m^2h and achieved up to 42% divalent ions dilution. While the outcome of this study is still preliminary, the results are promising and can highlight the potential of using the FO system for MSF brine dilution.

Chapter 1: Introduction

1.1. Background

Water scarcity is an escalating global challenge for the 21 century due to the worldwide population growth, industrial activities and the climate change effect. Since the world's population is predicted to reach 9.7 billion by 2050 (Qureshi, 2020), the current water shortage might worsen if alternative energy and cost-efficient sources are not developed. Nowadays, the different countries where natural resources of fresh water are limited, seawater desalination is an alternative supply for water demand. While RO is the desalination process that is widely implemented, only in the Gulf Cooperation countries 70 % of the desalination techniques are thermal plants (Aende et al., 2020). Thermal desalination technologies use extensive energy, causing detrimental issues for the ecosystem. The cost of a desalination technique can be determined using different factors: the operation and maintenance, the system's capacity, the operational energy and the feed water constituents, and the brine reject. For instance, the harsh water quality in the oil-rich region of the Middle East requires the utilization of thermal separation techniques for their tendency to produce final high-quality product water. The GCC seawater's properties are high temperature, high impurity, and high salinity. These water properties are considered unattractive for the RO operational characteristics. Multi-stage flushing (MSF) and Multi-Effect Distillation (MED) are the thermal technologies used in the GCC countries, with MSF dominating the MED in some countries, such as Qatar. The MSF plants' serious drawback is the accumulation of non-alkaline scale on the internal pipes of the heat exchangers. The heat transfer efficiency weakens due to the scale accumulation, which reduces the process efficiency. The scale formation restricted the top brine temperature (TBT) to only 112 °C. Antiscalants are added to the feed water to control the precipitations of soluble metal ions to minimize scale formation.

Research on tackling scale formation dates back to as early as the nineties, and the literature shows the ascendant research trend in the last few years. Since the ions causing the scale are highly concentrated in the seawater, the feed water treatment was proposed as an anti-scaling strategy. Minimizing the ions count in the FS to the MSF plant decreases the scale formation and allows the TBT to reach more than 112 °C. However, antiscalants cannot completely avoid the process of scale deposition; hence, periodic mechanical cleaning of the fouled parts must be applied. It is worth not at high TBT (Altaee et al., 2014a). At first, Nanofiltration (NF) membranes were studied to be applied to remove the multivalent ions. Bench-scale experiments and pilot plants showed the feasibility of applying NF as a pretreatment step to the FS. However, the price of the NF process at the time was the main obstacle to the development of such a system.

Similarly, RO was theoretically and experimentally employed to minimize the fouling materials; however, it was observed that the feed containing high salt concentrations is not preferred for RO. An alternative membrane separation named Forward osmosis (FO) was proposed to be used instead of NF and RO; however, the cost of the generation step of the FO increased the overall cost of the process. A novel proposed by Altaee indicated the use of the MSF brine reject as a DS in the FO pretreatment step. This innovation diminished the regeneration step as the product of the FO process will be used as FS to the MSF plants.

FO is an osmotically driven membrane separation technique. The water molecules flow naturally through a semi-permeable membrane from a low-concentrated solution to a high concentrated solution. The osmotic pressure difference between the solutions is the driving force in the FO process. FO process has several advantages, including simple equipment configuration, low energy consumption, high rejection to contaminants and considerably low membrane fouling. On the other hand, the most critical requirements for the FO process are selecting an ideal DS and the appropriate membrane (Wang et al., 2018). There is a remarkable rise in research studies on DS investigations and FO membrane modification and development. Until now, the tailored FO membrane compatible with the ideal DS is yet to be defined. In the proposal of

using the brine reject of the MSF plants as a draw solution, one of the main difficulties of the FO process was eliminated. Another requirement for the FO process on the energy requirement level is the regeneration process, which is considered the energy-intensive step in the FO process. This step is not required in the FO pretreatment due to the direct use of the diluted brine reject. In the simulation, the recovery rate recorded was 32%, with 62% reductions in the counts of Ca^{2+}, Mg^{2+} and SO_4^{2-}. In the experimental study conducted by Thabit et al. to study the feasibility of the FO as a pretreatment method using real seawater and Qatar MSF brine reject as the feed and draw solutions in the FO process. The variables investigated in the study were the stream solutions temperature, the flow rate of the draw and FS, and the FO membrane orientation. An average water flux of 16.9 $L/m^2.h$ was achieved at a 2 LPM flow rate for both fed and draw solution. The water flux was higher when the temperature increased. The dilution of the DS was shown to be 8.5% at 40 °C compared to 3% at 25 °C. In addition, at higher flow rates, the PRO mode showed higher membrane permeability. Thabit's study delivered positive and promising preliminary results that shed light on the performance of the FO process when varying the operational parameters (Thabit et al., 2019). However, deeper lab-scale investigations are needed to confirm these results. The amount of literature on implementing FO as a pretreatment for MSF is low compared to the wealthy research on improving the overall FO system's characteristics and performance.

A new concept named pressure-assisted forward osmosis (PAFO) was in order to increase the water flux in the FO process, introduced and investigated for the ability to increase the water flux in the FO process. PAFO differ from FO by applying a small hydraulic pressure on the feed side of the FO membrane. The additional hydraulic driving force could impact the membrane water permeability (Blandin et al., 2013; Jamil et al., 2016) and might overcome the FO limitations of reverse solute flux (Kim et al., 2017a).

Another concept was established to overcome the limitations of a standalone desalination technique. Coupling two or more processes through hybridization in a hybrid system encompasses a broad spectrum of desalination and water reclamation research. Selecting an effective hybrid system requires a deep

understanding of the operational parameters of each standalone technique, the feed water, and the final product quality. For example, MSF-RO hybrid systems have been applied to existing and new MSF plants in UAE and Saudi Arabia since 2007. Studies on the hybrid system's performance concluded that such hybridization was feasible on an economic and technological level compared to the newly designed plants (Ahmed et al., 2020).

1.2. Research Hypothesis

Scale formation in thermal desalination processes is a major drawback affecting the MSF plant performance. Multi-Stage Flashing (MSF), which is Qatar's main desalination technology, is facing the problem of the non-alkaline scale that is caused due by the precipitation of calcium (Ca^{2+}) or magnesium (Mg^{2+}) ions with sulfate (SO_4^{2-}) as calcium sulfate ($CaSO_4$) or magnesium sulfate ($MgSO_4$) salts on the heat exchangers. Unfortunately, the non-alkaline scale is not responsive to acid cleaning and requires mechanical cleaning, leading to an increase in the maintenance and operating costs of the MSF plant. Seawater FS pretreatment was proposed to tackle the scaling agents.

FO technique has been proposed as an alternative to the RO process in water purification and seawater desalination. FO process is considered an emerging energy-efficient technology for pharmaceutical and juice concentration applications, protein enrichment, and power production. Implementing the FO process in wastewater treatment and seawater desalination is attractive in the research field. FO has been investigated in removing contaminants and fouling matters from feed water before RO, NF, PAO, MED and MSF processes. The results regarding FO hybridization are promising in terms of overall performance and energy saving compared to the standalone FO process. FO seawater desalination has been commercialized in limited areas in Oman, China and Gibraltar (Aende et al., 2020). Whilst FO is a potentially energy-efficient process, and its efficiency is associated with the solute recovery step, using the separation step of FO to improve the feed quality to other desalination technology is theoretically feasible.

On the other side, a high salinity draw solution can enhance the spontaneous transfer of water molecules through the FO membrane because of the osmotic pressure between the two solutions. The MSF brine a highly concentrated DS that does not require any regeneration process (Altaee et al., 2014a). Rejected brine from desalination plants characterized by high temperature, high salt concentration, chemical compounds and a trace of heavy metals from the antiscalants solutions and the cleaning agents. In the previously published papers, MSF brine reject was used as DS in the FO process, and fresh seawater was used as FS. The water flux achieved in the experiments and the decrease in the concentrations of the ions in the DS constitute a significant finding that further evaluation of the FO process for the recycling of the MSF brine is accomplishable.

Therefore, the principal hypothesis for this research is that the FO technique can potentially remove scale-causing ions from the MSF brine by high permeability membranes. Commercially available FO and NF membranes will be evaluated under specific operational parameters. Feed streams with different total dissolved solids (TDS) will be examined. Hence, this work aims to develop a FO system with high permeability, high solute retention ability and minimal membrane fouling. The issue of scale formation can be tackled when using the highly diluted brine that is the product of the FO system as a feed stream to the MSF plants.

1.3. Research Objectives and Goals

The current research aims to study the feasibility of the FO process in removing the scale ions, i.e. Ca^{2+}, Mg^{2+} and SO_4^{2-} from the feed water to the MSF plants. To achieve that, a list of specific objectives was set out:

i) To evaluate the introduction of pressure-assisted Forward osmosis (PAFO) for the dilution of the MSF brine. The laboratory work will investigate the impact of FO operating parameters on the dilution of the MSF brine reject. The specific power consumption of the PAFO process will be calculated and compared with that of the FO process. The impact of membrane materials on the performance and fouling propensity of the FO process will be evaluated.

ii) To investigate the potential of using treated wastewater as an FS for indirect desalination of the MSF brine reject. The low osmotic pressure on treated wastewater will promote water flux in the FO membrane and hence the brine dilution due to its low osmotic pressure.

iii) To assess the use of commercial NF membranes in the FO system instead of the FO membrane to reduce the capital cost of brine dilution. NF membranes have higher water permeability than FO membranes, which are inexpensive. Laboratory research will evaluate the performance of several commercial NF membranes in the FO setup for brine dilution and the impact of operating parameters on the scale ions rejection.

iv) To examine the fouling properties and the appropriate physical cleaning methods for FO membrane cleaning. Hot water at 40 °C and osmosis backwash will be evaluated for membrane cleaning. The laboratory work will study the effectiveness of seawater and brine pretreatment with a 20 μm filter to reduce the FO membrane fouling.

1.4. Research significance

MSF scaling is a commercial problem causing an increase in the energy and maintenance cost of seawater desalination. The current method of using antiscalants is ineffective for long-term scale control. As a result, mechanical cleaning is practised, but it requires shutting down the MSF plant. Different separation membrane technologies have been studied to treat the feed solution to the MSF plants to reduce the scaling matters. Minimizing the scale of the ion causing in the feed solution to the MSF plants resulted in lower scaling and increased operational temperature and, therefore, the MSF plants' recovery rate. This project seeks to evaluate the feasibility of the FO technology for diluting the FS to the MSF plant. FO is an emerging osmotic process attracting researchers for its low energy requirements. In this project, FO experiments will be held using different types of FO membrane materials in a laboratory-size FO system using

concentrated seawater brine at 40 °C to mimic the concentration of the MSF brine. The MSF brine will be the draw solution, while seawater or wastewater will be the FS. The performance of the FO process will be evaluated in terms of water flux, water recovery, consumed energy and draw solution dilution at different operating conditions.

Developing a lower-cost seawater desalination system is crucial for countries like Qatar, where 99 % of the municipal water supply is desalted seawater from thermal plants. Thus, enhancing the performance of the currently installed MSF plants can lead to the least cost and most efficient thermal desalination (Darwish et al., 2016a). FO process as an energy-efficient technique was experimentally studied for MSF fresh brine dilution, and the preliminary outcome was promising for further research (Thabit et al., 2019). In this project, the FO process will be evaluated under specific operational parameters to reach the highest percentage of brine dilution. The recycling of the MSF brine can control the environmental impact of the current improper treatment of the brine, reduce the usage of the antiscants chemicals substances and, most importantly, diminish the scale formation.

1.5. Thesis outline

This thesis is divided into eight chapters. The layout is as follows:

Chapter 1 is introductory. The introduction of this PhD study provides a background on the current state of the MSF plants and the FO process. The research hypothesis, objectives, goals and research significance are presented.

Chapter 2 is the literature review. It reviews the literature published in the desalination domain, including thermal and membrane separation techniques. The detailed state of the art of the FO process is presented.

Chapter 3, named “materials and methods”, layouts the activities, the experiments, and the materials used in this study.

Chapter 4 is titled “Pressure-Assisted Forward Osmosis-MSF Hybrid desalination plant performance”. In this chapter, hydraulic pressures (1-4

bar) were applied on the feed side of the FO process. The performance of the FO system under different applied pressures is discussed.

Chapter 5 is “brine reject dilution with wastewater for indirect desalination: Converting wastewater streams to water resources”. This chapter introduced treated wastewater as an FS in the FO process. The prefiltration of stream solutions and various fouled membrane cleaning methods are evaluated.

Chapter 6 is titled “Performance of NF membranes in a lab-scale forward osmosis system for brine recycling”. The FO system was run, including three different modules of NF membranes, respectively, using the PAFO process.

Chapter 7 discusses the FO system's performance when incorporating treated wastewater as an FS with the NF membranes. The efficiency of the fouled membrane cleaning is presented.

Chapter 8 is the “conclusions and future recommendations”; it highlights the significant finding of this study and proposes recommendations for further research.

Chapter 2: Literature Review

2.1. Global Water Situations

Water is one of the vital resources on our planet; it is unevenly distributed across the globe and covers almost three-quarters of the earth (Cosgrove and Loucks, 2015). Data reveals that approximately 1,4 billion m^3 is the total global reserve of water, with around 97.5% ocean water and 2.5% freshwater that is naturally found in the Ice Mountains, in the atmosphere and streams and lakes, as well as under the ground (Shatat and Riffat, 2012). Nowadays, the water demand will postpone personal needs and cover other sectors such as agriculture, industrial and thermoelectric power. Personal water consumption varies considerably from one geographical area to another; for example, in America, the average use per capita is between 376 to 666 litres/day per person, whereas the average in Africa is 20 liters per day per capita (Singh, 2017). In the past, rational and systematic use of renewable water resources met human demand and maintained a balanced environment. For the time being, the demographic and urbanization growth, the demands of the new quality of life and the large economic activities increase water usage. Data revealed that around 50% of the population worldwide rely on groundwater to supply freshwater, approximately 2.5 billion (Organization et al., 2015). Susceptibly, global warming, population growth, industrial demands, and contamination of groundwater are the main factors that exacerbate water scarcity. By causing a fluctuation in the rainfall pattern, global warming leads to a shortage of freshwater availability in numerous regions worldwide (Chadwick et al., 2014). With an expected growth in the world population to reach 9.4 billion by 2050, pressure on the freshwater supply and the underground reserve will increase (Pimentel et al., 2004). It is reported that human activities lead to the contamination of the natural water reserves (Shukla et al., 2017). As a result, the traditional physicochemical techniques used to treat the available water

resources are no longer sufficient for this century's demand (Micale et al., 2009). Climate change and drought are additional issues impacting water availability (Cosgrove and Loucks, 2015). A research study conducted in 2016 revealed that two-thirds of the global population might face water shortage by 2025 if water consumption maintains the current rate. Half a billion live in a severe permanent water deficiency yearly (Mekonnen and Hoekstra, 2016). The Middle East, North Africa, developing countries worldwide such as China and India (Shatat and Riffat, 2012), Texas and Florida in the United States and Mexico are suffering from water scarcity (Mekonnen and Hoekstra, 2016). Therefore, institutions and governments worldwide promoted research and projects to provide a sustainable supply of fresh water alternative to the natural supply using new technologies such as water reuse and desalination.

2.2. Technologies to reduce Water Shortage

In addition to the natural resources of water, countries are striving for alternatives to address water shortage issues following the economic and population crisis. Water reclamation and water desalination are globally invested as a substitute for freshwater reserves (Cath et al., 2010; Salgot and Folch, 2018).

2.2.1. **Water Reclamation**

Turning wastewater into a new usable water source is called water reclamation, also known as water reuse or water recycling. Wastewater is the water used by different sources such as homes, businesses, and industrial processes. There are two types of water reuse i) non-potable and ii) potable reuse. In the latter, recycled water is high-quality water safe for drinking. However, ethical and social factors have limited the reuse of recycled wastewater for potable purposes, especially in the Arabian Gulf countries, where social, cultural and religious barriers limit the reuse of wastewater-sourced water (Shomar and Dare, 2015). For non-potable reuse, clean water can be used in various domains, including agriculture, land irrigation, and industrial uses (Rao et al., 2018). Literature has shown that microfiltration (MF), ultrafiltration (UF), Nanofiltration (NF), and reverse osmosis (RO) are the pressure-driven membranes techniques employed in the wastewater recycling field with scientifically high-quality water (Lutchmiah

et al., 2014b). The pore size of these processes and the operational hydraulic pressure required an increase in the order MF>UF>NF>RO. Forward osmosis (FO) with the pore size of RO and no hydraulic pressure requirement, in its turn, has been allocated as an alternative technique in treating wastewater; however, it is not yet commercially applied. The limited application of FO in the treatment of wastewater is due to economic and technical concerns (Ibrar et al., 2020a; Korenak et al., 2017)

2.2.2. **Desalination techniques**

Desalination is derived from the root word *desalt,* meaning “remove salt from”. Desalination is defined as the “process of removing dissolved solids such as salts and minerals from water” (Kucera, 2014). Desalination dates back to the 1950s and has gained exponential growth in facilities and techniques. Several desalination techniques have been developed in order to meet all municipal, agriculture and industrial needs for adequate water. The current commercially available desalination technologies are Reverse osmosis, Multi-stage Flash Distillation, Multi-effect distillation, Electrodialysis and NF. Recording 65%, 21%, 7%, 3% and 2% of the total global installed capacity, respectively. MSF, MED and RO are predominant in the seawater desalination field, while ED and NF are more implemented in brackish water desalination. MSF and MED are thermal-driven technologies that convert water to vapor and recover the fresh water in subsequent condensations. RO, ED and NF are pressure-driven processes that separate salt from water using semi-permeable selective membranes known as membrane desalination techniques.

Desalination is currently providing a sustainable supply option for areas with water scarcity, such as the Gulf Cooperation countries (GCC). In this area of the Middle East, the largest thermal desalination plants are stationed where MSF dominate with a share of 96% compared to MED (63%) and RO (30%). The GCC countries include Saudi Arabia, United Arab Emirates, Qatar, Kuwait, Bahrain and Oman. Despite the importance of thermal desalination as an alternative for clean water production in the GCC, the high-energy cost and the environmental consequences remain the main drawbacks (Li et al., 2018).

With the advanced research and development in membrane science, RO is currently considered the leading desalination technology producing freshwater globally. It is documented that RO desalination plants produce around 50% of the desalinated water worldwide and are characterized along with the other membrane technologies by their energy efficiency and practical operations compared to thermal desalination (Qasim et al., 2019). NF process, in its turn, has been used in the desalination market and is characterized by removing multivalent scaling ions and requiring less hydraulic pressure than the RO process (Abdel-Fatah, 2018; Zhou et al., 2015). Despite the predominance of pressure-driven membrane desalination technologies, they encounter several issues, including high hydraulic pressure requirements, the demand for major pretreatments and the continuous replacement of membranes (Li et al., 2018). Recently, hybrid desalination techniques have been developed and designed for implementation on a large spectrum. Coupling two or more desalination techniques showed promise compared to a standalone process (Ahmed et al., 2020). When FO was coupled with RO as a pretreatment step, the RO membrane fouling decreased with an increase in the recovery rate and a reduction in chemical use (Chun et al., 2017).

It is mentioned in the literature that according to the International Desalination Association, statistics showed that from June 2015 to June 2016, the desalination capacity increased by 3.7 million m^3 per day (Bennett et al., 2016). Other studies predicted that 50% of the population worldwide might be at risk of water shortage by 2030. Hence, governments and countries worldwide have been putting extensive efforts into solving the problem of water scarcity and sustaining an alternative source of clean water.

2.3. A brief insight into the current GCC Desalination techniques

Amongst the different desalination technologies available worldwide, thermal desalination, especially MSF and MED, have dominated the GCC countries. The thermal desalination industry is one of the key players in the GCC governments' economy. Maintaining the current thermal plants' infrastructure while enhancing

performance, decreasing energy consumption, and cutting costs are taking place. The RO is the membrane-based technology that is shown interest in the GCC but on a narrow scale.

2.3.1. **MSF system**

MSF is one of the oldest desalination techniques that remains important and dominant mainly in the Gulf area, and it reports around 22% of the worldwide desalination plant production (IDA, 2014). Thermal desalination plants provide up to 70% of the total freshwater demands in the Gulf Countries Council (GCC) (Mabrouk, 2013), with only MSF plants participating in the production of approximately 100,000 m^3/d (Energy, 2011). Since MSF acquires thermal inputs, desalination plants are usually built as cogeneration plants for desalting water and electrical power generation. Part of the steam produced by the power station is used to heat the brine (seawater), which is the first step in the MSF. The electricity powered by the station is used for pumping and maintaining the vacuum in the desalination plant (Al-Mutaz and Al-Namlah, 2004). MSF plant requires between 20-27 kWh/m^3 to generate the unit mass of freshwater. The energy required is the total summation of the electrical and thermal needs (Al-Karaghouli and Kazmerski, 2013).

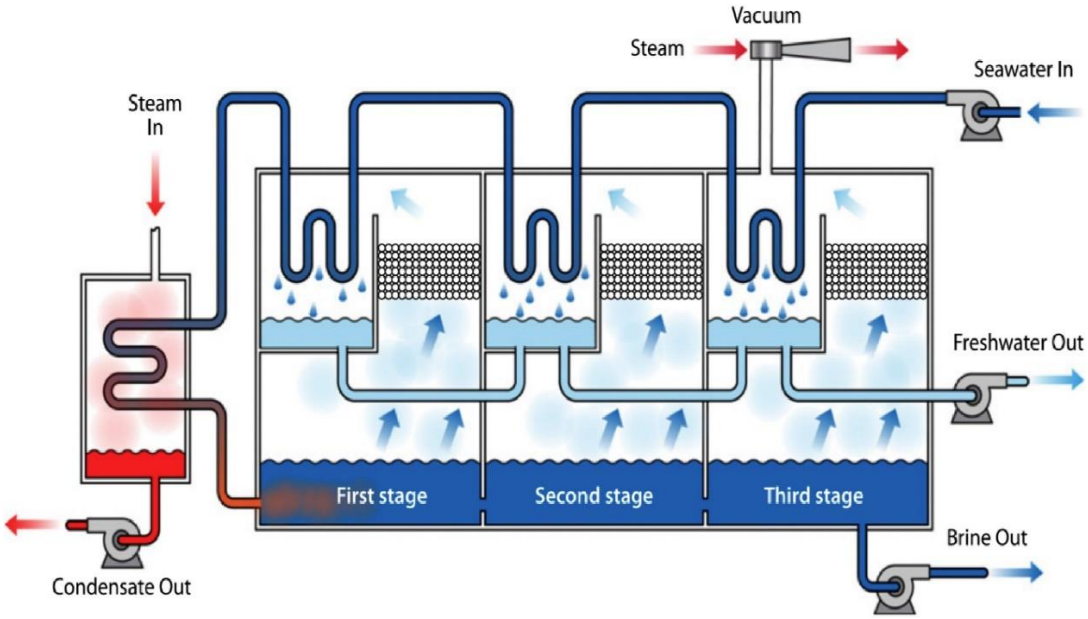

Figure 2.1. Schematic diagram of the MSF Process (Zhao et al., 2018).

As shown in **Figure 2.1**, MSF contains a series of consecutive flashing stages; each stage consists of a flash chamber and a heat exchanger (Baig et al., 2011). The number of stages varies from 15 to up to 40 stages (Baig et al., 2011; Feria-Díaz et al., 2021), allowing an average production of 50.000 to 70.000 m^3/d (Shahzad et al., 2017). The largest MSF plant in the world is located in Saudi Arabia, with a capacity of 815.120 m^3/d (Feria-Díaz et al., 2021). Basically, in the MSF process, seawater is evaporated using the heat provided by the power plant; the evaporated steam will then condense on the surfaces of cooling tubes implanted in the upper section of each chamber, producing distilled water collected in trays (Ettouney et al., 1999). Flash evaporation occurs at the heat input section in order to drive the flashing process from the brine into the bottom of the stages. When the hot brine passes into the first flashing stage, where the pressure is lower, a fraction of vapour is created, and the temperature of the remaining brine is dropped. By reducing pressure when passing from one stage to another, seawater in the chamber evaporates without adding extra heat. Distillate are collected in trays in each stage, throughout the plant and pumped into a storage tank (Khawaji et al., 2008). The operating temperature of the MSF plants ranges from 90 °C and 120 °C, known as top brine temperature (TBT). Rising the TBT enhances the flash evaporation and hence the plant's overall performance; however, fouling and scaling problems increase at higher temperatures (Shahzad et al., 2017). Among the advantages of the MSF desalination technique, there is mainly the production of high-quality distilled water that is not influenced by the salinity of the feed water and can handle large capacities (Australia, 2002; Borsani and Rebagliati, 2005). However, the intensive energy consumption, the high production cost, the environmental impacts of brine reject and the scale formation are the problems that have encountered the MSF techniques (Altaee et al., 2016; Lattemann and Höpner, 2008; Sanaye and Asgari, 2013).

One of the serious issues facing the MSF system is scale formation. The latter problem results in a remarkable reduction in heat transfer rate and hence the efficiency of the overall technique (Al-Rawajfeh et al., 2014). Crystallization of the reversible dissolved salts calcium carbonate ($CaCO_3$), magnesium hydroxide ($Mg(OH)_2$), Magnesium sulfate ($MgSO_4$) and calcium sulfate ($CaSO_4$) is the

essential elements forming the scale in the distiller plants (Al-Rawajfeh et al., 2005). $CaSO_4$ scale is mitigated by keeping the TBT under 110 °C to reduce its deposition. Whereas $Mg(OH)_2$ can be controlled by bicarbonate depletion or by adding organic polymeric (Al-Sofi, 1999). The non-alkaline formation, such as $MgSO_4$ and $CaSO_4$, was found specifically in the MSF plants within the condenser tubes due to the high TBT (Altaee et al., 2013).

2.3.2. **The status of RO in the Gulf area**

RO is the leading worldwide membrane process that dominates the desalination market (Anis et al., 2019; Feria-Díaz et al., 2021). The market share in the GCC countries is 70% for thermal technologies and the remaining 30% for the RO technique. RO differs from the natural osmosis phenomena in that hydraulic pressure greater than the osmotic pressure gradient of the solutions is applied on the feed side. The hydraulic pressure of a range between 20 to 80 bar will force water molecules to navigate across the membrane in the opposite direction to that of the natural osmosis. In the latter, pure water flows spontaneously from a low concentration to a high-concentration solution across a semi-permeable membrane. Interest has been directed toward RO due to its specific energy consumption, and overall operational costs are dramatically lower compared to thermal desalination (Qasim et al., 2019). However, the seawater quality in some parts of the world, specifically in the Gulf area, made RO less attractive. The high salinity and turbidity of the Gulf seawater put extra challenges to the performance of the current RO system (Mabrouk, 2013; Nassrullah et al., 2020). Despite the RO process dominating the other pressure-driven membrane technologies, research to address and tackle the drawbacks is an ongoing strategy. The progress in RO technology involves the membrane structure and materials, the pretreatment technique, and the system design to achieve cost reduction. RO has also been implemented in a hybrid system with thermal desalination plants in the GCC, but not on a large scale. Coupling RO with other thermal plants in Saudi Arabia and UAE generated better configuration in terms of water production and energy efficiency however addressed some difficulties usually associated with the RO system design (Al Bloushi et al., 2018)

2.4. Forward Osmosis-Emerging desalination technology

Although RO is the most feasible and efficient among the pressure-driven desalination technologies, it suffers from high pressure and energy requirements and higher operational costs. However, FO, a natural osmotic filtration driven by the difference in the solute concentrations between two solutions, has recently gained great interest among researchers as an alternative seawater desalination technique. FO has been found in various domains, such as fertigation, the pharmaceutical industry, protein enrichment and concentrating solutions (Suwaileh et al., 2020). Other applications include car manufacturing, oil and gas, and electronic industries (Haupt and Lerch, 2018).

FO is promising for its efficiency in removing divalent salts from water and remarkably requires less energy since it occurs spontaneously without applying hydraulic pressure. In spite of the fact that the FO technique in the desalination domain has great attraction from scientists and researchers, the technology remains at its early commercialization level. FO is currently operated in limited commercial desalination plants in Al Khaluf, Oman, Gibraltar and China (Aende et al., 2020). Over the last decade, interest in the FO process in water research has increased tremendously in academic and industrial fields worldwide. **Figure 2.2** recorded the statistical data showing the FO publications trend between 1992 and 2020.

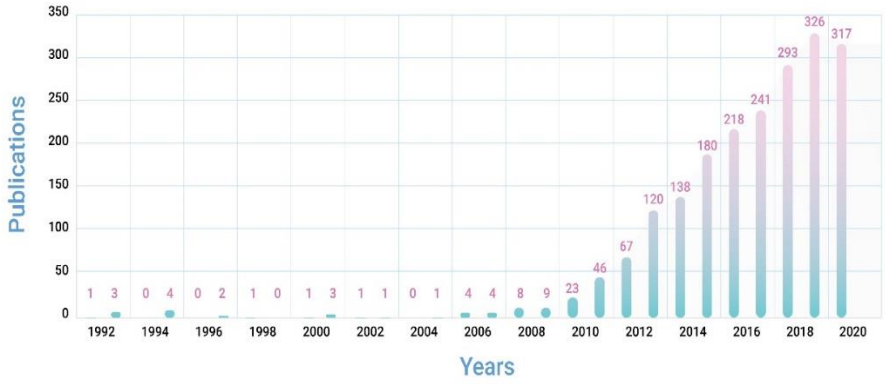

Figure 2.2. FO publications trend between 1992 and 2020 (Aende et al., 2020).

A systematic literature review conducted by Ang et al. in 2019 revealed that the publications' focus was on the FO membrane fabrication, the draw solute recovery, and the energy efficiency in the regeneration process (Ang et al., 2019). The review indicated that 59 countries have contributed to the FO publication records. Among these countries, China-326, United States-325, Singapore- 247, Australia-228 and South Korea-215 were the top 5 countries that contributed to FO technology publications (Ang et al., 2019). In addition, wealthy review articles presented the state of the art of the FO process on a wide spectrum (Aende et al., 2020; Cath et al., 2006; Zhao et al., 2012). Other literature was more specific, considering the aspects of the FO technique, including membrane characteristics (Kim et al., 2017b; Ndiaye et al., 2021), membrane fouling (Ibrar et al., 2019; Li et al., 2017a) and draw solutions (Johnson et al., 2018; Luo et al., 2014). In addition to hybrid systems (Blandin et al., 2016a; Chekli et al., 2016), utilization in wastewater treatment (Ibrar et al., 2020a; Lutchmiah et al., 2014b), applications in seawater desalination (Abou El-Nour, 2016; Linares et al., 2014; Qasim et al., 2015) and in municipal wastewater (Ansari et al., 2017). A noticeable increase in the number of publications on each FO topic was recorded in 2019. According to Suwaileh et al. (2020), the topics studied in terms of number of publications included fouling (576 articles), fabrication and modification (437), DS (404), recovery system (396), modelling and simulation (167), energy consumption (139) and techno-economic (95) (Suwaileh et al., 2020).

2.5. Basic Principles

FO is a filtration phenomenon where water molecules are transported across a semi-permeable membrane due to the osmotic pressure gradient of the stream solutions (**Figure 2.3**). The freshwater flows naturally through a semi-permeable membrane from the low-concentration solution to the high concentration. The latter is called draw solution (DS) or the extraction solution, and the low-concentration solution is known as feed solution (FS) or the donor solution. The primary outcome of the FO process is a diluted DS and, conversely, a concentrated FS due to the water loss. The product freshwater that is considered

the outcome of the FO process can be extracted from the DS using a recovery system or regeneration step.

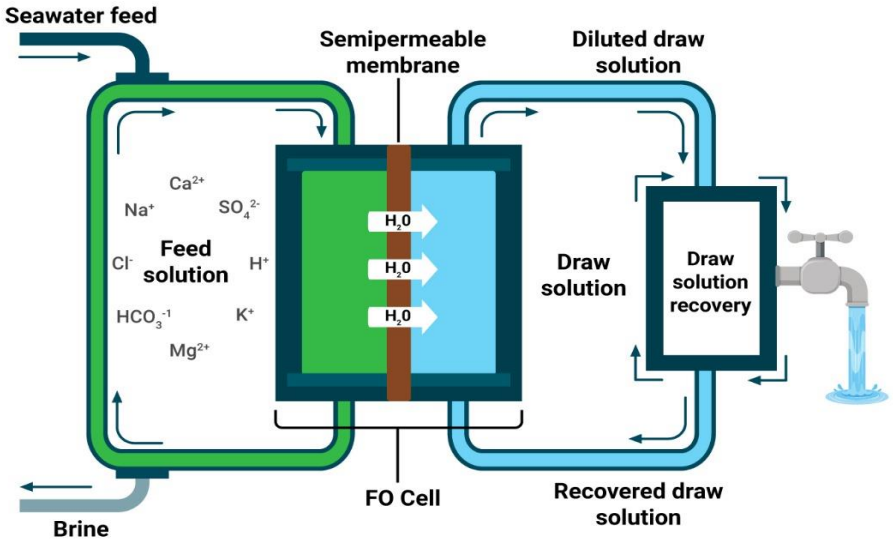

Figure 2.3. Illustration of the principle of FO process including the separation step and the regeneration (recovery) step.

The water flow in osmotically driven processes called water flux (Jw) and mathematically calculated using (Cath et al., 2006):

$$Jw = A\ \sigma\ \Delta\pi$$

Where A ($Lm^{-2}\ h^{-1}\ bar^{-1}$) is the pure water permeability coefficient of the membrane used in the FO process, σ is the reflection coefficient equal to 1 in the FO process.

Consequently, the water flux equation in FO experiments is $Jw = A\ \Delta\pi$

$\Delta\pi$ is the osmotic pressure gradient between the two streams, and the equation can be written $Jw = A(\pi_{draw} - \pi_{feed})$

Where π_{draw} and π_{feed} are the osmotic pressures of the DS and FS, respectively. Analytically experimental water flux in the FO process can be determined by

$Jw = \Delta V / A_m \Delta t$

ΔV is the change in FS volume, Δt is the interval of operational time, and A_m is the membrane area of the FO membrane (m^2).

Generally, the FO process consists of two steps or stages; the first stage is the separation of freshwater from the FS and diluting of the draw solution. The second stage is the regeneration of the DS and the extraction of pure water from the highly diluted draw solution. The selection of the DS directly affects the quality of the water produced at the end of stage two of the FO operation. Thus, a successful FO process relies on a DS that offers high osmotic pressure and a facile recovery process in addition to a well-designed FO membrane (Aende et al., 2020).

Recently, pressure-assisted forward osmosis (PAFO) has been introduced, and research on its potential to improve water production is being assessed. The principle of the PAFO is to apply low hydraulic pressure on the feed side. The PAFO process was used instead of the FO process to purify the RO concentrate and showed promising results of increasing the water permeability across the flat sheet CTA membrane. The maximum pressure applied in the study was 4 bar (Jamil et al., 2016).

2.5.1. **FO membranes**

One of the advantages of the FO technique is the simple equipment instalment and configurations. The membrane is a vital part of the FO process. Thus, the design and development of an ideal membrane for effective FO technique is ongoing research in academic and industrial domains. FO membrane consists of a selective and a support layer. The active or selective layer rejects particles and solutes from the stream solutions, while the support layer provides mechanical strength and stability to the membrane (**Figure 2.4**). The ideal FO membrane requirements include high water flux and low reverse solute permeation for the active layer and a support layer that permits higher mass transfer with lower concentration polarization, integrated with sufficient mechanical structural strength and antifouling properties (Li et al., 2016). These requirements remain a challenge in FO membrane manufacturing and development. A considerable amount of studies investigated the performance of FO membrane following the

introduction or the addition of novel materials, various polymers and different concentrations also by including changes in the structure of the support layer or altering the design of the thin selective layer (Suwaileh et al., 2018). FO membranes are provided in cellulose triacetate (CTA) and thin-film composite TFC) polyamide. They are available in flat sheet, spiral wound and hollow fibre configurations (Li et al., 2017b). Flat sheet FO membrane configuration recorded the highest usage in the laboratory experiments. The Hydration Technology Innovations (HTI) Company has provided cellulose-based membranes for approximately 20 years. Later, the company developed TFC membranes in flat sheet and spiral-wound configurations. Toyobo, in turn, introduced the hollow fibre CTA FO membrane, followed by Porifera, which developed plate and frame modules. Recently the Aquaporin Inside provided TFC aquaporin flat sheet membranes where aquaporin proteins are incorporated into the selective layer.

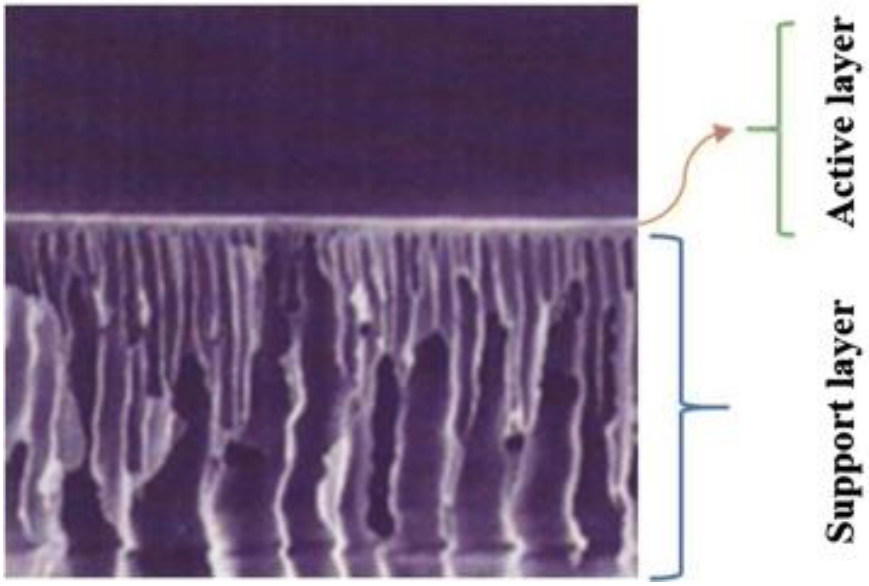

Figure 2.4. The typical TFC FO membrane structure: active and support layers (Khan et al., 2019).

Literature showed that the TFC membrane demonstrated better water flux compared to the other examined membranes (Li et al., 2017b). Since the ideal design of the FO membrane is not met yet, the research and the manufacturing have focused on the alteration of the support layer by adding new materials or on the modification of the selective layer to increase its selectivity towards ions and

contaminants (Suwaileh et al., 2018). Silica, carbon nanotube and graphene materials are among the most common additives to the support layer of the FO membranes presented in the documented research; however, the commercialization of these membranes is still low. The thin selective layer undergoes modifications such as introducing Nanofillers, coating and grafting parallel to the support layer. The considerable research in delivering the perfect FO membrane design for each application is promising in delivering FO membranes with improved hydrophilicity, lower ICP, higher selectivity, and mitigating fouling and scaling (Emadzadeh et al., 2014; Suwaileh et al., 2020). Besides the membrane structure, the cost is another critical obstacle affecting the FO commercially. It is documented that the cost of the FO membrane is ten times higher compared to the RO membranes –specifically mentioning the 16.5m^2 HTI. The high cost of the FO membrane might result from the low market demand. The cost of the 700m^2 FO membrane provided by Toboyo is equal to that of the RO membrane. This available size is for the full-scale module; however, it is not available in flat sheet laboratory size. The price of each membrane module within the same manufacturer or between different providers can differ depending on the descriptions and the details provided in the manufacturer catalogues. The main FO membrane suppliers are fluid technology solutions, Oaysis water, Porifera, Toyobo, Moderna water and Trevi Systems. From a cost perspective and longer usage of the membrane, it was demonstrated that the hybrid system could increase the membrane lifetime and therefore decrease the cost, specifically in the desalination of high-salinity seawater (Altaee et al., 2017).

2.5.2. **Draw solution for the forward osmosis**

The concentrated stream is called the draw solution on the permeate side of the FO membrane. In addition to brine, the latter is the common term used in the literature; however, other terms such as driving solution, sample solution, and osmotic agent are among the used terminologies. The osmotic gradient difference between the draw and the FSs drives the FO process. The highly concentrated DS drag the water across the FO membrane from the feed side towards the draw side. The higher the draw solute concentration, the higher the osmotic pressure in the FO process. Unlike the other pressure-driven separation

membranes, the product is a diluted draw solution, not separated clean water. A second step, known as regeneration or water recovery, is needed to deliver the final product. Unless the FO process is designed to dewater the feed product and dilute the draw solution, the latter requires a second separation step to re-concentrate and produce the purified water. The FO's regeneration step requires more energy that can be intensive compared to the first step. Selecting the effective draw solute is one of the significant challenges as it is essential for the effectiveness of the FO process. The progression of the draw solute over time since 1965 is well documented in the literature. The DS that has been utilised include volatile solvents such as Sulfur dioxide, gas and volatile compounds such as alcohol, organic compounds such as fructose and glucose solutions, ammonia carbonates, inorganic salts, dendrimers, magnetic nanoparticles, Ionic polymer hydrogel, inorganic fertiliser, switch polarity solvent and carbonised quantum dots (Suwaileh et al., 2020). Overall, going through the literature, it became evident that there is still a lack of ideal solutes with all the proposed and investigated draw solutes requiring regeneration for freshwater extraction. The characteristics of the ideal draw solution that can affect the FO performance and efficiency involve:

- Provide high osmotic pressure.
- Compatible with the membrane structure.
- It should be water-soluble.
- Small molecular weight but not too small to prevent reverse solute flux.
- Low reverse solute flux.
- Not very expensive
- High diffusivity with low viscosity.
- Not toxic.
- It can be regenerated in an energy-efficient process (Johnson et al., 2018).

The ongoing research on the draw solutions indicates that none of the studied draw solutes met an ideal draw solute criteria. For example, NaCl is a small size solute with a high diffusion coefficient that can minimise the effect of ICP and increase the reverse solute flux. In the case of magnetic nanoparticle solutes, regeneration was an easy process using magnetic power. However, the aggregation of the nanoparticles resulted in low osmotic pressure, low flux, and the loss of particles during recovery (Ge et al., 2011). Divalent ion solutes in draw

solutions such as $MgCl_2$ and $MgSO_4$ show low reverse salt, but these ions' presence can increase the organic fouling. After using NH_4HCO_3 as a draw solution, 85% water recovery was recorded. However, the low amount of non-rejected ions such as NO_2^- and Br^- and metals such as Al, Fe and Ba can cause toxicity to drinking water. Thus, the final product's type and quality affect the determination of the appropriate draw solute and its recovery technique. The selection of the ideal draw solute can influence the overall efficiency and outcome of the FO process. Since regeneration is the highest energy-consuming step, the draw solute chosen should be regenerated in an energy-efficient technique (Ge et al., 2013). Overall, the regeneration methods are categorised into chemical precipitation, stimuli-responsive such as solar, magnetic field and electricity, membrane separation (MF, NF, UF, RO), thermal separation and in some cases, a combination of processes (Long et al., 2018; Luo et al., 2014).

2.5.3. **FO process- transport phenomena**

2.5.3.1. *Mass transfer*

Mass transfer or Mass transport includes a number of processes that involve transferring matter within a system on a molecular scale. It refers to the mass in transit as a result of the concentration gradient. In the case of FO and unlike other pressure-driven membrane techniques, the asymmetric structure of the membrane affects the mass transfer (Cath et al., 2006). Generally, the support layer of asymmetric membrane design prevents mixing, leading to a reduction in the mass transfer. This phenomenon is known as concentration polarization.

2.5.3.2. *Concentration polarization*

In both osmotic and pressure-driven membrane processes, the accumulation and the reduction of solutes near the surface is called concentration polarization. In the FO process, where the membrane is asymmetric and consists of active and support layers, CP might develop internally in the support layer and externally at the borders of the membrane's active layer surface. On the broad spectrum, there are two types of CP, external and internal, that occur in four aspects, called concentrative external concentration polarization (CECP), dilutive external

concentration polarization (DECP), concentrative internal concentration polarization (CICP), and dilutive internal concentration polarization (DICP). It is documented that the effect of ECP in FO models is mild to negligible compared to the other pressure-driven membrane techniques. This is explained by the absence of hydraulic pressure (Cath et al., 2006), the high mass transfer (Lutchmiah et al., 2014a) and the considerably low flux.

In the FO mode, where the FS faces the active layer, solute accumulation occurs on the active layer, increasing the feed concentration at the active layer. This phenomenon is known as CECP. In the same mode, the DS becomes less concentrated inside the support layer leading to DICP. DECP, in turn, occurs when the DS faces the active layer (PRO mode), a dilution of the active layer- DS interface due to the water flux from the FS. Simultaneously, the FS becomes concentrated in the support layer creating CICP. The CP phenomena mentioned above affect the osmotic gradient that decreases the dragging force across the FO membrane, lowering the water flux. **Figure 2.5** in the FO process shows that two phenomena can occur depending on the operational mode. When the active layer faces the FS, also known as AL-FS orientation or FO mode, and as water navigates the active layer, an increase in the osmotic pressure at the active layer-FS interface leads to concentrative external CP and dilutive internal CP (**Figure 2.5a**). In **Figure 2.5b,** the porous support layer faces the FS, the AL-DS orientation or the PRO mode. As water and solute penetrate the support layer, dilutive external CP and concentrative internal CP occur (Ibrar et al., 2019).

The internal CP has more impact in reducing the water flux in the FO process than the external CP due to the asymmetric membrane structure. The saline solution flow within the porous layer is carried by direct diffusion. In the TFC FO membrane, the thickness of the support layer plays an important role in the CP, and smaller structural parameters are desirable for lower DICP (Tiraferri et al., 2011). The amount of solute that can penetrate the active layer and the solute accumulation in the support layer contributes to an internal CP. Since the solute build-up occurs in the porous layer, increasing the flow turbulence might not mitigate the CP. There has been a wealth amount of research to tailor a FO membrane with reduced ICP. The work has been done on increasing the porosity

and reducing the thickness of the support layer, using double-skinned membranes, reducing the support layers' tortuosity and increasing the membrane's hydrophilicity (Ibrar et al., 2019).

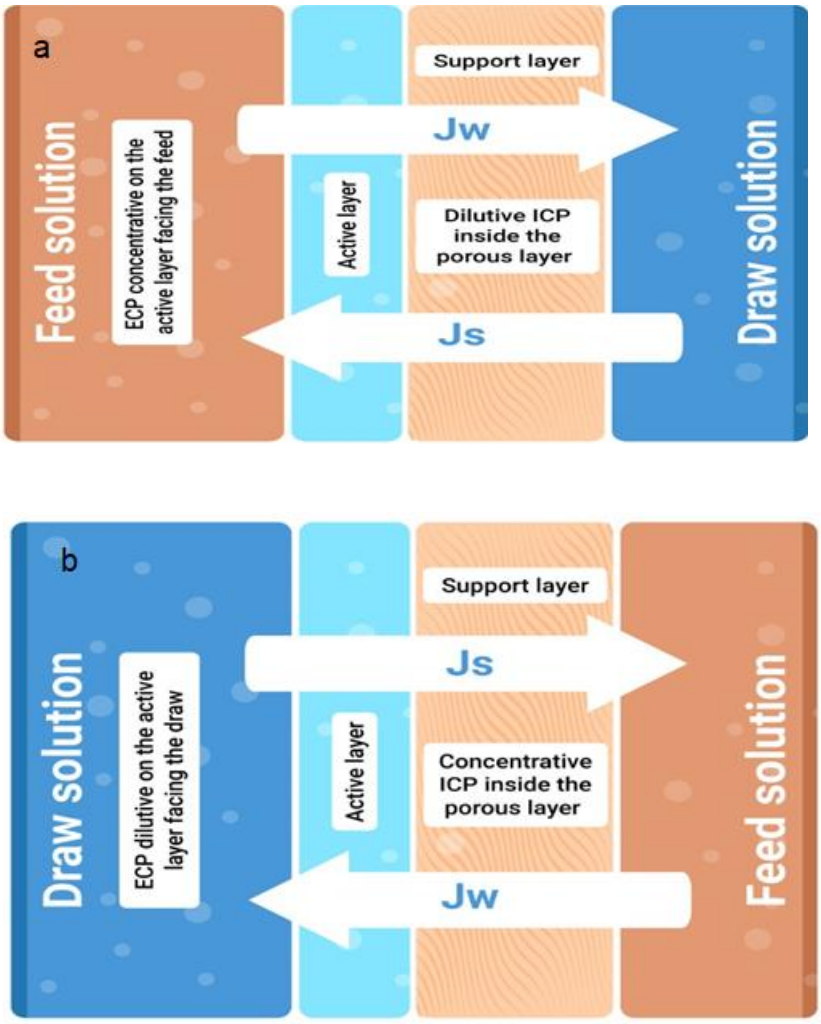

Figure 2.5. Illustration of ICP and ECP in a) FO mode and b) PRO mode. J_w and J_s are the water and the permeate flux, respectively.

2.5.3.3. *Reverse Solute Flux*

RSF is among the major issues affecting the progress of the FO technique. RSF, also called reverse salt diffusion, is described as the diffusion of DS across the FO membrane towards the feed side driven by the solute concentration gradient between the feed and draw solution. The considerable difference in concentrations between the feed and DS enhances the RSF and weakens the driving force. The reverse diffusion is correlated to the membrane parameters

such as thickness, porosity, tortuosity, and DS characteristics such as ion charge, viscosity, and aqueous diffusivity. For example, most FO membranes are negatively charged, allowing solution cations to navigate easier than anions (Sarkar et al., 2010). The damaging effects of RSF involve the loss of DS, the reduction in the osmotic pressure, the increase in fouling tendency, and the need for periodical regeneration of DS that can elevate the operational cost (Zou et al., 2019).

The control or the reduction of the RSF is one of the critical areas of study. RSF controlling and reduction is related to developing a selective membrane coupled with a novel appropriate draw solution. The literature showed a significant amount of lab-scale research regarding the material fabrication and development techniques of the FO membrane to tackle the FO process drawbacks. Very few studies focused on RSF reduction (Zou et al., 2019). Achilli et al. presented that the reverse solute flux is lower when the DS contains large-sized anions such as $NaHCO_3$, $MgSO_4$, K_2SO_4, $KHCO_3$, and $(NH_4)_2SO_4$. Results showed that the draw solutes with high osmotic pressure and larger molecules might exhibit lower salt back diffusion (Achilli et al., 2010).

2.5.4. **FO Membrane fouling**

Fouling is one of the major downsides affecting the performance of the membrane in the osmotic membrane separation processes. Even though the FO technique is believed to exhibit lower membrane fouling than other membrane processes, especially pressure-driven membranes, fouling is still a critical issue in the progress and efficiency of the FO process (Li et al., 2017a).

2.5.4.1. *Foulants composition and properties*

Membrane fouling occurs when solutes or other particles accumulate on the surface of the membrane or within the pores inside the membrane. During the separation technique, the build-up of the particles can form a cake layer or a gel-type layer on the surface and block the pores. Fouling affects the performance of the membrane by reducing the water flux, stimulating the concentration polarization, and weakening the rejection rate.

In the FO process, fouling occurs on the surface of the active and support layers and inside the support layer. It is classified and depends on the membrane orientation into internal and external fouling. The foulants will deposit on the active layer in the FO mode, leading to a microscopic cake-type layer (Ibrar et al., 2019). However, in the PRO mode, the fouling matters smaller than the membrane support layer pores can penetrate the support layer along with the water flow. These small particles will be attached to the wall of the support layer or deposited inside the support layer. The smaller foulants can adhere to the pore of the membrane causing internal fouling and pore-clogging. The latter is the severe kind of fouling. It is difficult to clean and can reduce porosity and stimulate the internal CP. Both External and internal fouling can occur in the PRO mode. External fouling is controllable and can be eased using physical and chemical cleaning methods (Ibrar et al., 2019). Depending on the feed water quality, both types of fouling can be irreversible. Membrane fouling in the FO process has been classified based on the type of foulants. Organic, mineral scaling or inorganic fouling, colloidal or fouling and biofouling are the four categories of FO membrane fouling. The fouling in the membrane-based processes is usually a combination of different types of fouling, rarely a single type of fouling (Li et al., 2017a). The foulants vary depending on the FS's quality and contents in the FO process. There are diverse foulants such as particulate matter, inorganic components, microorganism species, dissolved organics, microbial species and chemicals (Suwaileh et al., 2020).

2.5.4.2. *Fouling detection techniques*

A range of techniques is used for real-time fouling monitoring that can be used to study better and understand the fouling layer formation mechanism. On the broader spectrum, some of the used techniques are namely: i) ultrasonic time domain reflectometry (UTDR), direct observation through the membrane (DOTM), nuclear magnetic resonance (NMR), electrical impedance spectroscopy (EIS), optical coherence tomography (OCT) and confocal laser scanning microscopy with multiple fluorescent labelling. Only a few publications on real-time monitoring of FO membrane fouling are available (Ibrar et al., 2019).

There are analytical methods to study the characteristics and the type of the foulants of the fouled membrane, such as Scanning electron microscope (SEM), Energy dispersive X-ray (EDX), interfacial force measurement (AFM), spectroscopy and confocal laser-scanning microscope (CLSM). These modern techniques have been applied successfully in the studies of FO-fouled membranes (Li et al., 2017a).

2.5.4.3. *Fouling mitigation*

The Fouling control and cleaning methods are related at first to the type of foulants accumulated on or within the membrane layers. Many studies reported that the fouled membrane could be physically removed by flushing DI water. However, other techniques, e.g. chemical cleaning protocols, are needed when treating FSs such as wastewater, landfill leachate, and other complex mixture (Ibrar et al., 2020b). The combination of organic and colloidal fouling is irreversible, where particles aggregate and cause severe flux decline. The pretreatment of FS using UF or MF processes was proposed to avoid organic-colloidal fouling. According to Kim et al., results showed the successful removal of colloidal particles from the pretreated FS. Osmotic backwash was evaluated in cleaning CTA-fouled membranes with colloidal and combined organic and colloidal matters, effectively restoring the water flux (Kim et al., 2014).

The effect of the membrane orientation on fouling formation and fouling cleaning has been investigated. The FO mode, where FS faces the active layer, showed more stability and high cleaning efficiency than the PRO mode, especially for high saline water and wastewater (Ibrar et al., 2019). The membrane material and structure play an important role in controlling fouling and in cleaning methods efficiency. Polyamide membranes exhibit higher fouling than cellulose acetate. However, osmotic backwash and physical cleaning were more effective in flux recovery for TFC membrane than CTA (Li et al., 2012). Other fouling mitigation techniques were reported, such as Air scouring, pulsed flow method, and feed spacers (Ibrar et al., 2019).

2.5.5.**FO energy consumptions**

The energy requirements of the membrane desalination technique have been investigated to be affected by the concentration of the draw solution, the flow rate of the FS and the structure and orientation of the membrane (Nassrullah et al., 2020). The specific energy consumption of the RO for sweater desalination was reduced from 20kWh/m^3 to 2.5kWh/m^3 but is still considered an intensive energy process. The RO energy consumption reduction was achieved by developing energy recovery devices, providing pumps with better energy efficiency, and improving the membrane design and performance (Park et al., 2019). On the other hand, the FO process energy requirement is about 2% to 4% of the energy required in the RO process since the natural osmotic pressure drives the FO process (Altaee et al., 2014c). The separation phase of the FO process does not require high-energy consumption; however, the recovery step or regeneration process is the FO step with intensive energy demand (Suwaileh et al., 2020). Studies on coupling FO with other desalination techniques in a hybrid system have significantly influenced the desalination process's energy consumption. In experimental study by Altaee et al. (2017), the specific power consumption of RO in the FO-RO system for seawater desalination was lower than in the standalone RO process. The energy depends on the salinity of the seawater; the higher the salinity, the more energy is required (Altaee et al., 2017). In another study by Attarde et al., using hollow fibre membranes in the FO-RO system resulted in 25% energy savings compared to the RO process alone (Attarde et al., 2017). In addition, secondary wastewater effluent and red sea seawater were used in an FO-RO hybrid system for an operational period of 14 days. The energy consumed in the hybrid system was 1.5 kWh/m^3, around half of the standalone RO process's energy, usually around 2.5-4 kWh/ m^3. Furthermore, the performance of FO-RO process was investigated on a pilot study scale during a period of 5 month to study the fouling performance and the energy requirements. The results were promising, a significant reduction of fouling was reported and the energy consumption was reduced by 15% compared to the typical RO process (Nassrullah et al., 2020). Optimization of the energy requirements of the regeneration step of the standalone FO process is intensively attracting the researches to improve the overall outcome of the FO technique.

2.5.6. **Analysis of the FO process cost**

FO membrane cost has been stated to play a major component in the capital cost of the FO system. The expensive price of the FO membrane compared to the other membrane separation techniques can be related to the limited commercial applications of the FO process. The price of FO membrane from HTI was around ten times higher than that of RO membrane. According to the HTI company catalogue, the cost of the 8040FO-FS-P FI membrane was 1719 USD/element compared to 600 USD per element for the FILMTEC RO membrane. The HTI 8040FO-FS-P spiral wound of 16.5 m^2 was about 104 USD /m^2. Toyobo offers a more affordable FO membrane; the HP10130 series has a similar cost per m^2 to the RO membrane due to its membrane area. It has been calculated that a 10,000 m^3/d FO plant that uses TFS CTA FO membrane will cost 5,426,136 USD. The cost is based on 16.5 m^2 CTA FO membrane model 8040FO-FS-P at 1,719 USD/ element.

Although the membrane cost is the capital cost in the FO process, other operating expenses can be added to the overall cost. The regeneration process of the DS and regular membrane cleaning and maintenance are among the overall FO cost.

2.6. Hybrid System: A key for improved seawater desalination

The FO principle has attracted the seawater and wastewater treatment processes for the potential of FO as a low-energy technique. The low energy advantage of the FO process can only be achieved in applications where no further treatment is required or, in other words, when the regeneration process is not needed. For example, the diluted DS is the final product (Johnson et al., 2018). FO can be coupled with another thermal or membrane separation process in a so-called hybrid FO system. Recently, the ascendant trend in the literature studying the performance of hybrid systems in various applications is remarkable. The FO hybrid system research is taking great place in wastewater treatment, seawater, and brackish water desalination.

It has been claimed that integrating FO as a pretreatment process with other desalination processes has improved its overall outcome. Especially when desalinating harsh, low-quality feed water with high salinity, high total dissolved

solids or various contaminants. The reported FO hybrid desalination systems include FO-RO, FO-LPRO, FO-MD, FO-MSF and FO-NF. In the FO-RO hybrid system, water is transferred from the FS across the FO membrane; the diluted DS will be later used in the RO membrane. Coupling FO with RO improved the water flux and showed higher water recovery. The selection of the DS plays a major role in the energy requirement for the FO-RO system. $MgSO_4$ and NaCl were the DS used in two FO-RO pilot scale studies in Oman (Al-Zuhairi et al., 2015) and Australia (Chun et al., 2016) with seawater four types of brackish water FSs, respectively.

The outcome of the plant located in Oman was a significant improvement in energy consumption, lower fouling and a higher rejection rate compared to the conventional RO. The case study results in Australia showed that the performance of the FO pretreatment declined due to the inorganic scaling due to feed water quality. However, the overall performance of the FO-RO system demonstrated higher performance than the RO standalone. It has been presented that using FO-RO for seawater desalination combined with secondary effluent wastewater treatment achieved around 50% energy saving compared to the conventional single-pass RO. Furthermore, in a proposed FO-MSF hybrid desalination system. FO process was used as a pretreatment step before the MSF desalination process. Brine from the MSF plant was used as a DS in the FO system in order to dilute the brine. When comparing the NF-MSF with the FO-MSF, the latter was preferable for its lower energy consumption and less fouling (Altaee et al., 2013; Altaee et al., 2014a). The proposed system was evaluated for the first time using real MSF brine reject as the DS in the FO step and seawater as FS. The results were promising, with 8.5% brine dilution at 40 °C following the reductions in divalent ions count in the DS (Thabit et al., 2019). According to Darwish et al., using FO membranes for seawater pretreatment prior to the MSF with a 40% recovery rate would increase the TBT of the MSF plant without increasing scale formation (Darwish et al., 2016b). For the successful implementation of hybrid systems, further work is required to address challenges such as tackling the limitation of the mass transfer, the drop in the pressure, and the various fouling on a lab scale and later on a full scale. Economic assessment,

including energy requirements and operational cost, is expected for each hybrid system before commercialization (Blandin et al., 2016a).

2.7. Desalination research trend in GCC

The GCC countries are located in an area where water scarcity is severe due to the poor source of natural freshwater resources and the socio-economic growth. To meet the water demand, especially the drinking water, the GCC countries rely on seawater desalination using thermal desalination plants. Although the GCC countries are considered the leading in desalination capacity, there is an ongoing investment and research on developing energy-efficient and cost-saving desalination techniques. On the governmental level, there are long-term plans to increase the share of renewable energy by 2040 and launch nuclear power plants in Saudi Arabia and the UAE (Qureshi, 2020). On the research level, lab-scale experiments, pilot-scale plants and study cases have been employed to increase the efficiency of the current thermal desalination systems. For example, a case study in Abu Dhabi was conducted due to increased portable water demand. MSF, MED and RO are the most commonly used technologies in the UAE; 63% of the water produced by MSF and 12% accounts for RO. Hybrid MSF-RO plants were installed in UAE plants to investigate their performance. The impact of the MSF hybridization in the UAE plants has shown a significant reduction in energy consumption and cost while maintaining the same water production capacity (Al Bloushi et al., 2018).

Hybrid systems have been widely proposed as an energy and cost-saving strategy for the desalination processes, in addition, to decreasing the intensive energy requirements of the MSF plants in Qatar and the harsh conditions of the brine in the marine environment. The thesis work will focus on MSF brine recycling using the FO technology with various membranes. The integration of membrane separation techniques prior to the MSF plant is promising in removing the divalent ions, i.e. Ca^{2+}, Mg^{2+} and SO_4^{2-} responsible for the scale formation in the MSF plant. Redirecting the brine into the FO process as a draw solution can potentially decrease the ions concentration in the feed water to the MSF plants.

In parallel with the main objective, the introduction of pressure-assisted forward osmosis for the dilution of the MSF brine will be tested in terms of water flux and specific power consumption. The impact of membrane materials and orientation on the performance and fouling propensity of the FO process will be evaluated. Several membranes with different water permeability will be assessed by calculating the water flux, evaluating fouling properties and testing the most effective cleaning strategy to increase the performance of the FO process. Commercial NF membranes were tested in the FO process for feed pretreatment to the MSF plant for the first time to reduce the capital and operation costs. Experimental work also evaluated the impact of feed solution composition and concentration on the FO system.

Chapter 3: Materials and Methods

3.1. Introduction

The experimental work studied the performance of the FO process under various operational parameters. Hydraulic pressure of up to 4 bar was applied on the feed side in the PAFO techniques. Experiments were conducted with seawater and tertiary sewage effluent (TSE) subsequently for feed water. The MSF brine reject was the only DS used in this study. The temperature of the feed side was maintained at 25 °C, while 40 °C was the DS temperature. Two membrane categories were included in the FO system, FO and NF membranes. These membranes were evaluated in the AL-FS and the AL-DS orientations. The pristine fouled and washed membranes were studied using SEM, SEM/EDS, and FTIR characterisation technologies. Various cleaning methods were investigated for their effectiveness in removing foulants following each FO process. The overall behavior of each FO process conducted in this work was analyzed based on the following performance measurements: water flux values, water flux reduction, the reserve solute flux, energy consumption and the level of DS dilution. The flow chart in **Figure 3.1** presents the order of the tasks carried out during the research frame. All laboratory experiments were performed at the University of Technology, Sydney, Australia.

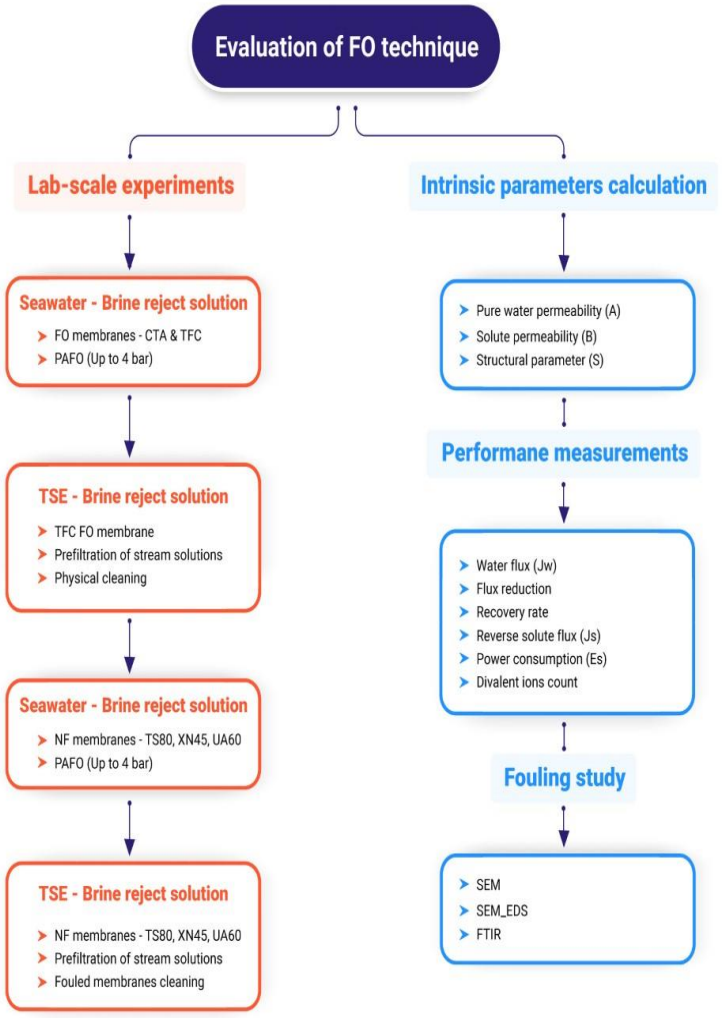

Figure 3.1. Key map of the research activities.

3.2. Experimental Materials

3.2.1. **Stream solutions**

Fresh seawater of 32 g/L was collected from the Sydney area and left for several days to settle. Then, it was heated to reach the seawater salinity of the feed water to the MSF plants in the Middle East. The concentration of the seawater FS used in the FO process was 45 g/L. In the other set of experiments, treated wastewater (TSE) was used as FS. The Blacktown wastewater plant in Sydney, Australia, provided TSE samples. The temperature of the FS was maintained at 25 °C. Only one DS was used in the experiments; seawater from the Sydney area was heated

to reach 80 g/L, the MSF brine reject concentration. The characteristics of each stream solution, e.g. TDS, conductivity, turbidity and the TOC, were provided in detail in **Table 3.1.**

Table 3.1. Characteristics of feed and draw solutions used in this study.

Ion / parameter	Seawater (45g/L)	TSE	Brine solution(80g/L)	Measuring Instrument
Ca^{2+} (ppm)	855.2		1040.9	7900 ICP-MS
Mg^{2+} (ppm)	1895.3		2199.6	7900 ICP-MS
SO_4^{2-} (ppm)	3171.6		6566	DIONEX AS-AP
Cl^- (ppm)	9832		22351.6	7900 ICP-MS
Na^+ (ppm)	16372.9		19151.6	7900 ICP-MS
K^+ (ppm)	692.9		872.3	7900 ICP-MS
TDS (g/L)	45.1		80.2	HQ14d Conductivity
Conductivity (mS/cm)	68.9	3.91 ± 0.27.5	106.7	HQ14d Conductivity
pH	8.0	7.2 ± 0.2	8.35	HQ40d multi
Turbidity (NTU)	1.47	0.967	2.43	2100P Turbidimeter

3.2.2.**FO membranes**

Thin Film Composite (TFC) from Porifera and Cellulose triacetate membrane form FTSH_2O was the FO membrane studied in the experiments. It is mentioned in the manufacturer guideline that the thin-film composite membrane from Porifera has a structural parameter (*S*) of 344 microns and can tolerate pressure up to 12.41 bar, 40°C feed temperature and has salt rejection up to 90% (Blandin et al., 2016b). Similarly, the cellulose triacetate membrane can tolerate up to 50°C feed temperature and hydraulic pressure of 5 bar. **Table 3.2** summarizes the membrane's chemical and physical characteristics. A represents the water permeability constant, B represents the coefficient of solute permeability, and S is the membrane structural parameter.

Table 3.2. Characteristics of Porifera and FTSH_2O membranes.

Parameter	Porifera (TFC)	FTSH_2O (CTA)
Membrane chemistry	Thin-film composite	Cellulose triacetate
A (L/m^{2}h.bar)	2.1	0.69
B (kg/m^{2}h)	1.2	0.34
S (μm)	344	707
Contact angle active layer	68.5°±0.7	68.1°± 1
Contact angle support layer	53.9° ± 2	60.2° ± .5
Zeta potential	-41.9 ± 2.44	-12.8 ± 1.18

The virgin Porifera TFC and CTA FTSH_2O membrane's Wettability measurements and hydrophilic behaviour were investigated by measuring the contact angle using the sessile drop method at various places on the same membrane using FACE Automatic Interfacial Tensiometer, Japan. Images of the water contact angle measurement are represented in **Figure 3.2.** Using a scanning electron microscope (SEM, Zeiss Supra 55VP), the surface morphology of the used and cleaned membranes for AL-DS direction was obtained. Before characterisation, all the membranes were washed with deionized (DI) water and subsequently dried in a vacuum chamber.

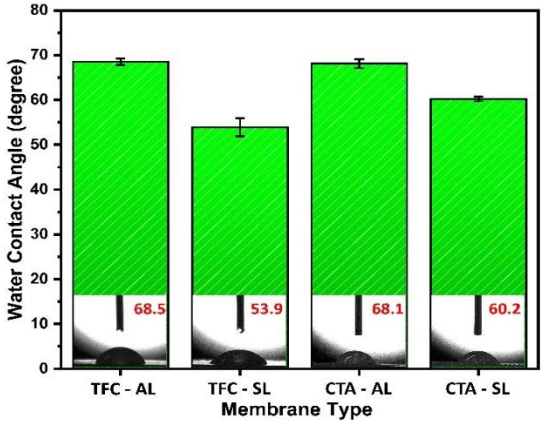

Figure 3.2. Water contact angle for virgin Porifera TFC and FTSH_2O CTA membranes.

Zeta potential measurements were run for the membranes using Malvern instruments. The wetting angle between the water-membrane surface interface was measured. The active layer (AL) of the Porifera TFC and FTSH_2O CTA membrane shows almost an equal water contact angle ~ 68.5 and 68.1, respectively (**Figure 3.2)**. As for the support layer, Porifera TFC showed a lower water contact angle, ~53.9, than the FTSH_2O CTA membrane, ~60.2.

3.2.3.**NF membranes**

Three commercially available NF membranes from TRISEP® were used in the FO process experiments. Namely, TS80, XN45 and UA60. The thickness of all membranes is between 130 to 170 µm, the chlorine tolerance is less than 0.1 ppm, and the pH range is between 1.0 and 12.0. The UA60 NF membrane is between a tight UF membrane and a loose NF membrane with an 80% rejection rate to $MgSO_4$. The XN45 NF membrane has a 96% rejection rate to Mg^{2+} and SO_4^{2-} and the TS80 membrane has a 99.5% rejection rate to $MgSO_4$. Table 3.3 summarises the NF membranes characteristics according to the TRISEP® guideline.

Table 3.3. NF membranes characteristics (7.6 bar, 25°C and 30 min operation).

Membrane	A_w (L/m^{2}h.bar)	B (L/m^{2}h)	Membrane chemistry	Thickness (µm)	$MgSO_4$ rejection (%)	Flux (L /m^{2}h)	Zeta potential (mV)	Contact angle (active layer)
TS80	8.63	1.33	Thin-Film Polyamide	130-170	99.2	49.3-81.6	-55.6	17.4°±2.3
XN45	7.96	2.51	Thin-film Polypiperazine	130-170	96	47.6-73.1	-52	8.2°±2.8
UA60	14.01	26.55	Thin-film Polypiperazine	130-170	80	76.5-136	-60	15.7°±3.1

A_w represents the water permeability constant, B represents the coefficient of solute permeability, and S is the membrane structural parameter.

3.2.4.**FO laboratory-scale setup**

A CF042A-FO Cell manufactured by Sterlitech was used in the FO system. The FO cell is a clear cast acrylic cube-shaped filtration unit of 5×4×3,25-inch exterior dimensions of 42 cm^2 (6.5 $inch^2$) membrane area. It can tolerate 88°C maximum temperature and 27.6 bars of hydraulic pressure. The system was provided with two flow meters, F-550 (Blue-White Industries Ltd), connected on each side of the cell to measure the FS and DS flow rates. Both sides of the cell were furnished with pressure gauges (USG U.S. Gauge) ranging between 0 and 4 bar to measure the hydraulic pressure on the FS and DS. Water circulation in the system was maintained using two pumps manufactured by Cole-Parmer, providing up to 5 bar. The conductivity of solutions, the TDS, and the salinity were measured using HQ 14d portable conductivity and TDS meter (HACH, Australia). The turbidity of the solutions was measured using a turbidity meter, HACH 2100P. A digital scale balance connected to a computerized system was used to detect the variation in the DS weight. **Figure 3.3** shows the installation of the FO system used in the experimental work.

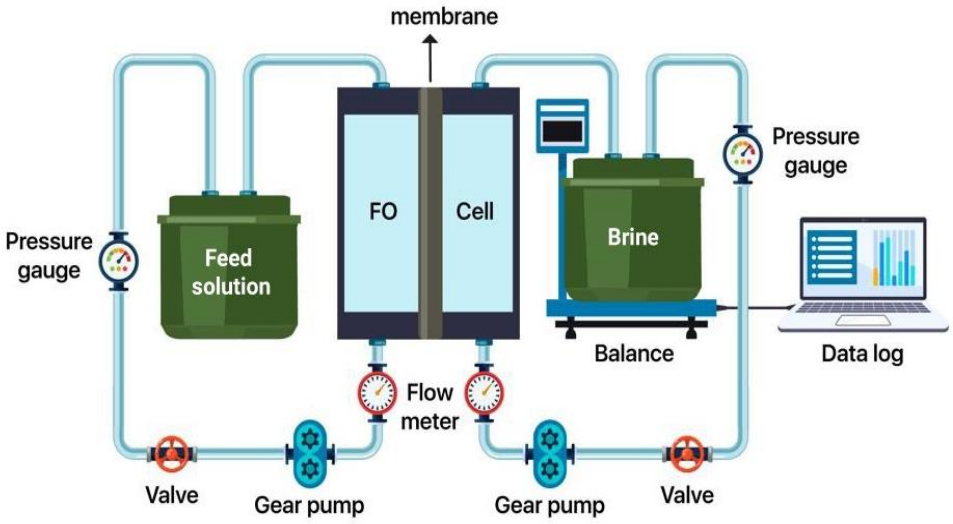

Figure 3.3. An illustration of the FO lab-scale installation.

3.2.5. **Prefiltration**

A microfilter of 20 µm size was used for removing the turbidity and particulate organic matter from seawater and wastewater in selected FO experiments. The filtration was conducted using an HP4750 dead-end stirred cell. A 20-micron Whatman membrane sheet was cut and placed against the porous support disc and sat perfectly without bending or extending outside to avoid leakage. The diameter of the flat sheet is 47-48 mm, with an active membrane area of 17.3 cm^2. The experiments were carried at a constant pressure of 1 bar and 20 °C on the stream solutions.

3.3. Analytical methods

3.3.1. **Intrinsic parameters calculation**

3.3.1.1. *Pure water permeability (A)*

The selectivity of the active layer is explained as selecting the water molecules to penetrate the membrane while rejecting other matters. The selectivity can be quantified by the pure water permeability A (L m^2 /h.bar), which can be calculated in **Equation 3.1** using values determined in standard procedures under specific operational parameters.

$$A_w = \frac{J_w}{\Delta P} \qquad (3.1)$$

J_w is the water flux (L/m^2h), and ΔP (bar) is the osmotic pressure difference between the draw and FSs.

To determine A and B of the FO membranes, an RO test was conducted with DI water FS (23 to 24 °C) with a feed pressure of 1 to 6 bar with 0.5 bar increment to calculate A_w. To adjust the transmembrane pressure, a backpressure control valve was used. Also, to avoid membrane deformation, the AL of the FO membrane was facing the DI water. At first, the hydraulic pressure applied was 6 bar to reach the steady-state of the system. Following the membrane compaction, the next reading was noted after 12 hours, with pressure ranging from 1 to 6 bar. The collected values were used in the equation to calculate A.

3.3.1.2. *Solute permeability (B)*

The back diffusion of the solute t is due to the difference in solute concentrations between the two solutions. The solute transport is an indication of solute permeability (B). B (L/m^{2}h) can be calculated using the equation where values of the variables were obtained from the experiment mentioned above.

$$B = \frac{(1-R_j)}{R_j} exp\left(\frac{-J_w}{k}\right) \qquad (3.2)$$

R_j is the rejection rate, k is the mass transfer coefficient.

3.3.1.3. *Structural parameter (S)*

Since the Support layer of the FO is responsible for the mechanical strength of the active layer, the thickness of this layer as well as its tortuosity and porosity, play a major role in membrane performance. The structural parameter S determine the characteristics of the support layer. S (μm) is usually provided in the manufacturer guideline, or it can be expressed as follow.

$$S = \frac{l\tau}{\varepsilon} \qquad (3.3)$$

Where l (μm) is the thickness, τ is the tortuosity, and ε is the porosity of the support layer (Ibrar et al., 2020b; Kim et al., 2017b; Madsen et al. 2017).

3.3.2.**Basic performance measurement**

3.3.2.1. *Water flux*

The amount of water transferred across the membrane during a period is the permeation flux or water flux J_w (L/m^{2}h). Water flux was calculated, after measuring the variation in weight of the FS during the process, according to the following equation:

$$J_W = \frac{\Delta W}{A.\Delta t} \qquad (3.4)$$

ΔW is the difference in the weight of FS in kg, A represents the membrane area in m^2 and Δt is the time interval in hours (h) (Zhang et al., 2014a).

3.3.2.2. *Flux Reduction*

Flux reduction (FR) was calculated after each cleaning method to study the effectiveness of these methods in water flux recovery. The latter was calculated by applying the following expression:

$$FR = \left(1 - \frac{J_c}{J_f}\right) \times 100 \qquad (3.5)$$

J_c: is average water flux after cleaning, and J_f: average water flux before cleaning.

3.3.2.3. *Reverse solute flux*

The reverse solute flux (RSF) was calculated to understand the behavior of the FO membrane. RSF is the penetration of the solute in the membrane from the DS side towards the FS side, resulting in the difference in the solute concentrations. The values of RSF (J_S, g/m²h) were studied and analyzed according to the following equation

$$J_S = \frac{(Ct.Vt - C0.V0)}{A.\Delta t} \qquad (3.6)$$

C0 and Ct in (g/L): solute concentrations at the beginning and at time t, respectively. V0 and Vt in (L): volumes of the FS measured at the beginning and at time t, respectively, A in (m²): the membrane area, and Δt in (h): the allocated time.

3.3.2.4. *Recovery rate*

The recovery rate is estimated as the ratio of permeate flow to the feed flow according to the following expression:

$$Re = \frac{Q_p}{Q_f} 100\% \qquad (3.7)$$

Where, Q_p and Q_f are the flow rate of permeate and FS (L/min), respectively

3.3.3. **Energy consumption**

To investigate the impact of the FO technique conducted in the experiments, it is important to calculate the specific power consumption (E_s, kW h/m^2) in the standalone FO process as per the following:

$$E_S = \frac{P_f Q_f + P_D Q_D}{n Q_p} \qquad (3.8)$$

Regarding the prefiltration step, the energy consumed in the prefiltration method that can be added, when appropriate, to the FO process was calculated using the expression below:

$$E = \frac{P_f Q_f}{n Q_p} \qquad (3.9)$$

P_f: wastewater hydraulic pressure in bar, Q_f : FS flow rate in m^3/h, P_D: brine hydraulic pressure in bar, Q_D: DS flow rate in m^3/h, n= 0.8: the pump efficiency, Q_p : permeation flow in m^3/h.

3.3.4. **Ions count measurements**

At the beginning and the end of each FO run, the concentrations of Ca^{2+} and Mg^{2+} in the brine solution were measured using an ion chromatography machine 7900 ICP-MS provided by Agilent technologies. The concentrations of SO_4^{2-} were measured using Dionex VWDIC manufactured by HPIC. All the ion concentrations were reported, and the reduction percentage was calculated and presented separately for each ion in the FO experiments.

3.3.5. **Fouling detection techniques**

3.3.5.1. *SEM-EDS analysis*

Scanning electron microscopy (SEM) effectively analyzes organic and non-organic matter on nano and micrometre scales. Coupling the SEM with the Energy Dispersive X-ray Spectroscopy (EDS) can provide images with fundamental information on the composition of the fouling materials. An energy-dispersive spectrometer is an instrument used to determine EDS. This study took SEM and SEM-EDS images of new membranes, fouled membranes, and washed

membranes when appropriate. Specialized images showing fouling materials are produced using the SEM Quanta device.

3.3.5.2. *FTIR spectroscopy*

FTIR (Fourier transform infrared) technique has been applied widely to identify the functional groups of the foulants on the membrane by attenuated total reflection (ATR). In other words, inorganic and organic fouling compounds that absorb the radiation-specific compound can be characterized by FTIR spectra. Both membrane layers of the fouled and washed membranes were scanned using an FTIR scanning microscope and later compared to a new membrane's spectra.

Chapter 4: Performance of the Pressure-Assisted Forward Osmosis-MSF Hybrid Desalination Plant

This chapter is based on the following publication.

Khanafer, D., Yadav, S., Ganbat, N., Altaee, A., Zhou, J. and Hawari, A.H. 2021b. Performance of the Pressure Assisted Forward Osmosis-MSF Hybrid Desalination Plant. Water 13(9), 1245.

Abstract

An osmotically driven membrane process was proposed for seawater pretreatment in a multi-stage flashing (MSF) thermal plant. Brine reject from the MSF plant was the draw solution (DS) in the forward osmosis (FO) process in order to reduce chemical use. The purpose of the FO process is to remove divalent ions from seawater prior to thermal desalination. This study used seawater at 80 g/L and 45 g/L concentrations as the DS and FS, respectively. The temperature of the brine reject (DS) was 40 °C and of seawater was 25 °C. Commercial thin-film composite (TFC) and cellulose triacetate (CTA) membranes were evaluated for the pretreatment of seawater in the FO and the pressure-assisted FO (PAFO) processes. Experimental results showed 50% more permeation flux by increasing the feed pressure from 1 to 4 bar, and permeation flux reached 16.7 L/m^{2}h in the PAFO process with the TFC membrane compared to 8.3 L/m^{2}h in the PAFO process using CTA membrane. TFC membrane experienced up to 15% reduction in permeation flux after cleaning with DI water, while permeation flux reduction in the CTA membrane was >6%. The maximum

recovery rate was 11.5% and 8.8% in the PAFO process with TFC and CTA membranes, respectively. The maximum power consumption for the pretreatment of seawater was 0.06 kWh/m^3 and 0.1 kWh/m^3 for the PAFO process with a TFC and CTA membrane, respectively

4.1. Introduction

Seawater desalination has become a strategic source of clean water worldwide, specifically in the Middle East, where the natural resources are limited (Intelligence et al., 2011; Yadav et al., 2020c). Reverse Osmosis (RO) represents the primary membrane technology for desalination. In contrast, thermal technologies are mainly Multi-Stage Flushing (MSF) and, to a less extent, Multi-Effect Distillation (MED) (Al-Karaghouli and Kazmerski, 2013; Gilron, 2014; Nassrullah et al., 2020). Despite RO being more energy-efficient (Qasim et al., 2019), thermal desalination is still prominent in the Middle East, especially in the Gulf countries, due to their high performance in treating FS of high salinity and low-quality, reliability, and no need for intensive pretreatment of FS (Mabrouk, 2013; Nassrullah et al., 2020; Yadav et al., 2020b). Hence, thermal desalination is responsible for 70% of the total freshwater supply in the Middle East (Mabrouk, 2013). Besides that, thermal desalination plants produce high-quality drinking water; nevertheless, they suffer from scale formation on the heat exchangers, which is one of the drawbacks that affect the efficiency of the desalination process (Nassrullah et al., 2020). At elevated temperatures, alkaline scales such as calcium carbonate ($CaCO_3$) and non-alkaline such as calcium sulfate ($CaSO_4$) and magnesium sulfate ($MgSO_4$) deposit on the heat exchangers, causing a reduction in the heat transfer rate and therefore lowering the plant's efficiency. Scale precipitation adversely impacts the performance of thermal desalination plants and the energy requirements for desalination (El Din et al., 2002; Hassan, 2006). Periodic cleaning and antiscalants are often applied to minimize scaling problems; however, they cannot prevent it (Mabrouk, 2013), particularly the non-alkaline scale in the MSF plants, which requires regular shutting down of the MSF plant for cleaning (Lyster et al., 2010). Recently, FO was suggested for the pretreatment of seawater to the MSF plants to remove multivalent ions, causing scale problems. When coupling the FO process with the MSF, the MSF brine

concentrate will be used as the DS for the FO process in order to reduce the operation cost (Altaee et al., 2014a). The feed water in the FO process is seawater that would be pretreated to remove divalent ions (**Figure 4.1**). The purpose of the FO process is to dilute the concentration of divalent ions in the brine reject before recycling to the MSF unit to minimize/prevent the precipitation of magnesium sulfate and calcium sulfate on the surface of heat exchanger tubes. Previous research revealed the viability of applying the FO process in minimizing scale problems and increasing the top brine temperature (TBT) in the MSF plants (Altaee et al., 2014a; Thabit et al., 2019). It is noticeable that research on the FO technology for the treatment of seawater to MSF/MED systems is scarce, and more work is required to understand the role of membrane materials and applied feed pressure on the FO process (Yadav et al., 2020c).

Driven by the osmotic pressure gradient across the membrane, FO was introduced as a pretreatment process in the cycle of the MSF desalination plant (Altaee et al., 2014a). The proposed innovation in the model is that the brine rejected from the MSF plants plays the role of DS in the FO process and the seawater, in turn, is used as the FS. The outcome is promising in minimizing the concentration of multivalent ions in the feed water to the MSF plant. The diluted brine will return to the MSF system as a lower salinity FS with the potential to reduce scale deposition and allow the MSF plant to work at elevated TBT. Moreover, the proposed FO-MSF system might solve the issue of hot brine rejection to the sea and reduce the seawater intake. The FO-MSF system was theoretically designed, and its feasibility has been investigated to reveal a potential reduction in Ca^{2+}, Mg^{2+} and SO_4^{2-} ions concentrations (Altaee et al., 2014a).

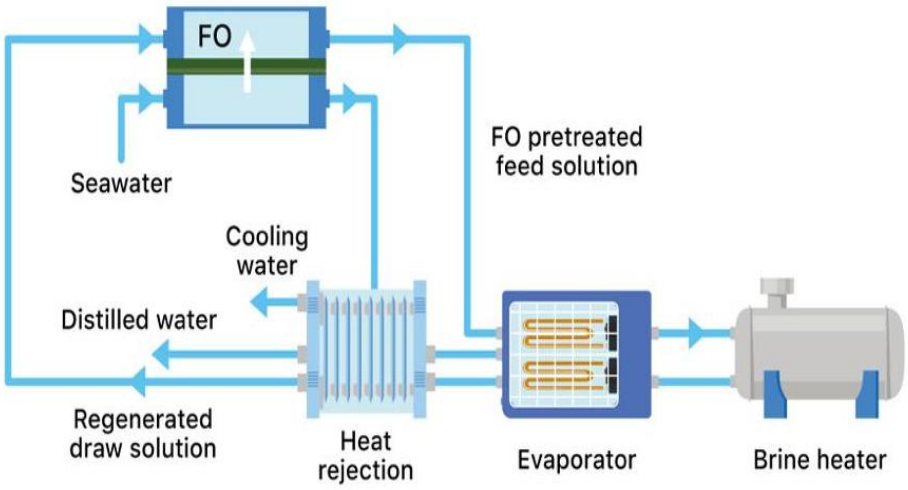

Figure 4.1. Schematic diagram illustrating the proposed FO pretreatment of seawater to the MSF plant.

Although theoretical studies underpinned the potential of the FO-MSF system, there were only a few experimental studies in this field. Thabit et al. (Thabit et al., 2019) studied the efficiency of the FO technology for seawater treatment using cellulose triacetate FTSH_2O membrane and actual brine reject DS at 40 °C. The FO membrane tested in the PRO mode (DS-AL) achieved 22.3 L/m^{2}h permeation flux exceeded and 8.5% dilution of the DS brine at the end of the experiment. The study outcomes formed a foundation that needs building upon with more experiments to investigate and evaluate the adoption of the FO-MSF system in the Middle East. The membrane materials and operating modes also affect membrane fouling propensity and permeation flux (Lee, 2020; Li et al., 2020). To understand the impact of membrane materials, researchers investigated the impact of membrane materials on the efficiency of the FO process (Chung et al., 2012; Mazlan et al., 2016; Yadav et al., 2020c). A study investigated the efficiency of the FO technology in CTA and TFC membranes, revealing that the permeation flux in the TFC was greater than that in the CTA membrane (Chung et al., 2012). Previous work also examined the impact of operating parameters on the efficiency of the FO process. A study by Alaa et al. (Hawari et al., 2016) evaluated the impact of the temperature of the stream solutions on the FO process. It revealed that permeation flux could be increased when the temperature of the DS

increased from 20 to 26 °C. Although the permeation flux in the FO technology is mainly driven by the osmotic pressure gradients across the membrane, several studies tested pressure-assisted FO (PAFO) to improve the permeation flux and tackle the influence of concentration polarization (CP) on the membrane (Blandin et al., 2013; Linares et al., 2014). The concept of PAFO consists of applying low feed pressure to increase the permeation flow under the effect of both osmotic and hydraulic pressures (Coday et al., 2013) since the AL-FS orientation is known for causing severe dilutive internal concentration polarization (ICP). A study by Jamil and co-workers evaluated the feasibility of PAFO for treating RO brine. The results showed a 2% and 29% increase in the permeation flux by applying 2 and 4 bar, respectively (Jamil et al., 2016).

The current study evaluated the performance of the PAFO process in the pretreatment of seawater to the MSF plant owing to its energy efficiency (Van der Bruggen and Luis, 2015). A seawater brine of 80 g/L concentration and 40 °C was the DS in the FO process to resemble the concentration and temperature of the MSF brine reject in the Middle East. The FS in the FO membrane was seawater of 45 g/L concentration and 25 °C representing seawater conditions in the Middle East. Also, there is no information available yet on the influence of membrane materials on the performance of the FO-MSF system, knowing that both TFC and CTA FO membranes are commercially available. Porifera TFC and FTSH_2O CTA membranes were tested to determine the influence of membrane materials on the efficiency of the FO process and permeation flux recovery after membrane cleaning. Both membranes were tested in the AL-FS and AL-DS modes/orientations using 0 to 4 bar feed pressure. Previous studies showed discrepancies in the process efficiency when it operates under different membrane orientations (Ibrar et al., 2020b; Thabit et al., 2019). The permeation flow, the rejection rate of Ca^{2+}, Mg^{2+} and SO_4^{2-} ions, and the process recovery rate were calculated in the FO and the PAFO processes for TFC and CTA membranes. The study also estimated the specific power consumption for the CTA and the TFC membrane.

4.2. Methodology

4.2.1. **FO membranes and characterization**

Porifera TFC and FTSH_2O CTA membranes were implemented in this study to test their performance under different operating parameters. As shown in **Table 3.2, Chapter 3** and referring to the manufacturer guideline, the TFC membrane from Porifera has a structural parameter (*S*) of 344 microns. The membrane can tolerate pressure up to 12.41 bar, 40 °C feed temperature and salt rejection capability up to 90% (Blandin et al., 2016b). Similarly, the datasheet from FTSH_2O summarised the characteristics of the CTA presented in **Chapter 3, Table 3.2** (Madsen et al., 2017). This membrane can tolerate up to 50 ˚C feed temperature and hydraulic pressure of 5 bar.

A and B were calculated using **Equations 3.1** and **3.2,** mentioned in **Chapter 3**. The Values of A and B presented in this paper were also reported in previous studies (Madsen et al., 2017). Wettability measurements and hydrophilic behaviour of the virgin Porifera TFC and FTSH_2O CTA membranes were investigated by measuring the contact angle using the sessile drop method at various places on the same membrane, and it is measured using FACE Automatic Interfacial Tensiometer (Japan) (Yadav et al., 2020a). Images of water contact angle measurement are represented in **Chapter 3, Figure 3.2.** The surface morphology of the used and cleaned membranes for the AL-DS direction was obtained using a scanning electron microscope (SEM, Zeiss Supra 55VP). In addition, SEM was performed to locate and analyse the fouling materials. SEM images were taken on fouled and washed membranes in both AL and SL. Before characterisation, all the membranes were washed with deionized (DI) water and subsequently dried in a vacuum chamber. Using Malvern instruments, Zeta potential measurements were carried out for virgin Porifera TFC and FTSH2O CTA membranes. The wettability of membranes measures the wetting angle between the interface of the surface of the water and the outline of the membrane surface. The active layer (AL) of the Porifera TFC and FTS*H₂O* CTA membrane shows almost an equal water contact angle ~68.5 and 68.1, respectively. As for

the support layer, Porifera TFC showed a lower water contact angle, ~53.9, than the FTSH_2O CTA membrane, ~60.2 (**Chapter 3, Figure 3.2**).

4.2.2. Feed and Draw solutions

In this study, fresh seawater was collected from the Sydney area with a salinity of 32g/L and concentrated by heating to increase its concentration to the level of brine reject and seawater from the MSF plants. In all experiments, the concentration of the FS was 45 g/L, and the DS was 80 g/L. Also, the temperature of FS was 25 °C, and the DS was 40 °C to resemble the temperature of brine reject (Thabit et al., 2019). As a primary step, seawater was stored in containers and left for at least two days for the large particles to settle. (**Table 3.1, Chapter 3**) shows the compositions and characteristics of the FS and the DS used in the experimental work.

4.2.3. FO system components

In Chapter 3 (Section 3.2.4), the laboratory set-up is described in detail and presented in **Figure 4.2**.

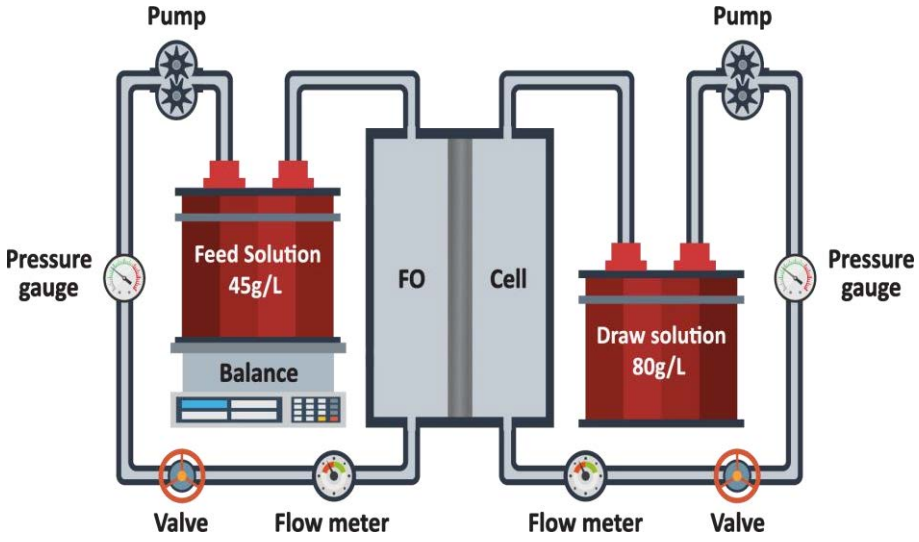

Figure 4.2. FO bench-scale unit configuration used in the seawater-brine FO and PAFO experiments.

4.2.4. **Experimental work**

Each run of the FO process lasted 5 hours, and each membrane was washed with DI water for 30 minutes at the end of the process before using it in the next run. For all FO processes, permeation flux collected in the first 10 minutes was discarded until the membrane filtration process was stabilized. The first set of FO tests was designed to calculate permeation flux at a hydraulic pressure gradient equals to zero (ΔP=0), and then a feed pressure in a range of 1 to 4 bar was applied in the PAFO process. Divalent ions, Ca^{2+}, Mg^{2+} and SO_4^{2-} concentrations were measured before and after each experiment.

Permeation flux in L/m^2h was calculated after measuring the variation of the weight of the FS during the process according to **Equation 3.4** (**Chapter 3**) (Zhang et al., 2014a).

At the beginning and the end of each FO run, the concentrations of Ca^{2+} and Mg^{2+} in the DS were measured using an ion chromatography machine 7900 ICP-MS provided by Agilent technologies. The concentrations of SO_4^{2-} were measured using Dionex VWDIC manufactured by HPIC. These three ions were the only ions studied and measured in this study as they are accountable for the non-alkaline scale development in the MSF plants in the form of $MgSO_4$ and $CaSO_4$ (Tang et al., 2010). Reducing the concentration of the mentioned ions in the DS using the FO process will help control scale formation and depositions using a diluted FS in the MSF process (Hawari et al., 2016).

4.3. Results and Discussions

4.3.1. **Impact of membrane materials and orientations**

4.3.1.1. *Permeation flux*

The impact of applying hydraulic pressures on the FS side was investigated in terms of permeation flux. The first set of experiments measured permeation flux at feed pressure between 0 and 4 bar for 5 hours in the AL-FS mode, and both membranes (TFC & CTA) were tested for this orientation. In the PAFO experiments, a feed pressure between 1 and 4 bar with a 1 bar interval was

applied to the FS. The DS and the FS temperature was 40 °C, and 25 °C, respectively, representing the temperature of the brine reject from the MSF plant and the seawater in the Middle East (Thabit et al., 2019). **Figures 4.3A and 4.4A** present the variation in the permeation flux throughout 5 hours of tests at different applied pressures on the FS in the AL-FS mode for the TFC and the CTA membranes, respectively. Results also show that permeation flux at 0 bar was around 7.4 L/m^{2}h compared to 14.8 L/m^{2}h at 4 bar for the TFC FO membrane and 6.4 L/m^{2}h and 8 L/m^{2}h at 0 and 4 bar, respectively, for the CTA FO membrane. Indeed, increasing the feed pressure from 0 to 4 bar resulted in 50% more permeation flux in the TFC membrane and 25% more permeation flux in the CTA membrane.

The thicker support layer of the CTA membrane might lead to an intense ICP, which reduced permeation flux compared to the TFC membrane with a 50% thinner support layer (**Table 3.2, Chapter 3**). Generally, results show a drop in the permeation flux over time because of the concentration of the FS and the dilution of the DS, which caused a sharp drop in the osmotic driving force and lowered the permeation flux (Thabit et al., 2019). There is a remarkable decline in permeation flux over time, particularly in the PAFO test performed with a TFC membrane. The decline in the permeation flux when using TFC was quick in the first 30 minutes and became steady until the end of the experiments. The drop in the permeation flux in the CTA membrane was gradual throughout the 5 hours of tests. For example, there was a 22.6% and 19.9% reduction in the permeation flux in the FO tests with TFC and CTA membranes, respectively. Indeed, there was a 65% and 27% decrease in the permeation flux in the PAFO tests at 4 bar feed pressure with the TFC and CTA membranes, respectively. This decrease in permeation flux is probably due to the higher permeation flux in the TFC membrane that caused a sharp fall in the osmotic driving force in the PAFO tests. The TFC membrane from Porifera achieved higher permeation flux in the FO and PAFO tests in comparison with the CTA membrane, knowing that higher permeation flux was recorded in the PAFO tests. The results suggested that higher dilution of the brine reject (DS) would be accomplished in the PAFO test using the Porifera TFC membrane in the AL-FS orientation (**Figure 4.3A**).

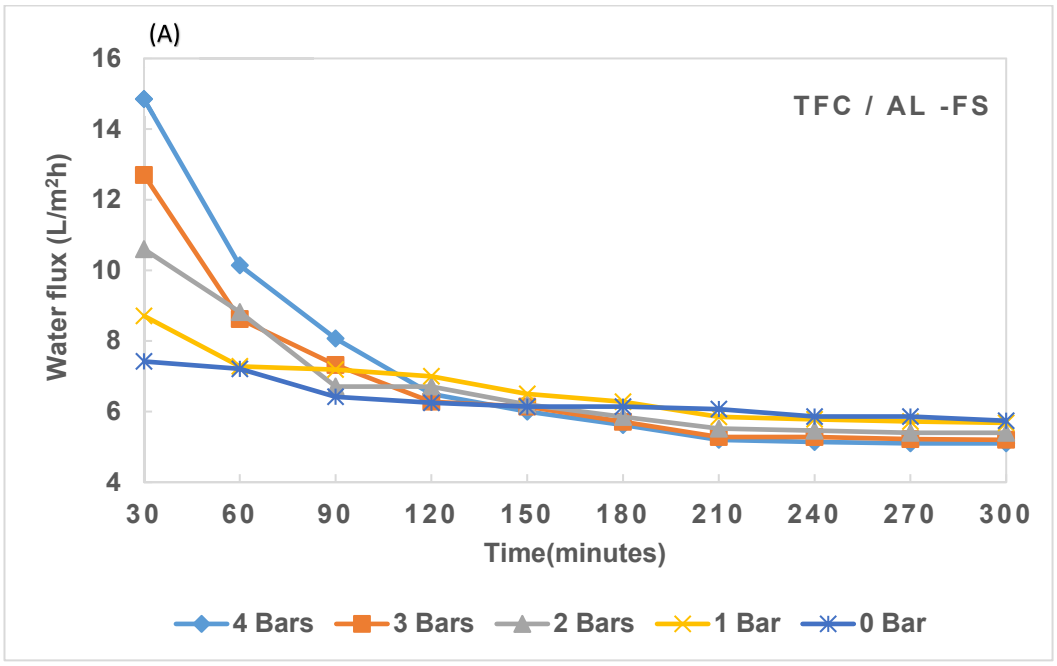

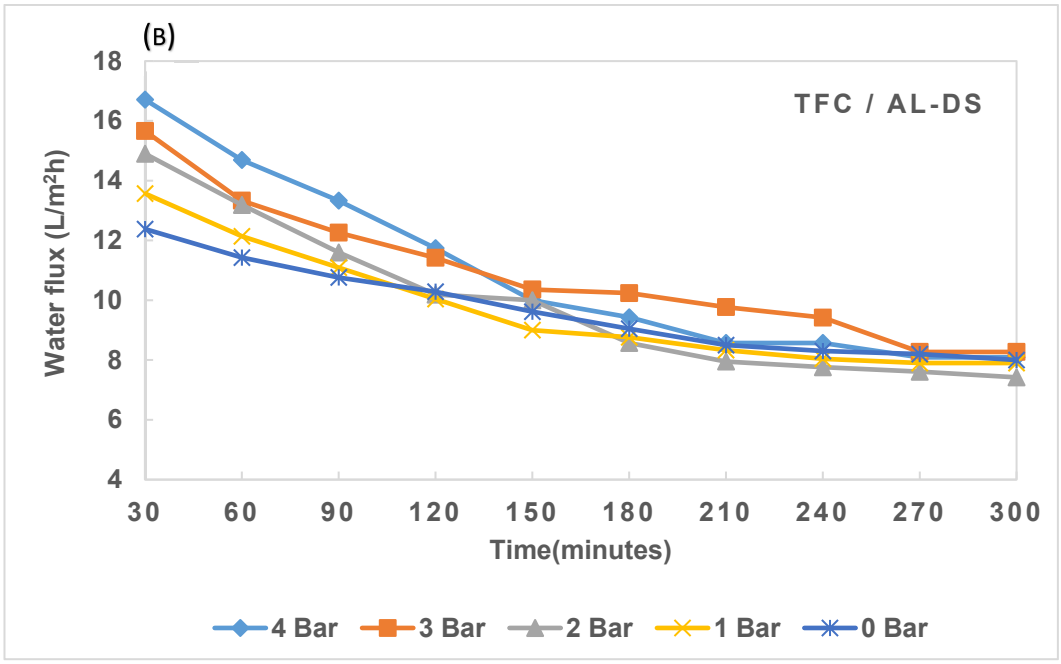

Figure 4.3. Permeation flux of the FO process over the operating time at applied hydraulic pressures between 0 and 4 bar using TFC membrane in (A) AL-FS and (B) AL-DS orientations.

In the next set of experiments and under the same conditions, both types of membranes were tested with AL facing the DS and results are presented in

Figures 4.3B and 4.4B, respectively. These two graphs illustrated the profile of permeation flux in the FO and PAFO tests when the AL-DS mode was applied using TFC and CTA membranes. What is noticeable on a large scale is that a greater permeation flux was achieved in all experiments tested in the AL-DS mode compared to the AL-FS operating mode. According to **Figures 4.3A and 4.3B**, the permeation flux in the TFC membrane tested in the AL-FS at 0 bar feed pressure was 7.4 L /m^2h. In contrast, the permeation flux was 12.4 L/m^2h in the membrane tested in the AL-DS. Permeation flux increased by 67% by altering the membrane mode from the AL-FS to the AL-DS, indicating that more permeation flux and dilution of the brine reject DS were achieved. For the PAFO process at 4 bar feed pressure using a TFC membrane, the permeation flux in the Al-FS direction was 14.8 L /m^2h. At the same time, it was 16.7 L/m^2h in the PRO mode, recording more than a 12% increase in the permeation flux after changing the membrane orientation. For the CTA membrane at 0 bar, there was a 29% increase in permeation flux by altering the orientation of the membrane from the AL-FS to the AL-DS mode (**Figures 4.4A and 4.4B**). In contrast, there was 34% more permeation flux in the CTA membrane operating at 4 bar due to altering the orientation from the AL-FS to the AL-DS mode. The results are compatible with previous studies in which FO membrane operating in the PRO mode exhibited greater permeation flux; there was an agreement in these studies that CP is lower and more controllable in the AL-DS mode (Hawari et al., 2018; Hawari et al., 2016; Mazlan et al., 2016; Tang et al., 2010; Xu et al., 2010).

Furthermore, the permeation flux was higher in all the experiments using the TFC membrane than when CTA membranes were used. For example, the TFC membrane tested in the AL-FS (**Figure 4.3A**) at 0 bar exhibited 83% more permeation flux in comparison with the CTA membrane tested in the AL-FS direction (**Figure 4.4A**). Results also showed that at 4 bar feed pressure, the permeation flux in the TFC membrane tested in the AL-DS direction was 54% more than that in the CTA membrane tested under the same operating conditions. This is due to the hydrophilicity of the TFC membrane and its thinner support layer (**Table 3.2, Chapter 3**), which led to a higher permeation flux in the TFC membrane. Another probable reason for the higher permeation flux in the TFC

membrane in AL-DS is the higher hydrophilicity of its support layer that promoted the permeation and diffusion of the FS to the DS (**Figure 3.2, Chapter 3**).

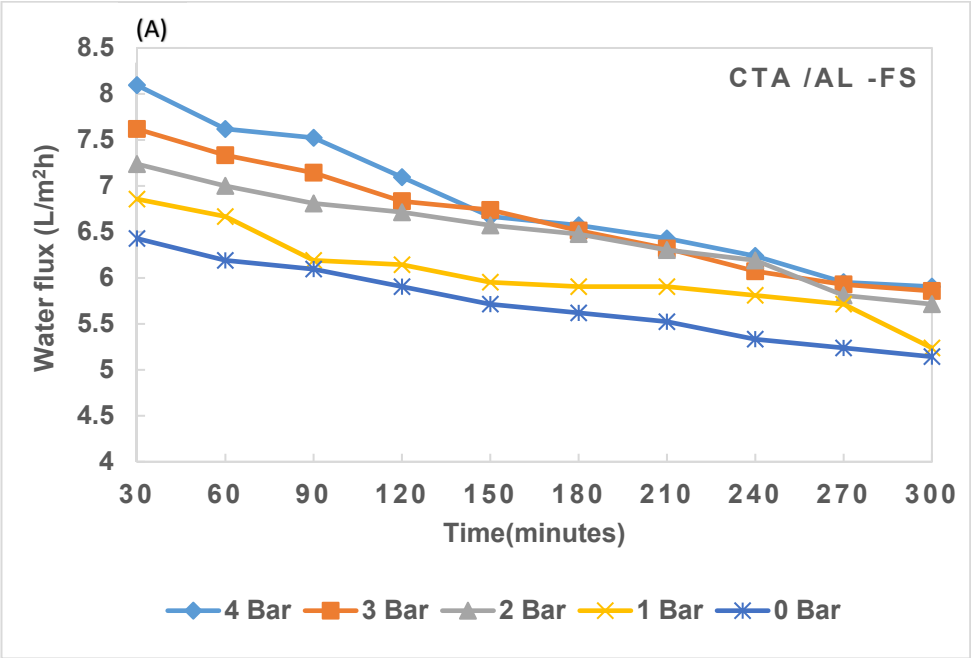

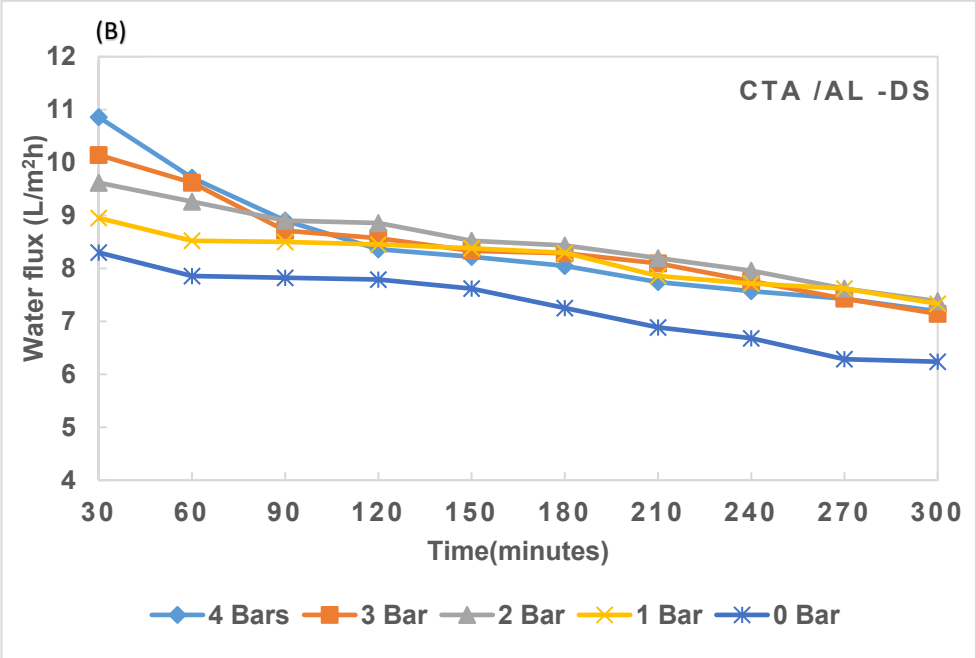

Figure 4.4. Change of permeation flux with time at different applied pressures using CTA membrane, (A) AL-FS and (B) AL-DS orientations.

Reduction in the permeation flux due to membrane fouling was evaluated for both membranes and under different operational parameters to determine the most efficient type of membrane for the FO-MSF system. Figure 4.5 shows the calculated average permeation flux at 0 to 4 bar feed pressure for both TFC and CTA membranes and in the AL-FS and AL-DS orientations. For the TFC membrane, results show that a maximum average permeation flux of 9.57 L/m^{2}h was achieved at 4 bar hydraulic pressure in the AL-DS direction. Under the same operating conditions, the CTA membrane's maximum reported average permeation flux was 8.4 L/m^{2}h, 12% less than the average permeation flux achieved in the TFC membrane. For the TFC and CTA membrane operating at 4 bar in the AL-FS orientation, there was an 8.6% difference in the average permeation flux favouring the TFC membrane. Compared to the AL-DS mode, the difference in the average permeation flux between the TFC and CTA membrane working in the AL-FS mode was lower. And this was caused by the complexity of the ICP phenomenon, which affected the driving force across the membrane despite the thinner structural parameter of the TFC membrane. In general, permeation flux declined more rapidly in the PAFO process due to the greater permeation flux, which caused a steep decline in the osmotic pressure. A faster decline in the osmotic driving force requires fewer FO modules, which will reduce the capital cost for seawater pretreatment by the FO process.

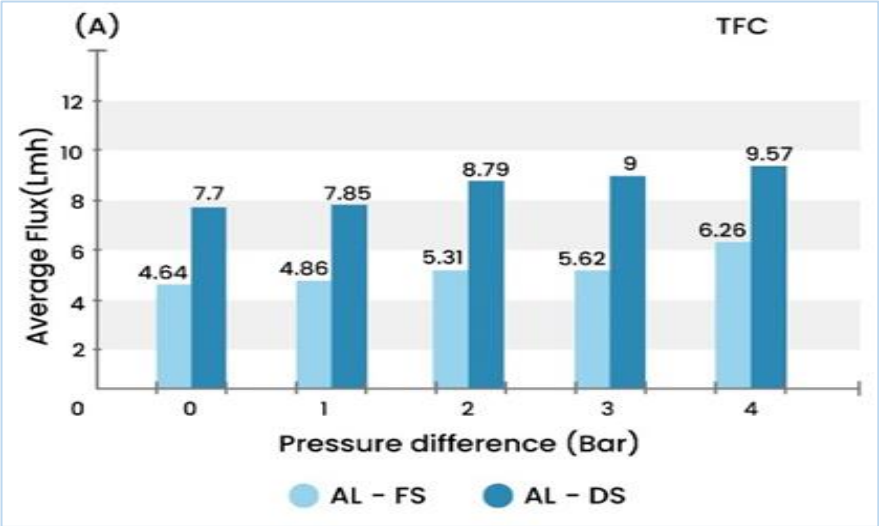

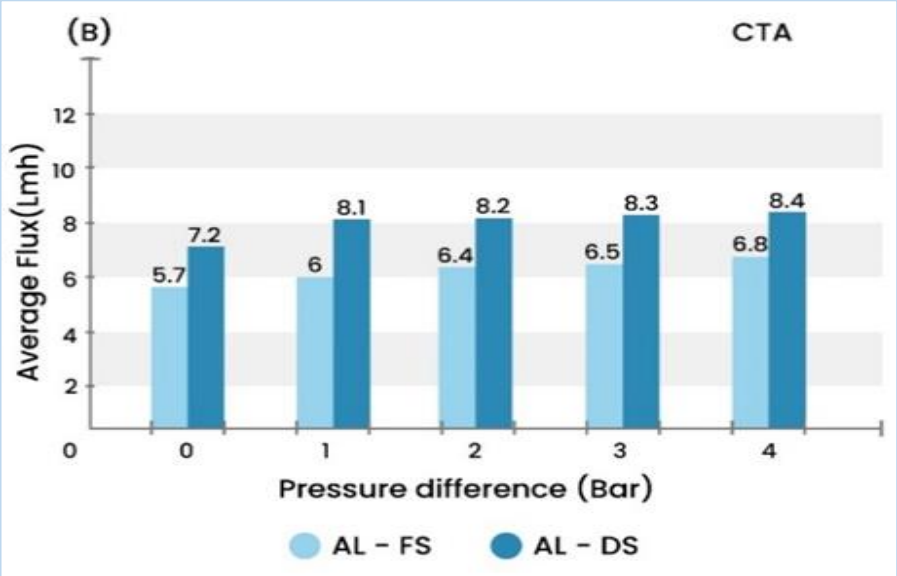

Figure 4.5. The average membrane flux was calculated at different applied pressures of the FO process using (A) TFC membrane and (B) CTA membrane in both orientations, AL-FS and AL-DS.

4.3.1.2. *Flux reduction*

Each used membrane was washed for 30 minutes with DI water at the end of the first test and reused in another run. Then, the permeation flux was estimated at the end of the second test to investigate the reduction in the permeation flux due to irreversible fouling of the membrane. Losses in the permeation flux before and after cleaning with DI water are attributed to the membrane fouling that cannot be removed by simple cleaning with DI water. It is worth mentioning that the DS and FS were not pre-treated before the FO process; hence, fouling would happen on the active and support layer of the membrane. **Table 3.1 (chapter 3)** shows that the DS and the FS turbidity are 2.43 and 1.47 NTU, respectively. The fouling layer on the FS side is expected to be denser due to the build-up of foulants on the membrane surface by the convective flow.

In contrast, permeation flow from towards the DS side will remove loosely attached fouling materials away from the surface in a mechanism similar to that in a backwash cleaning. **Figures 4.6A and 4.6B** show the reduction of

permeation flux in the FO experiment using TFC and CTA membranes, respectively. In the case of the TFC membrane, the reduction in the permeation flux in the FO mode was 5.2% at 0 bar feed pressure and increased to 6.9% at 4 bar feed pressure (**figure 4.6A**). For the TFC membrane operating in the PRO mode, the reduction in the permeation flux was 14.6 % in the PAFO test at 4 bar feed pressure and 10.4 % in the FO test. Apparently, FO tests performed in the PRO mode experienced a higher permeation flux reduction due to poor mixing inside the support layer, reducing the effectiveness of the cleaning process. The permeation flux decline in the PAFO tests was also observed as more severe at elevated feed pressures due to the dense and compacted fouling layer inside the SL.

Similarly, **Figure 4.6B** shows that the CTA membrane's permeation flux reduction was greater at 4 bar feed pressure. In contrast, the TFC membrane exhibited a greater permeation flux reduction than the CTA membrane (**Figure 4.6B**). The highest recorded permeation flux reduction was 5.9% in the FO mode operating at 4 bar feed pressure; this is about 15% less than the reduction in the permeation flux in the TFC membrane tested under the same working conditions. The decline in the permeation flux in the CTA working in the AL-DS direction was three times less than that recorded in the TFC membrane under the same operating conditions. On the contrary, when tested in the AL-DS direction, the CTA membrane demonstrated a lower decrease in the permeation flux. For example, the reduction in the permeation flux at 0 bar feed pressure was 3.2% in the AL-DS and 4.2% in the AL-FS direction. The corresponding results at 4 bar feed pressure were 5% in the AL-DS direction and 5.9% in the AL-FS direction.

The reason for a lower permeation flux reduction in the CTA membrane when the FS was opposite to the SL and experiments with the DS opposite to the SL is attributed to the combined effects of permeation flux in the membrane and the turbidity of FS and DS. The fouling layer was probably denser and compacted when the DS was against the SL due to the accumulation of the fouling materials from the high turbidity DS (2.43 NTU) in the porous SL. Unfortunately, low permeation flux in the CTA membrane aggravates the problem since fouling materials would not be flashed away from the membrane surface by the

permeation flow, especially in the AL-FS mode. For this reason, cleaning with DI water was ineffective in removing the fouling layer accumulated inside the dense SL of the membrane operating in the AL-FS direction. Accordingly, the CTA membrane performed better in the AL-DS direction due to the greater permeation flux (**Figure 4.4B**) while maintaining a lower reduction in the permeation flux. On the contrary, FO mode is the desirable working mode of the TFC membrane because of the high efficiency of the cleaning method in maintaining a low permeation flux reduction. For the TFC membrane, permeation flux in the AL-FS mode at 4 bar feed pressure is almost twice that in the CTA membrane under the same operating conditions.

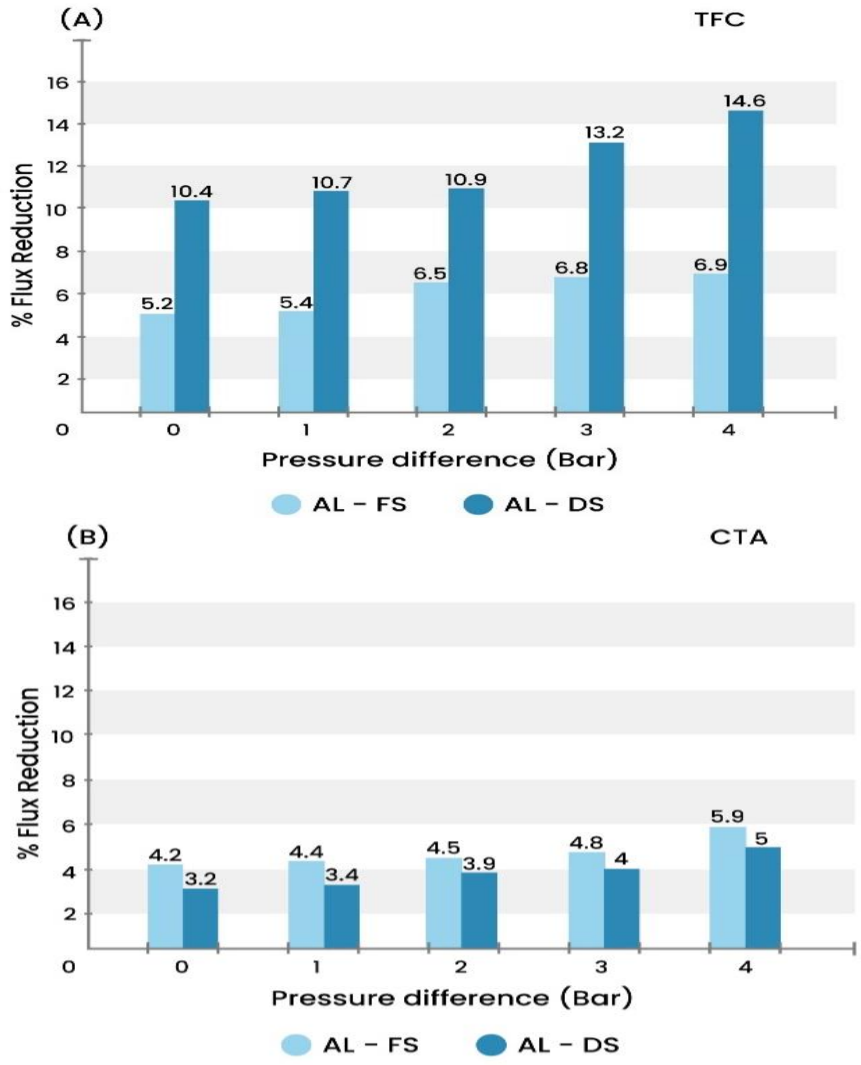

Figure 4.6. Flux Reduction in the FO process at different applied pressures using (A) TFC membrane and (B) CTA membrane in AL-FS and AL-DS orientations.

SEM images (**Figure 4.7**) reveal that the CTA membrane is more responsive to cleaning by DI water than the TFC membrane. A notable change in the morphology of the active and the support layer of used and washed Porifera TFC and FTSH_2O CTA membranes. For the TFC membrane, cleaning with DI water partially removed fouling materials from the active membrane layer. At the same time, it was less successful in removing the fouling layer on the support layer side. Ineffective cleaning with DI water of the TFC membrane explains the high reduction of permeation flux after cleaning. In contrast, cleaning with DI water was more effective in washing the fouling layer off the surface of the CTA membrane. The latter showed little fouling materials left on the washed active layer, and fouling materials became sparse after washing. These results explain the lower reduction in the permeation flux of the CTA membrane obtained after washing.

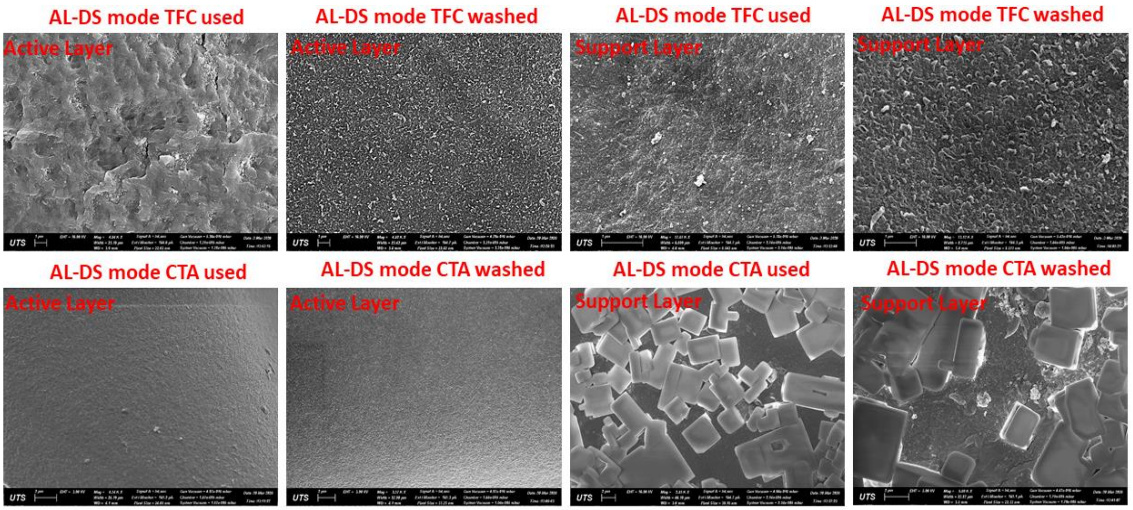

Figure 4.7. SEM images of the active and support layer of used and washed TFC and CTA membranes. Images show the fouling layer in the active and support membrane layers used in the FO process conducted with 2 bar hydraulic pressure.

4.3.2. **Recovery rate**

The recovery rate is estimated as the ratio of permeate flow to the feed flow according to **Equation 3.7** in **Chapter 3**. Results show that the water recovery rate was higher in the AL-DS orientation due to the greater permeation flux. **Figure 4.8** also revealed that the recovery rate in the FO process was greater at

4 bar feed pressure. TFC membrane achieved higher recovery rates than the CTA membrane due to higher membrane permeability and thinner structure parameter, which lessened the impact of CP inside the support layer (**Table 3.2, Chapter 3**). The TFC membrane achieved the highest recovery rate of 11.48% at 4 bar feed pressure in the AL-DS direction (**Figure 4.8A**). As for the CTA membrane, the highest recovery rate was 10.05% in the PRO mode at 4 bar (**Figure 4.8B**). Changing the orientation of the membrane from the AL-FS to the AL-DS orientation led to a more than 50% increase in the recovery rate. The increase in the recovery rate could be attributed to the greater permeation flux and low ICP. When it is compared with the CTA membrane, the TFC membrane achieved greater permeation flux and recovery rate at 4 bar feed pressure. The desirable operating mode for the TFC membrane is the AL- FS direction since such membrane orientation assures lower permeation flux reduction after cleaning with DI water only (**Figure 4.6A**). For the TFC membrane, results in **Figure 4.8A** shows that 93.1% of the permeation flux was recovered in the FO test at 4 bar while 94.8% of the permeation flux was recovered in the FO tests at 0 bar. However, the latter operating conditions resulted in ~66% lower permeation flux in comparison with the FO process at 4 bar. Therefore, the FO process performed better in the AL-FS mode at 4 bar feed pressure using TFC membranes.

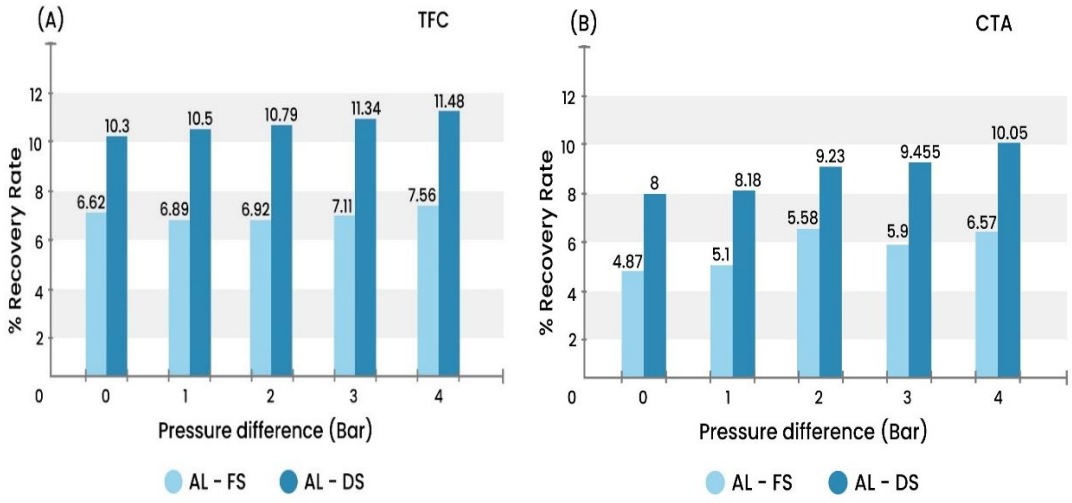

Figure 4.8. Recovery rate (%) of FO process at different applied pressures, using TFC membrane (A) and CTA membrane (B). In AL-FS and AL-DS orientations.

4.3.3. **The concentration of Divalent Ions**

It is discussed in the literature that the decrease in the concentration of the scale-causing divalent ions will minimize the formation and deposition of non-alkaline scale on the surface of heat exchanger tubes (Hawari et al., 2016). It is important to mention that ion reduction is the decrease in the concentration of divalent ions in the DS after the pretreatment using the FO process. As mentioned earlier, the concentration of Mg^{2+}, Ca^{2+} and SO_4^{2-} in the DS was measured before and after each FO test to record the concentrations after the FO pretreatment. All ion concentrations were reported, and the percentage of reduction of the ions under different operational parameters is presented separately in **Figure 4.9**.

At first sight, results reveal that applying ascending feed pressure led to an increasing permeation flux and dilution of the DS. Compared to the FO process at 0 bar, up to a four-time higher dilution of the DS was achieved by increasing the feed pressure from 1 to 4 bar. For example, a 6% dilution of Mg^{2+} was achieved by the TFC membrane at 0 bar, but Mg^{2+} dilution increased to 23% at 4 bar, which is four times more than that at 0 bar. For Ca^{2+}, 7% and 24 % dilution was achieved at 0 and 4 bar, respectively, and for SO_4^{2-}, 9% and 28% dilution was achieved at 0 and 4 bar, respectively. There was also a slight increase in the dilution of ions when the membrane was operating in the AL-DS (**Figure 4.9B**) direction in comparison with the AL-FS direction (**Figure 4.9A**) due to the higher permeation flow. Furthermore, the TFC membrane showed a more substantial decrease in the divalent ions due to the higher permeation flux and ions rejection rate. Moreover, it is noticeable that for SO_4^{2-}, the reduction is the highest amongst all other divalent ions, which was attributed to its high rejection by the TFC membrane. When the CTA membrane was operating in the AL-DS direction (**Figure 4.9D**), the dilution of Mg^{2+} was 10% and 21% at 0 and 4 bar, respectively. The dilution of Ca^{2+} was 6% and 25% at 0 and 4 bar, respectively, and it was 7% and 21% for SO_4^{2-} at 0 and 4 bar, respectively. According to the data gathered about ions reductions, it is important to mention that applying 4 bar in the TFC test with AL-FS mode is promising in seawater pretreatment to the MSF plant due to the considerable decrease in the divalent ions and low permeation flux reduction (**Figure 4.6A**).

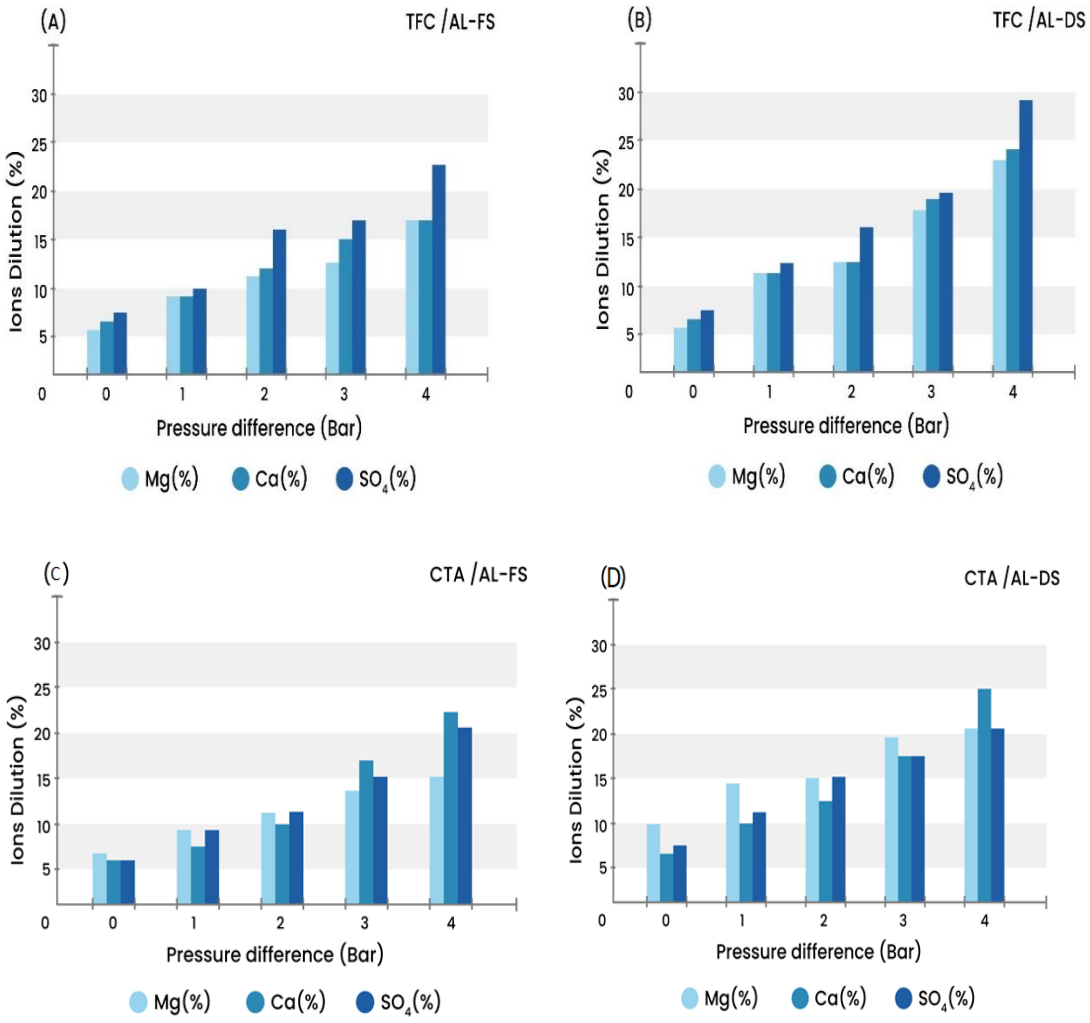

Figure 4.9. Mg^{2+}, Ca^{2+} and SO_4^{2-} dilution in the DS following the FO process at different applied pressures and in FO and PAFO modes using TFC and CTA FO membranes. (A) and (B) TFC membrane in AL-FS and AL-DS orientations, respectively. (C) and (D) CTA membrane AL-FS and AL-DS orientations, respectively.

4.3.4. **Power consumption**

Mathematically, specific power consumption (*Es*-kWh/m^3) can be estimated from the expression **3.8 (chapter 3)**. Figure 4.10 shows *Es* increased when the feed pressure was 4 bar. The results show that *Es* in PAFO tests were higher than in the FO tests. However, it is still low compared to the *Es* required for seawater desalination by RO technology (McGovern, 2014). The highest specific power consumption was 0.1 kWh/m^3 in the CTA membrane operating at 4 bar in the

PRO mode. Results also show that the amount of power consumed in the AL-FS orientation is slightly higher when it is compared with that of the AL-DS direction. For example, the *Es* in the CTA membrane at 4 bar was 0.08 in the AL-FS orientation and 0.1 kWh/m^3 in the AL-DS direction (**Figure 4.10B**). The corresponding values in the TFC membrane at 4 bar were 0.053 in the AL-FS mode and 0.065 kWh/m^3 in the AL-DS orientation (**Figure 4.10A**). According to **Equation 3**, the lower permeation flow in the AL-FS orientation in comparison with the AL-DS orientation caused a slight increase in power consumption. Results show that the highest *Es* in the FO pretreatment process is 0.1 kWh/m^3, while close to 2.5 kWh/m^3 in the RO technology for seawater desalination (McGovern, 2014). For the desirable operating condition with TFC membrane in the FO mode and at 4 bar, the specific power consumption was 0.065 kWh/m^3; this low power consumption underlines the great potential for applying the FO technology as a pretreatment process of seawater to the thermal MSF plant.

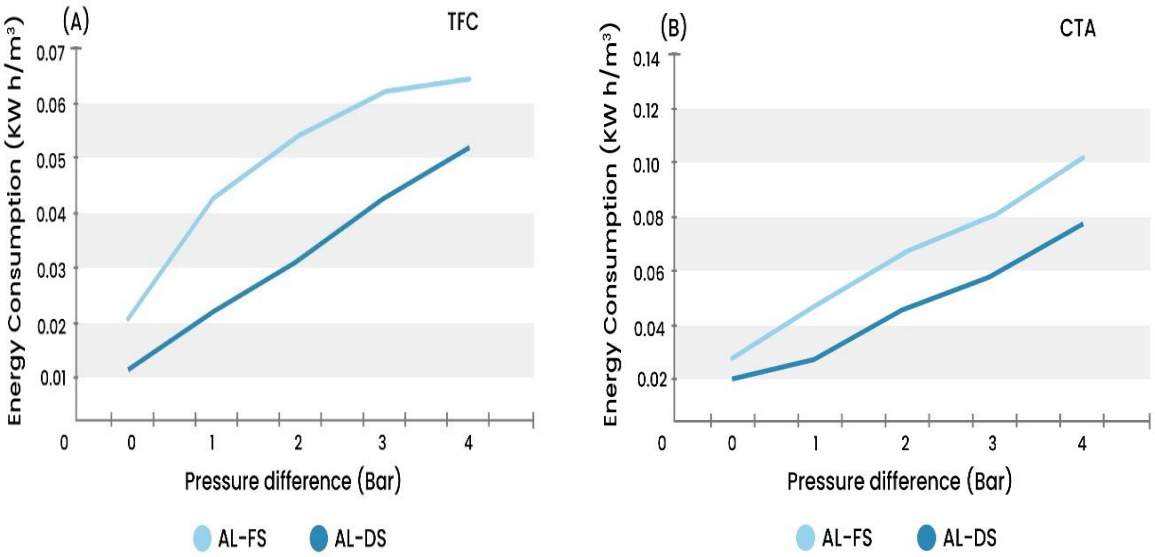

Figure 4.10. Energy consumption at different applied pressures, (A) using TFC membrane and (B) using CTA membrane.

4.4. Conclusions

FO and PAFO processes were tested for the pretreatment of seawater using commercial TFC and CTA membranes. The results showed that applying a small hydraulic pressure on the FS side increased the permeation flux. The permeation flux increased from 7.4 to 14.8 L/m^2 h by increasing the feed pressure up to 4 bar in the PAFO process with TFC membrane in the FO mode and at 4 bar. This significant improvement in permeation flux was achieved at a relatively trivial specific power consumption of 0.06 kWh/m^3 CTA membrane, in general, demonstrated lower permeation flux than TFC at 4 bar pressure, 10.9 L/m^2h, but the specific power consumption was slightly higher than that in the TFC membrane, 0.1 kWh/m^3.

Interestingly, the recovery of permeation flux in the fouled CTA after cleaning is higher than that in the TFC, and this was due to the characteristics of the fouling layer, which is loosely compacted due to the low water flux. Based on its low power consumption and high permeation flux, the PAFO process at 4 bar using TFC membrane in the FO mode would be the preferable operating conditions. After DI water cleaning, the latter operating condition has a considerable permeation flux recovery of 93%. The results reveal the great potential and feasibility of the PAFO process for improving seawater pretreatment for the MSF plant without compromising the advantage of low power consumption.

Chapter 5: Brine Reject Dilution with Wastewater for Indirect Desalination: Converting Wastewater Streams to Water Resources

---

This chapter is published as follows:

Khanafer, D., Ibrahim, I., Yadav, S., Altaee, A., Hawari, A. and Zhou, J. 2021. Brine reject dilution with treated wastewater for indirect desalination, Journal of Cleaner Production,129129.

Abstract

The forward osmosis (FO) process was suggested as a pretreatment to a multi-stage flashing (MSF) plant to reduce the environmental impact of brine discharge and the chemicals used. Yet, there is no study investigating the performance of the FO process pretreatment to the MSF plant using tertiary sewage effluent (TSE) as a feed solution. Combining MSF brine with the TSE generates a considerable permeation flux, reducing the membrane area and capital cost. This study evaluated the performance of the FO process for indirect desalination of the MSF brine, considering membrane fouling, cleaning, required membrane area and the specific power consumption. The FO process used a thin-film composite (TFC) membrane to dilute the brine reject from the MSF plant by the

TSE, converting waste solutions into a feasible water resource. A considerably high water flux (±35 L/m²h) was generated and slightly decreased throughout each experiment's 4 cycles. An enhancement in the water permeability was observed in the FO tests with a prefiltration of the brine reject and the wastewater with 20µm and an osmotic backwash cleaning of the used membrane. The prefiltration of the draw and feed solutions effectively minimised the impact of fouling. Maximum power consumption of 0.007 kWh/m³ was consumed in the forward osmosis process without prefiltration and decreased to 0.006 kWh/m³ in the FO process. The proposed FO system successfully diluted the brine reject' divalent ions, reducing their concentration to 43% in some cases. Depending on the FO membrane orientation, the TSE feed solution resulted in a 276% to 473% reduction in the number of FO elements required in the FO process compared to the seawater feed solution.

5.1. Introduction

Thermal desalination processes are broadly used to desalinate seawater in the Middle East (Mabrouk, 2013; Panagopoulos and Haralambous, 2020). MSF represents one of the main thermal desalination processes in the Gulf region, providing up to 75% of the desalinated water in some countries (Buros, 2000). It has been proposed that maintaining the current MSF plants in better conditions for future use in the long term is less intricate than installing other desalination technologies (Mannan et al., 2019). Researchers in this domain have focused on tackling the in-site issues of the MSF plants due to the high efficiency of the process and its capability to treat elevated salinity FS (Thabit et al., 2019). One of the main issues affecting the MSF plant's performance is the non-alkaline scale fouling caused by calcium sulfate and magnesium sulfate precipitation on the plant's heat exchangers (El Din et al., 2002). Antiscalants, periodic cleaning and membrane technologies were suggested to treat the seawater and minimize the fouling in the thermal plants, but they cannot inhibit it (Mabrouk, 2013). The NF membrane process was proposed for seawater treatment, but experimental and pilot plant results revealed that it is not a cost-effective approach for seawater softening due to the high operation cost of the NF process (Mabrouk et al., 2015). With the NF membrane, 15 to 25 bar are applied to remove magnesium, calcium

and sulfate ions from the FS to the MSF plant. Lately, the FO technique, a membrane separation process, has been investigated to remove scaling ions from seawater (Altaee et al., 2014a; Thabit et al., 2019). In principle, the FO technique relies on the osmotic pressure gradient between the FS and the DS for freshwater extraction across a semipermeable membrane (Cath et al., 2006). The FO technique showed promising results such as low energy consumption, less fouling, a high rejection rate and good water flux. However, the FO process experiences intense concentration polarization during operation, reducing water flux and diluting the brine reject. In addition, the relatively high osmotic pressure of seawater FS is another impediment controlling water flux in the FO process.

The hybrid system (FO-MSF) was proposed to remove undesirable multivalent ions from seawater using the MSF brine as a DS (Altaee et al., 2013). Combining the FO process with the MSF plant will reduce brine discharge to seawater since it will be the DS in the FO membrane for pure water extraction from the FS. Coupling the FO process with the MSF will prevent the thermal pollution caused by brine discharge at 40 °C to seawater and the chemicals used, such as antiscalants and antifoaming, to control scales deposition onto the heat exchanger (Altaee et al., 2013). A wealth of literature discusses the environmental impact of improper treatment of the brine reject and proposes appropriate regulations to control brine discharge (Ariono et al. 2016). Alternatively, researchers proposed brine reject recycling using the FO process. Preliminary results from laboratory tests demonstrated the feasibility of applying this process for seawater pretreatment to the MSF plant (Hawari et al., 2018; Thabit et al., 2019). In laboratory-size experiments using MSF brine as a DS and seawater as an FS, the average water permeability in the FO test was 16.9 L/m^{2}h at 25 °C DS temperature (Thabit et al., 2019). When the temperature on the DS side was 40 ºC, the average water flux reached 22.3 L/m^{2}h. Taking into consideration that 22.3L/m^{2}h water flux was high, a further enhancement in the water flux is always desirable for additional dilution of the DS. In the FO-MSF/MED system, the osmotic pressure between the brine reject and seawater is limited and cannot be increased due to the thermal plant's design conditions that operate at pre-designed top brine temperature (TBT). Recent studies revealed that the FO water flux increased by Brine reject, and tertiary was applied

on the feed side in a pressure-assisted FO (PAFO) process (Khanafer et al., 2021). Using PAFO for brine reject dilution brought an insignificant increase in the specific power consumption due to the higher permeation flow. Nevertheless, higher water flux is still desirable to dilute further the brine reject and ensure scale prevention.

Earlier studies underlined the environmental impact of the brine reject from the MSF on the marine ecosystem when discharged into seawater (El-Ghonemy, 2018; Panagopoulos and Haralambous, 2020). Brine reject contains chlorine, antiscalants, copper residues, and antifoaming agents of detrimental effects on flora and fauna when released into the seawater. The relatively high temperature of the brine reject results in thermal pollution when mixed with seawater. Some studies proposed the discharge of the brine reject into the sewer system. The latter approach would affect wastewater treatment because the brine reject high salinity that inhibits the growth of the microorganisms. Instead of disposal as wastewater, tertiary sewerage effluent (TSE) could be used as an FS in the FO process to treat the thermal plant brine. Despite the severe freshwater shortage in the Middle East, large amounts of TSE are disposed of every day (Yangali-Quintanilla et al., 2011). The TSE salinity is about 1 to 2.6 g/L (Hawari et al., 2018), which is significantly less than the salinity of seawater in the Middle East (45 g/L), indicating its great potential for the dilution of the brine reject. TSE was previously used in the FO process for indirect desalination of seawater (Choi et al., 2017; Yangali-Quintanilla et al., 2011; Zhang et al., 2014b; Zhao et al., 2012). Indirect desalination is an attractive concept in which wastewater streams, such as brine and TSE, are converted into freshwater sources. Victor et al. used secondary wastewater effluent for the dilution of Red Seawater in the FO process to reduce the cost of seawater desalination.

Coupling wastewater effluent with the Red Sea water resulted in a 50% reduction in the specific power consumption for desalination by 50%, around 1.5 kWh/m^3. The study reported a 28.8% water flux decline after ten days due to the FO membrane fouling. However, cleaning with air scouring and freshwater could recover 98.8% of the initial water flux. Another study by Choi et al. studied wastewater reclamation by the FO process using a NaCl (0.6 M) DS to resemble

the concentration of the seawater (Choi et al., 2017). The study used a special thin-film composite (TFC) membrane with functionalized carbon nanotubes (CTN). Results indicated that water flux was lower in the fabricated membrane than commercial TFC membranes. Experimental results also showed the great potential of coupling seawater with treated wastewater effluent for indirect seawater desalination. However, there is no experimental study on treated wastewater application for the dilution of thermal plant brine by the FO process.

The present study is the first experimental work on applying the FO technique to treat brine reject from the MSF plant using treated wastewater as FS (**Figure 5.1a)**. There are several advantages of using brine reject and treated wastewater in the FO process: reducing wastewater disposal to seawater, converting wastewater into a viable source of freshwater and minimizing scale fouling of the MSF thermal plant. Coupling low-salinity wastewater with brine reject at 40 °C can enhance water flux in the FO process and reduce the membrane required in the pretreatment process. The specific power consumption and the membrane elements required in the FO process using a TSE FS were compared with seawater FS. The targeted dilution percentage of the brine reject by the FO process is 14% or higher, corresponding to the recovery rate in the MSF plant operating at a performance ratio equal to 8 (Altaee and Zaragoza, 2014; El-Ghonemy, 2018; Morin, 1993). It also aimed to provide insights into the development of lower energy and cost-saving desalination hybrid systems.

5.2. Materials and experiments

5.2.1. **Stream solutions**

In this study, treated wastewater and brine reject the feed and DS of the FO process, respectively. The Blacktown wastewater treatment plant, Sydney, Australia, provided wastewater samples. The average (triplicate values) concentrations of the wastewater and the seawater brine were presented in **Table 3.1 (Chapter 3)**. The DS's temperature was maintained at 40 °C during the experiments, with 25 °C at the FS's temperature.

In selected FO experiments, a microfilter of 20 μm size was used to remove the turbidity and particulate organic matter from seawater and wastewater. **Table 5.1** shows the turbidity and the total organic carbon (TOC) of the stream solutions before and after microfiltration.

Table 5.1. Comparison of wastewater and brine turbidity and total organic carbon (TOC) before and after microfiltration.

Solution	Turbidity (NTU)	TOC (mg/L)
Wastewater (no prefiltration)	7.1 ± 0.1	49.69 ± 2
Wastewater (with prefiltration)	1.76 ± 0.12	28 ± 1.3
Seawater (no prefiltration)	2.43 ± 0.15	30.6 ± 0.5
Seawater (with prefiltration)	0.9 ± 0.05	9.4 ± 0.2

5.2.2. **Membrane and equipment**

The membrane implemented in the experiments in this study was the TFC FO membrane manufactured by Porifera. The selection of this membrane was based on its potential to achieve high water flux, which is usually attributed to the thin support layer (SL) structure of the TFC membranes that reduce the internal concentration polarization (ICP) (Wang et al., 2015). **Table 3.2 (chapter 3)** summarizes the membrane's chemical and physical characteristics.

Figure 5.1a shows the experimental design of the FO process used in this study, and **Figure 5. 1b** illustrates the wider spectrum of the proposed FO-MSF hybrid system.

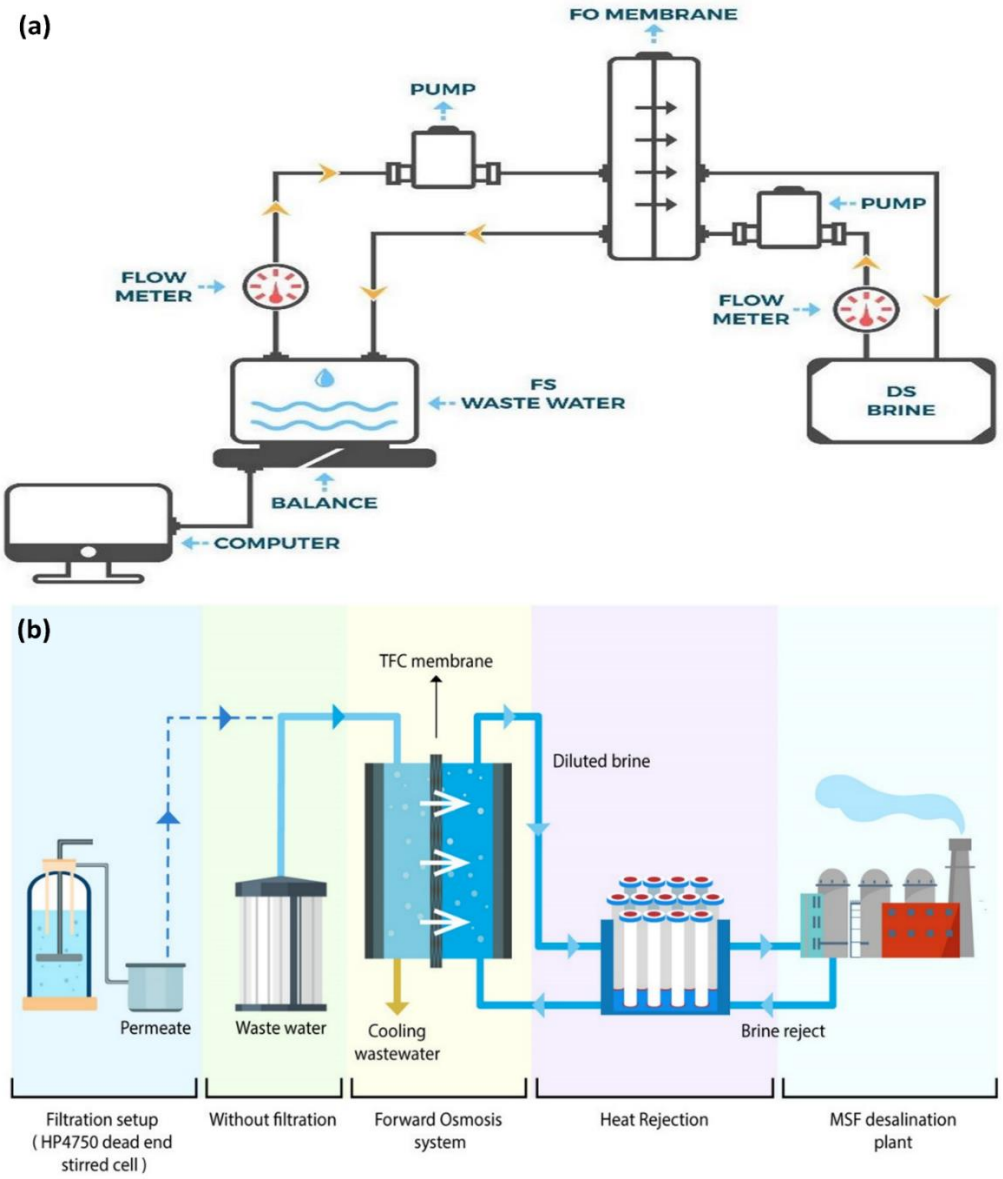

Figure 5.1. (a) Lab-scale experimental design of the FO system. Operational parameters: 2 LPM flow rate, 25 °C and 40 °C on the feed and draw sides, respectively. (b) An illustration of the proposed FO-MSF hybrid system.

5.2.3. **Experimental work**

Brine reject solution was prepared in the laboratory by concentrating seawater on the MSF brine's concentration level in the Middle East. The TSE was supplied by the wastewater treatment plant in Sydney, Australia. The wastewater and brine solution filtration was conducted using the HP4750 dead-end stirred cell. A 20 micron Whatman membrane sheet was cut and placed against the porous

support disc and sat perfectly without bending or extending outside to avoid leakage. The diameter of the flat sheet is 47-48 mm, with an active membrane area of 17.3 cm^2. All the prefiltration experiments were carried out at a constant pressure of 1 bar and 20 °C.

Each FO experiment was operated for 180 min, membrane washed for 30 min and then repeated 3 times to make 4 cycles in total for each experiment. The volume of wastewater and brine reject was 5 L at the start of each experiment, while the temperature was 25 °C and 40 °C, respectively. A constant flow rate of 2 LPM was used in the FO cell using the Porifera TFC FO membrane. Each experiment started with a new TFC membrane, the latter was soaked in DI water for 30 min before the first cycle, and at the end of each cycle, the membrane was cleaned and reused for the other 3 cycles. In **Table 5.2**, a summary of the experimental work is provided; each experiment was run 4 times using the same membrane following the same cleaning method. In all experiments, one variable was changed at a time, and its impact on the FO performance was investigated. In the FO filtration experiments, the FS and DS prefiltration and membrane orientation were the variables to investigate their impact on water flux, ions rejection, reverse salt flux, specific power consumption, and membrane fouling. In Exp1, AL-DS was the membrane orientation, and both layers were cleaned at a flow rate of 2 LPM with 40 °C DI water for 30 min. Experiments 1, 3, 5 &7 were run in the AL-DS orientation and Exp2, 4, 6 & 8 in the AL-FS mode. Exp1-4 was performed without the prefiltration of feed and DSs, while Exp5-8 was with prefiltration. In Exp2 and 4, membranes were cleaned with 40 °C DI water and a 3 LPM flow rate. The DS and the FS prefiltration were done in Exp5 and 7, and both membranes were washed with DI water at a 3 LPM flow rate.

Similarly, for Exp6 and Exp8, filtered streams were used in the FO experiment. The flow rate of the cleaning solution and osmotic backwash were varied in the cleaning process to evaluate their impact on water flux recovery. The membrane backwashing was performed with 40 g/L NaCl solution at 40 °C and 3 LPM flow rate on the SL of the membranes and DI water at 40 °C and 3 LPM flow rate on the AL. The strategy of backwashing with NaCl showed promising results as it helps remove foulants from the membrane's SL pores (Yu et al., 2017). In the

MSF desalination plant, a 40 °C temperature could be obtained from the brine reject using a heat exchanger.

Table 5.2. Summary of the operational conditions applied in the experiments conducted in this study.

Experiment (Exp)	Membrane orientation	Cleaning (30min,40°C)		FS & DS treatment
		Active layer	Support layer	
1	AL-DS	DI water, 2LPM	DI water, 2LPM	-
2	AL-FS	DI water, 2LPM	DI water, 2LPM	-
3	AL-DS	DI water, 3LPM	DI water, 3LPM	-
4	AL-FS	DI water, 3LPM	DI water, 3LPM	-
5	AL-DS	DI water, 3LPM	DI water, 3LPM	20 µm filter
6	AL-FS	DI water, 3LPM	DI water, 3LPM	20 µm filter
7	AL-DS	DI water, 3LPM	45g/L NaCl, 3LPM	20 µm filter
8	AL-FS	45g/L NaCl, 3LPM	DI water, 3LPM	20 µm filter

5.2.4. **Analytical processes**

The experimental plan was designed to inspect the effect of key parameters such as the membrane orientation, the reversible fouling, and the membrane cleaning strategies on the FO process. Eight experiments of 4 cycles were carried out under several operational parameters. The membrane cleaning methods, the orientation and the treatment of the brine reject, and the wastewater were the changing parameters

To examine the performance of the FO process under defined experimental conditions, the water flux was calculated for each run using the recorded weight change according to **Equation 3.4, Chapter 3**. Flux reduction (FR) was calculated after each cleaning method to study the effectiveness of these methods in water flux recovery using **Equation 3.5, Chapter 3.** The reverse solute flux (RSF) was calculated to understand the behavior of the FO membrane. RSF is the solute penetration in the membrane from the DS side towards the FS

side and is a consequence of the difference in the solute concentrations. The values of RSF (J_S, g/m²h) were studied using **Equation 3.6, Chapter 3**.

To investigate the impact of the FO technique conducted in the experiments, it is important to calculate the energy consumption (E, kWh/m^2) in the standalone FO process using **Equation 3.8, Chapter 3**.

5.3. Results and discussions

5.3.1. **Water flux in the FO process**

The water flux was calculated every 15 min in each cycle of 180 min, using **Equation 3.1**, and the results are presented in **Figure 5.2.** The latter showed the variation of water flux over the operational time without the prefiltration of the FS and DS. **Figure 5.2** illustrates the water flux decline that is explained due to the decrease in the pressure difference across the membrane as a result of the water permeation and membrane fouling. As such, the driving force is reduced, causing a reduction in the water flow (Zhang et al., 2014b). As shown in **Figure 5.2a**, water flux in Exp1 (AL-DS) was 33.6 L/m2h in cycle 1 but decreased 32%, reaching 22.7 L/m^2h after 180 min. The performance of the FO system was studied after cleaning the fouled membrane with DI water at 40 °C and 2 LPM flow rates. The reason for using DI water at 40 °C for membrane cleaning is its ability to dissolve and remove the fouling materials (Ibrar et al., 2020b). Compared to the initial water flux in cycle 1, it decreased to 29.5 L/m^2h in cycle 2. The initial water flux at the beginning of cycles 3 and 4 was 28.6 and 27.0 L /m^2h, respectively. The slight decline in the initial water flux in cycles 2 to 4 compared to cycle one is due to the irreversible membrane fouling that was not removed by cleaning with hot DI water. After cleaning with 40 °C DI water at a 2 LPM flow rate, the initial water flux in cycle 4 was 27.0 L /m^2h, and it declined to 21 L/m^2h at the end of cycle 4 of Exp1. Despite cleaning with 40 °C DI water at a 2 L/m^2h flow rate, the results show a 22% decline in permeation flux at the end of cycle 4 of Exp1. Exp2 was conducted in the AL-FS mode to study the membrane orientation's impact. For the same cleaning method (**Figure 5.2.b**), water flux in the first cycle of Exp2 was 30.7 L/m^2h and declined by 14% to 26.4 L/m^2h at the end of cycle 1. At the beginning of cycles 2, 3, and 4, the initial water

flux was 29.9, 28.6, and 27.6 L/m^2h, respectively, with a 17% water flux decrease by the end of cycle 4. At this point, the drop in the water flux under the AL-DS mode was quicker, which might be explained due to the combination of dilution and more intense membrane fouling. This observation could be due to the active and SL structure, leading to more severe concentration polarization in the FO mode, which has been investigated in previous works (Ibrar et al., 2020b; Vu et al., 2018).

Exp3 and Exp4 studied the effect of the flow rate of DI water in the cleaning cycle on the FO process in AL-DS & AL-FS modes. The 40 °C DI water flow rate in the cleaning process was increased to 3 LPM in Exp3 and Exp4. As presented in **Figure 5.2.c** and **Figure 5.2.d**, the initial water flux of cycle 2 was 30.0 and 30.9 L/m^2h, respectively, higher than the initial water flux of cycle 2 in Exp1 and Exp2 (**Figure 5.2.a** and **Figure 5.2.b)**. This suggests that cleaning at a 3 LPM flow rate has a better outcome than at 2 LPM as it was more efficient in removing fouling materials from the membrane surface. Therefore, DI water at 3LPM was used for the membrane cleaning for the rest of the FO experiments.

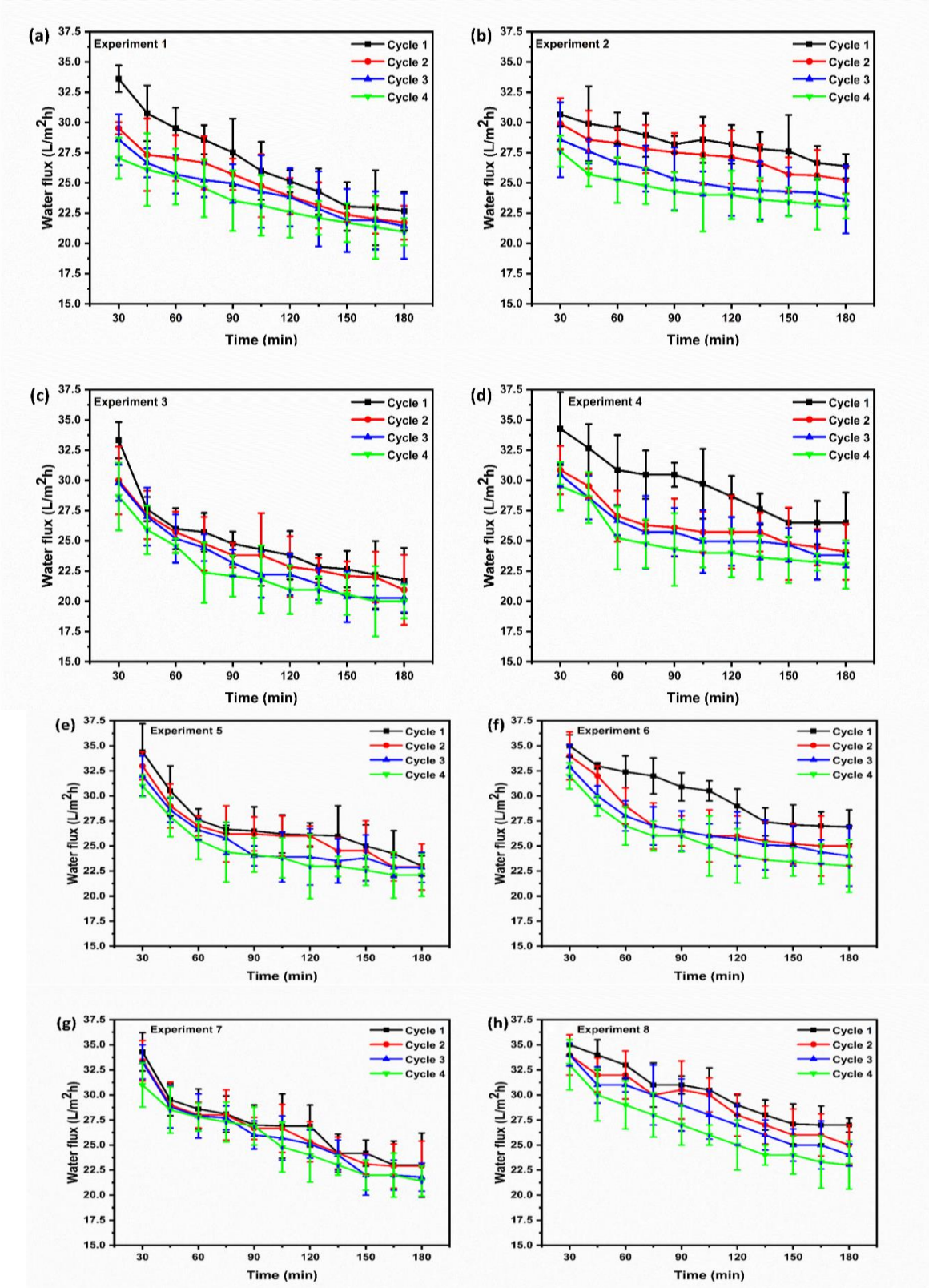

Figure 5.2. The water flux readings in the FO process, (a-d) without FS and DS prefiltration and (e-h) with FS & DS prefiltration, were conducted in both membrane orientations following three cleaning runs.

5.3.2. **Impact of prefiltration and osmotic backwash**

Since the flow rate of 3 LPM in the previous experiments has shown better performance, experiments 5 to 8 were performed with a 3 LPM cleaning flow rate. The stream solutions in Exp5-8 were prefiltered using a 20 µm Whatman filter to reduce the turbidity, and the TOC of both wastewater and the brine reject solution (**Table 5.1**). Water flux in cycle 1 was 34.4 L/m^{2}h in Exp5 and 35 L/m^{2}h in Exp6, as presented in **Figure 5.2.e and Figure 5.2.f,** respectively**.** After membrane cleaning with 40 °C DI water, the initial water flux was 33.0, 32.0, and 31.0 L/m^{2}h in cycles 2, 3, and 4 of Exp5 and 34.0, 32.9, and 32.0 L/m^{2}h in cycles 2, 3, and 4, respectively of Exp6. Water flux in Exp5 and Exp6 was higher than in Exp3 and Exp4, which was carried out without the prefiltration. This improvement is correlated with reducing the turbidity and the TOC of both FS and DS. The micro-size compounds that usually accumulate on the FO membrane were eliminated with the prefiltration. This finding agrees with a previous experimental work that achieved higher water flux in the FO membrane after the FS prefiltration (Hawari et al. 2018).

The study also investigated the impact of introducing the osmotic backwash of the membrane SL on the cleaning strategy at the end of each cycle. Exp7 showed the results of the osmotic backwash in which the SL was cleaned with 40 °C NaCl 45g/L at a 3 LPM flow rate and the AL with 40 °C DI water at a 3 LPM flow rate. This cleaning method removes fouling materials accumulated on the membrane layers by combining osmotic backwash and cross-flow cleaning with hot water. Results revealed a maximum water flux of 33.42 L/m^{2}h in cycle 2 that dropped to 23 L/m^{2}h at the end of cycle 3 (**Figure 5.2.g**)**.** Moreover, when comparing the same cleaning method in the AL-FS orientation in Exp8, it is shown that the initial water flux was 35.0, 34.0, 34.0 and 33.0 L/m^{2}h in all 4 cycles, respectively and declined steadily to reach 27, 25, 24 and 23.0 L/m^{2}h at the end of each cycle (**Figure 5.2.h**). All the water flux values measured in the TSE experiments were considered high compared with the water flux of the FO process conducted with seawater FS (Khanafer et al., 2021). The maximum water flux recorded using a TFC membrane with brine reject as DS and seawater as FS was 7.4 L/m^{2}h. The results highlight the effectiveness of applying the FO process for wastewater and

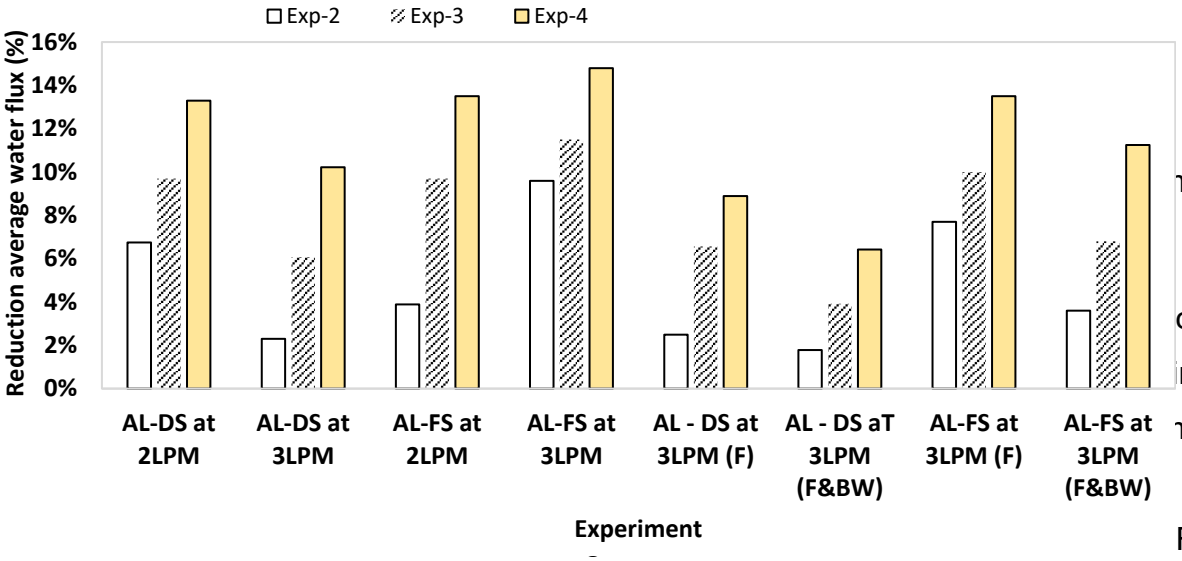

mize the cycles in rst cycle aximum and the FS tests yielded a better average permeation flux than the AL-DS tests.

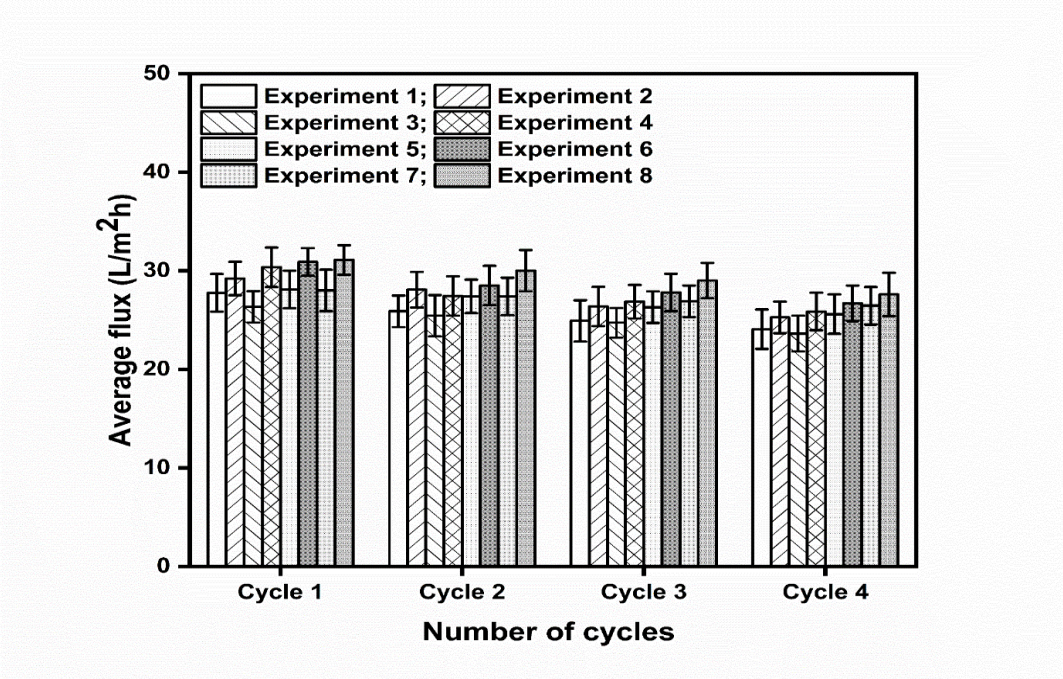

Figure 5.3. Average flux for each cycle in the FO experiments. Each FO process was run for 4 consecutive cycles. Each FO cycle was operated for 180 min, and the water flux was measured every 15 min. Experiment (1-4) without FS & DS prefiltration and (5-8) with FS & DS prefiltration.

5.3.3. **Flux reduction**

The used and fouled membrane was cleaned with 40 °C DI water or backwashed with 40 °C DI water and NaCl solution. The reduction in water flux was calculated using Eq. 2, and the results are available in **Figure 5.4**. Water flux reduction was generally lower in the AL-DS than in the AL-FS tests due to the greater membrane fouling in the latter test. For example, water flux reduction at the end of cycle 4 of

Exp1 and Exp2 was 13% and 14%, respectively, indicating that water flux reduction was higher in Exp2 when the FS faced the AL of the membrane. Experiments also revealed that a better cleaning process was achieved at a 3LPM flow than a 2LPM flow rate, especially when the DS is against the AL of the membrane. The water flux decrease at the end of Exp3 was 10% compared to 13% at the end of Exp1 (**Figure 5.4**). The higher flux reduction in the AL-FS could be due to the high hydrophilicity of the membrane AL (**Table 3.2, Chapter 3**), which promoted organic fouling. Fouling experiments showed that membrane fouling was more severe when the FS (wastewater) faced the membrane SL (Appendix A). The prefiltration of FS and DS improved the filtration process and reduced water flux reduction in the consecutive filtration cycles 1 to 4. For example, the water flux decline at the end of Exp5 was 9% compared to 10% at the end of Exp3, performed at the same operating and cleaning condition but without prefiltration. It should be pointed out that the prefiltration of FS and DS was less efficient in preventing fouling in Exp6 (AL-FS) due to the ineffectiveness of the cleaning process. Combining osmotic backwash with DI water cleaning at 40 °C resulted in better cleaning and water flux recovery. The osmotic backwash improved removing fouling materials trapped in the membrane SL while cleaning the AL with 40 °C DI water at a 3 LPM flow rate was considered effective for cleaning the AL in Exp7, recording 6% water flux reduction after 4 cycles. Therefore, the best operating and cleaning methods are presented in Exp7, in which 40 °C DI water and osmotic backwash at a 3 LPM flow rate are used for the membrane cleaning.

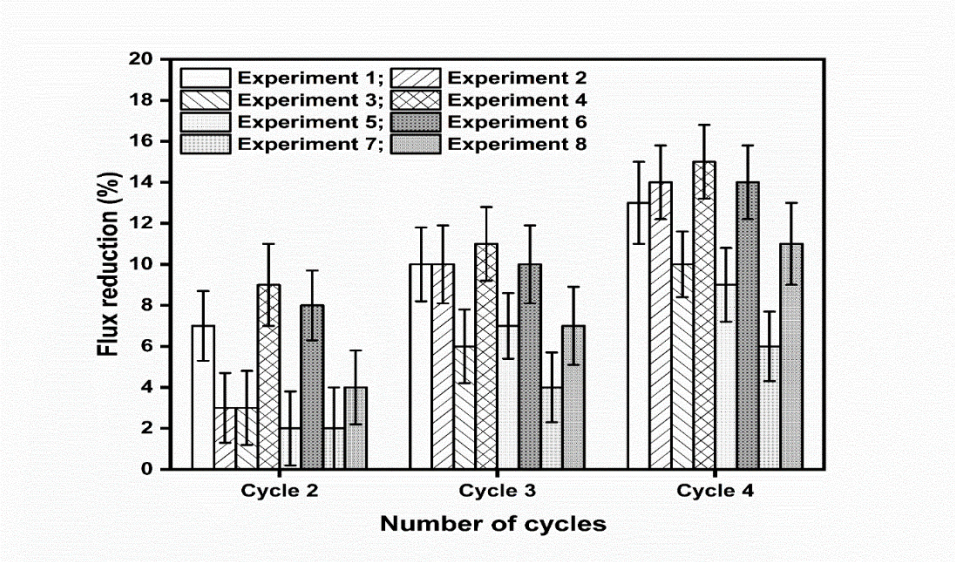

Figure 5.4. Flux reduction in the FO experiments after each cleaning method. Membrane cleaning was performed after each cycle for both AL-FS and AL-DS orientations. No FS & DS prefiltration in Experiments (1-4) and with prefiltration in (5-8).

5.3.4. **Reverse Solute Flux**

Reverse Solute Flux is a major challenge that needs investigation in the FO process due to the diffusion of salt leakage towards the FS side. RSF would decrease the concentration gradient, lose draw solute, and increase fouling (Oh et al. 2014). Controlling and reducing RSF was studied, and literature showed interest in operational strategies and membrane development that can collaborate in minimizing the reverse diffusion of draw solutes toward the FS (Zou et al., 2019). The reverse salt permeation is strongly related to the TDS of the DS. In this study, the TDS of the wastewater and seawater were 0.963 and 80.2 g/L. The RSF (J_S, g/m^{2}h) was calculated following **Equation 3.6**, and the results are presented in **Figure 5.5**. The latter shows the RSF in each cycle following different cleaning strategies. The RSF in the AL-DS for cycle 1 was 82.1 g/m^{2}h, and 80.2 g/m^{2}h for Exp1 and Exp3, respectively and 81 g/m^{2}h of Exp5 & Exp7 and decreased to 61.9, 59.0, 61.0, and 63.5 g/m^{2}h in cycle 4 of Exp1, Exp3, Exp5 and Exp7, respectively. Whereas for the FO experiments in the AL-FS mode, 59.1, 58.1, 54.4, and 61.0 g/m^{2}h were the RSF in cycle 1 of Exp2, Exp4, Exp6, and Exp8 reached 32.9, 35.1, 32.0, and 33.1 at the end of cycle 4. As for the orientation of the FO membrane, results revealed that the RSF is higher in the

AL-DS mode. This can be explained due to severe concentration polarization (CP) when the DS faces the membrane's SL, leading to a reduced concentration of the DS inside this layer; hence, the RSF was lower in the AL-FS tests. Permeation flux dilutes the draw solute, creating a dilutive internal CP, which, in turn, reduces the concentration of the DS in the SL. This phenomenon is less severe in the AL-DS mode as the DS faces the AL (Oh et al., 2014).

It is also shown in **Figure 5.5** that almost all the values of the reverse flux decreased after each cycle, i.e., cycle 1>cycle2>cycle3>cycle4. The decline in the RSF in each cycle after cleaning is due to the irreversible fouling of the membrane, which reduced the water flux and the RSF simultaneously in the FO process. In general, RSF is less in the FO processes performed in the AL-FS mode or when the FO membrane is fouled. In the current application, feed and DSs are waste streams, so contamination of the FS due to RSF is not a concerning problem. However, the diffusion of salts from the draw side could slightly reduce the driving osmotic force of the process. Nevertheless, wastewater FS of about 1 g/L initial TDS and brine reject DS from the MSF plant provide significant osmotic pressure for the FO process.

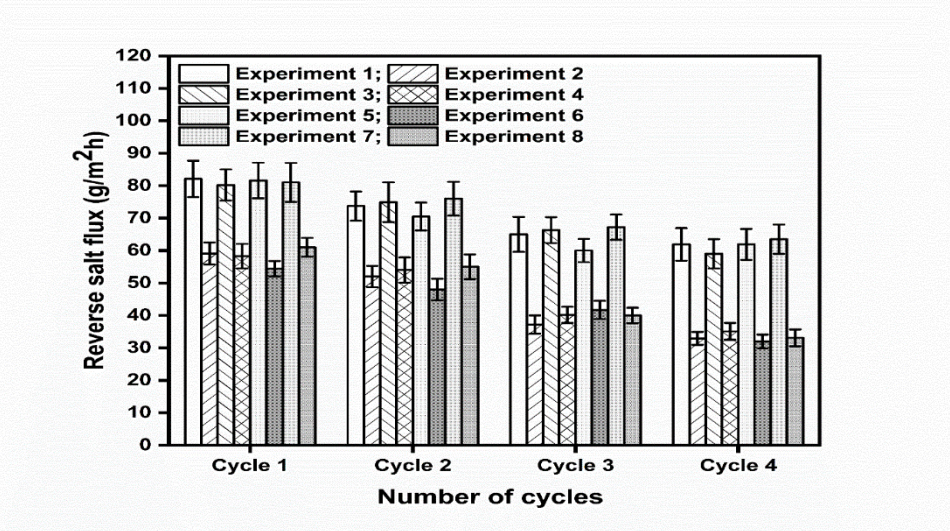

Figure 5.5. Variation of RSF without FS & DS prefiltration in Experiments (1-4) and with prefiltration in Experiments (5-8). Each experiment consists of 4 cycles of FO processes. The membrane was cleaned after each cycle.

5.3.5. **Tackling fouling materials**

The deposition of wastewater materials on the active and SL and within the porous SL reduces water transportation and affects the overall membrane performance. Fouling might result from ions scaling, organic or colloidal materials accumulation and microbial growth (Ibrar et al., 2019). External fouling occurs on the membrane AL in the AL-FS orientation; however, internal fouling is more intense where foulants of a smaller size than the membrane pores penetrate the SL, leading, in some cases, to pores clogging. This type of fouling is popular when the FS faces the SL (Zhao et al., 2016). In this study, physical cleaning strategies were implemented to mitigate the fouling materials, and a combination of analysis techniques was conducted on the tested membranes. Scanning Electron Microscopy (SEM) and Energy Dispersive X-Ray Spectroscopy (EDS) were used to identify the elemental composition of the fouling materials, and Fourier Transform Infrared Spectroscopy (FTIR) in its turn is best for identifying the presence of organic materials.

5.3.5.1. *SEM/EDS Scanning of fouled membranes*

It is important to mention that the fouling matters are not evenly located on the membrane surface (Ping Chu and Li, 2005). The scale morphology varies within the same membrane and with other membranes, illustrated in **Figure 5.6**. The deposited foulants mostly covered the membrane surface with various structures and shapes that might indicate a combination of different fouling compounds. The prefiltration of the stream solutions reduced the precipitated fouling compounds that were not highly presented in the SEM images compared to the images of the membranes when FO processes were conducted without prefiltration. The fouling compounds on the AL in the FO mode without prefiltration of the stream solutions were bigger and different in morphology. The prefiltration for the same membrane orientation minimizes the presence of a larger accumulation of foulants.

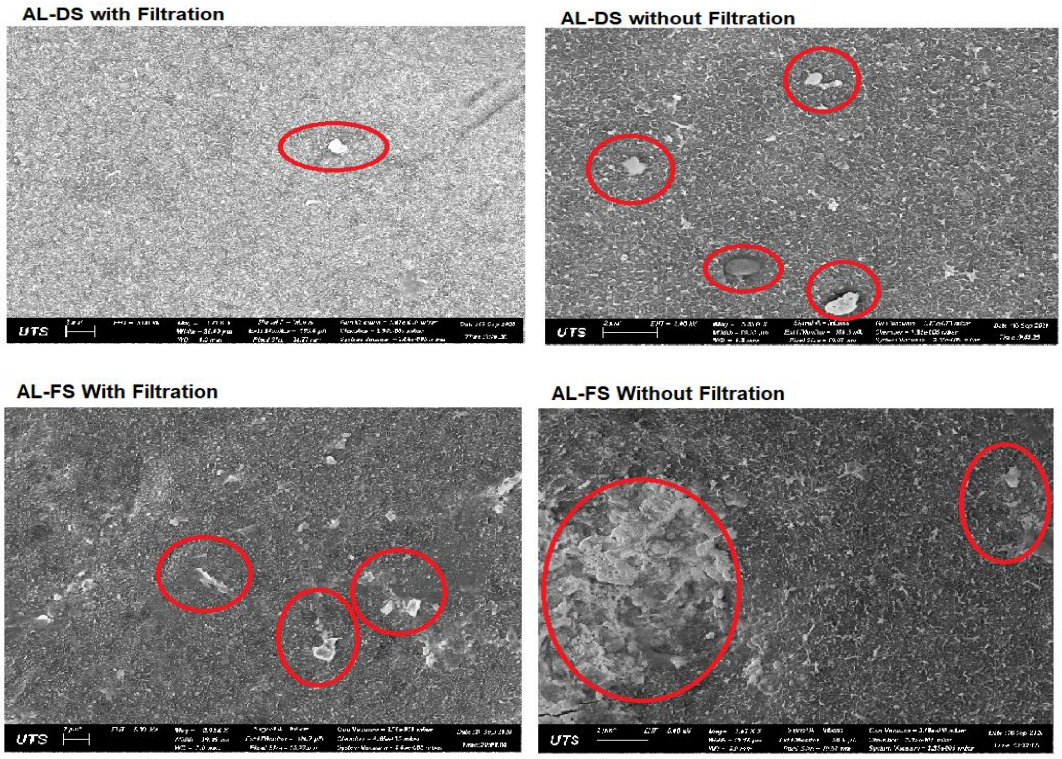

Figure 5.6. SEM images of the AL of the fouled FO membranes. Fouling on the AL are more remarkable without prefiltration and in AL-FS according to the membrane samples used.

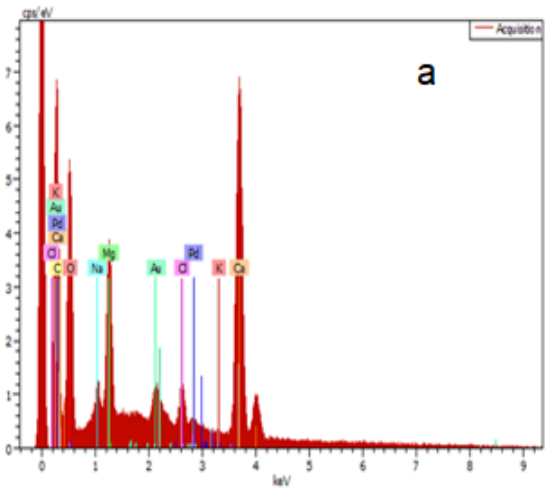

Spectrum: Acquisition **b**

El	AN	Series	un. C [wt.%]	norm. C [wt.%]	Atom. C [at.%]	Error (1 Sigma) [wt.%]
C	6	K-series	11.80	17.68	31.89	1.52
O	8	K-series	18.89	28.29	38.31	2.39
Na	11	K-series	0.50	0.74	0.70	0.06
Mg	12	K-series	3.28	4.91	4.38	0.20
Cl	17	K-series	1.25	1.87	1.14	0.07
K	19	K-series	0.04	0.06	0.03	0.03
Ca	20	K-series	28.50	42.69	23.08	0.98
Pd	46	L-series	0.41	0.62	0.13	0.05
Au	79	M-series	2.10	3.15	0.35	0.11
		Total:	66.77	100.00	100.00	

Figure 5.7: (a) Associated EDS spectrum of the sample membrane in the SEM-EDS analysis, (b) Table showing the elements of the spectrum in numbers in the SEM-EDS analysis.

SEM and EDS scanning were coupled to visualize the fouling compounds distinctly, characterize the fouling layer and obtain information on its chemical composition. According to the EDS spectrums, the organic compound (C &O) and other inorganic ions such as Mg, Ca, and Fe mainly showed spectra (**Figure 5.7**). This is in agreement with the SEM-EDS images, where fouling particles were displayed and identified in colors (**Figure 5.8**). DI water cleaning. C, O, Mg and Ca are clearly observed on the surface of the sample membrane.

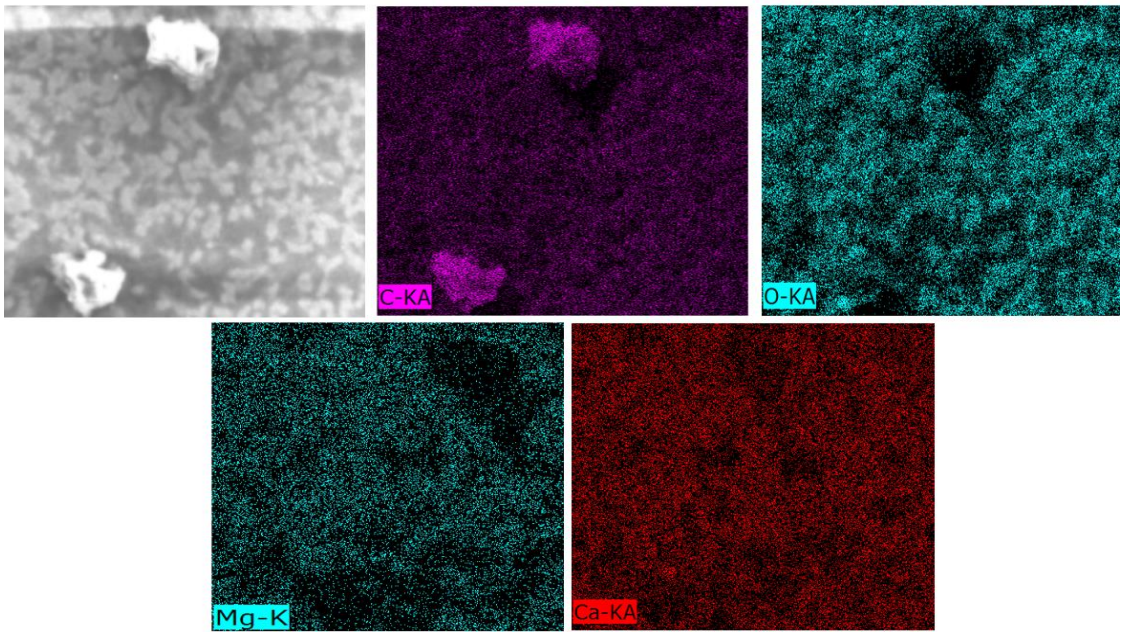

Figure 5.8. SEM-EDS analysis of the AL of the fouled FO membrane in the AL-DS orientation at the end of cycle 4 after hot DI water cleaning. C, O, Mg and Ca are clearly observed on the surface of the sample membrane.

5.3.5.2. *FTIR Analysis*

FTIR technique has been applied widely to identify the functional groups of the foulants on the membrane by attenuated total reflection (ATR). In other words, inorganic and organic fouling compounds that absorb the radiation-specific compound can be characterized by FTIR spectra. Both fouled and washed membrane layers were scanned using an FTIR scanning microscope and later compared to a new membrane's spectra. A clear change is observed in the FTIR

spectrum of the used membranes in both orientations compared to the pristine ones. The spectroscopy also shows that the spectrum of the membranes after cleaning resembles the new membranes, which can explain the efficiency of the cleaning strategy. On the used membrane (AL-FS) and the FTIR of the AL, the two peaks observed at a wavenumber of 875 cm^{-1} and 1875 cm^{-1} differentiate the fouled membrane from the new and washed membranes. In addition, the diminishing of a few peaks in the bands at wavenumber 500-850 cm^{-1} and 1000-1300 cm^{-1} is noticeable in the spectrum (**Figure 5.9a**). Similarly, the FTIR on the SL indicates the presence of fouling materials and how the cleaning methods enhanced the performance of the fouled membrane (**Figure 5.9b**).

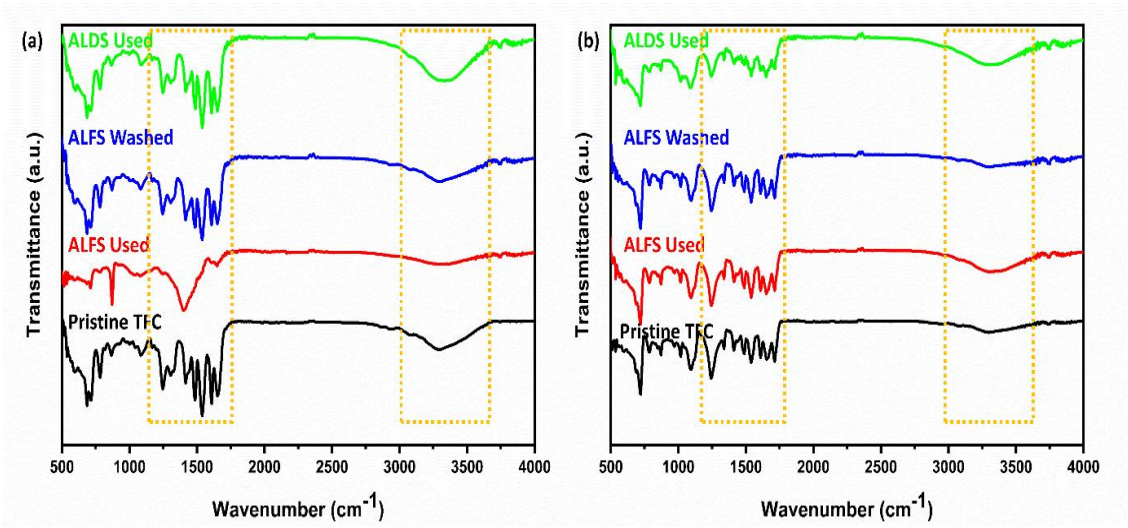

Figure 5.9. FTIR spectroscopy of the new fouled and washed membranes. (a) Scanning the AL in the AL-FS mode. (b)Scanning the SL in the AL-DS mode.

5.3.6. **Energy consumption and membrane cost**

The main component in the cost of desalination is the energy requirements; therefore, this section focuses on the energy consumed by the FO system during the ongoing process. The energy consumption was calculated using **Equation 3.8** (**Chapter 3**), and the results are illustrated in **Figure 5.10.** The energy consumed in the prefiltration process of the solutions was calculated using **Equation 3.9** (**Chapter 3**); 0.034 kW h/m^2 was the amount of energy consumed for the prefiltration before the FO process. This extra energy is not added to the

values presented in **Figure 5.10**. Results revealed that the specific power consumption increased from cycle 1 to 4. This might be due to the lower permeation flow in cycle 4 that caused an increase in the specific power consumption, as explained in **Equation 3.8, Chapter 3**. Increasing the flow rate from 2 to 3 LPM did not increase the power consumption in Exp3&4 (0.006 & 0.005 kW h/m^2); the explanation for this would be that the higher water flux was achieved after cleaning with 40 °C DI water at 3LPM.

For the same reason mentioned above, results revealed that the DS and the FS prefiltration decreased the energy consumption of the standalone FO process compared to the FO experiments without the prefiltration of the FS and DS. The FO process energy in this study is considered very efficient compared with the NF pretreatment process (Altaee et al., 2013). The FO process maximum energy consumption in this study was 0.007 kWh/m^2, which is considered very low compared to the energy consumption when seawater was used as FS. 0.020 kWh/m^2 was the power consumption in the FO process for the dilution of the brine reject using seawater as FS. The prefiltration step is more demanding in terms of energy consumption than the FO process itself. Generally, the overall energy demand in the FO process using TSE with prefiltration of the FS and the DS is considered low and efficient in terms of cost-saving perspective. It is noteworthy that the specific power consumption of the FO pretreatment is almost 142 times lower than the NF pretreatment of seawater to the MSF plant (Altaee et al., 2013).

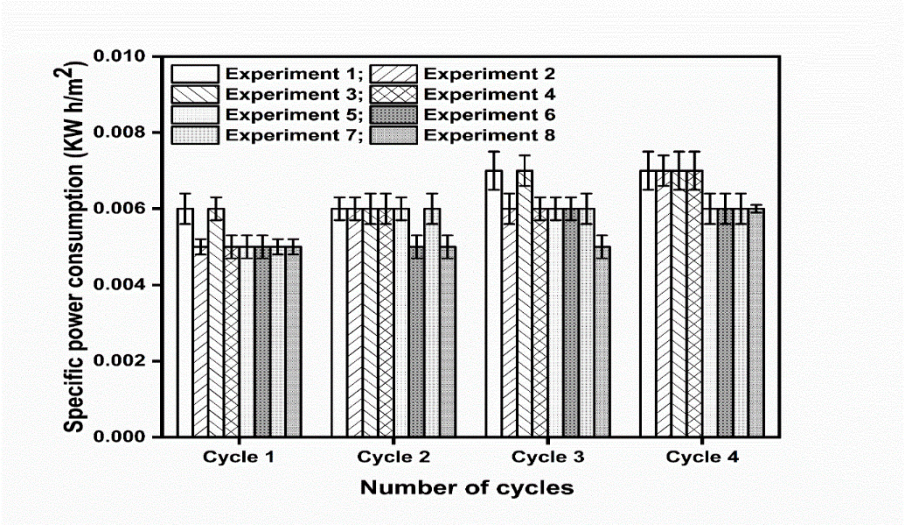

Figure 5.10. The performance of the FO experiments was conducted in terms of specific power consumption. (1-4) FO process without stream solution prefiltration, (5-8) FO process with prefiltration of FS & DS.

The membrane area required for brine reject pretreatment with seawater, and TSE was calculated for a desalination plant capacity of 10000 m^3/day. The results were compared to the FO process using seawater as an FS (Khanafer et al., 2021). The cost of Hydration Technology Innovation (HTI) FO element 8040FO-FS-P is USD 1719 per element and has a 16.5 m^2 active membrane area (Altaee et al., 2014b). The FO membrane area was slightly increased, ~2%, when the membrane orientation changed from AL-FS to AL-DS, whereas there was a 363% increase in the FO membrane area when the membrane orientation switched from AL-DS to AL-FS due to the sharp decrease in the water flux (**Table 5.3**). The drop in water flux is caused by the severe concentration polarization when seawater was the FS. Compared to the FO process using seawater FS, the results demonstrated that using TSE FS decreased the number of FO elements significantly. Using the TSE FS led to a 276% and 473% decrease in the number of FO elements required in the FO process, depending on the FO membrane orientation. The results indicate a significant advantage and cost-saving when TSE is used as an FS in the FO process.

Table 5.3. Membrane area and cost for TSE and Seawater FSs in the FO process as pretreatment for the MSF plant.

Type Feed	Membrane orientation	Membrane area	No. FO Elements	Cost (USD)	Specific power (kWh/m^3)
TSE	AL-DS	12148	736	1265571	0.005-0.007
Seawater	AL-DS	33602	2036	3500733	0.02
TSE	AL-FS	11905	722	1240260	0.005-0.007
Seawater	AL-FS	56306	3413	5866093	0.03

5.3.7. **Prefiltration and membrane cleaning effects on dilution of the Brine DS**

The penetration of pure water throughout the FO membrane diluted the brine reject; therefore, a reduction in the concentrations of the ions occurs (Thabit et al., 2019). In this study, the concentrations of Mg^{2+}, Ca^{2+}, and SO_4^{2-} in the DS were studied in all FO treatment cycles, i.e. in both membrane orientations, with and without prefiltration. The concentration of Mg^{2+} and Ca^{2+} were measured using ion chromatography (7900 ICP-MS provided by Agilent technologies) and SO_4^{2-} using Dionex VWDIC manufactured by HPIC. **Figure 5.11** shows the variation in the percentage of the concentration of the divalent ions from one cycle to another within the same experiment. Magnesium, calcium and sulfate ions are mainly responsible for scale formation in the MSF heat exchanger; reducing these ions will help in scale control (Thabit et al., 2019). The ions reduction after each FO experiment is illustrated in **Figure 5.11.** The percentage of ions reduction decreased due to the decline in water flux following the membrane cleaning within the same experiment. Overall, when the cleaning method's flow rate in the AL-DS orientation increased, it decreased the concentration of divalent ions of all three ions, where the reduction in Ca^{2+} is the highest. In the AL-FS tests, the reduction in Mg^{2+} and SO_4^{2-} was considerably greater than in the AL-DS, whereas the opposite was for Ca^{2+}. The higher dilution of ions in the AL-FS test resulted from the greater average ware flux in these tests than in AL-DS tests. For the same reason, in Exp1 (cycle 1), 37%, 41%, and 25% were the percentage of reduction of Mg^{2+}, Ca^{2+} and SO_4^{2-}, respectively. These values decreased to 34%,

38%, and 24% in Exp3 when the flow rate of the cleaning solution increased to 3 LPM**. (Figure 5.11a & c)**.

Cleaning the membrane with a 3 LPM flow rate in the FO tests without the prefiltration of the solutions raised the initial water flux, which in turn caused irreversible fouling in the FO membrane and hence lower average water flux (**Figure 5.3**); thus, a dilution of the DS. The prefiltration of solutions in the FO tests provided better performance in the chain of the FO processes, decreasing membrane fouling in the subsequent filtration cycles 1 to 4. According to the results in Exp3 (3LPM cleaning without prefiltration) and Exp5 (with prefiltration), the reduction is higher after prefiltration; for example, in cycle 3 of Exp3, the reduction was 34% compared to 39% in cycle 3 in Exp5 (AL-DS). The reduction was enhanced when an osmotic backwash was used; it counted 40% in cycle 3 (Exp7). In light of these results, the desired FO process would be in the AL-DS membrane orientation, prefiltration of feed and DSs, and cleaning with 40 °C DI water and osmotic backwash in order to tackle membrane fouling.

Compared to the FO process performed with seawater FS, using wastewater FS achieved a 40% decrease in calcium concentration and a 35% and 25% decrease in the concentrations of magnesium and sulfate, respectively (Exp7). This is more than 14%; the targeted dilution of the brine reject in an MSF plant operates at 112 °C (Morin, 1993). In effect, with the wastewater FS, the MSF plant could operate at a top brine temperature higher than 112 °C and without antiscalant. Therefore, the FO process will improve the MSF plant's performance, avoid antiscalant use, and reduce the environmental pollution associated with brine reject and wastewater disposal. Results revealed that the FO process has successfully diluted the brine using wastewater as FS.

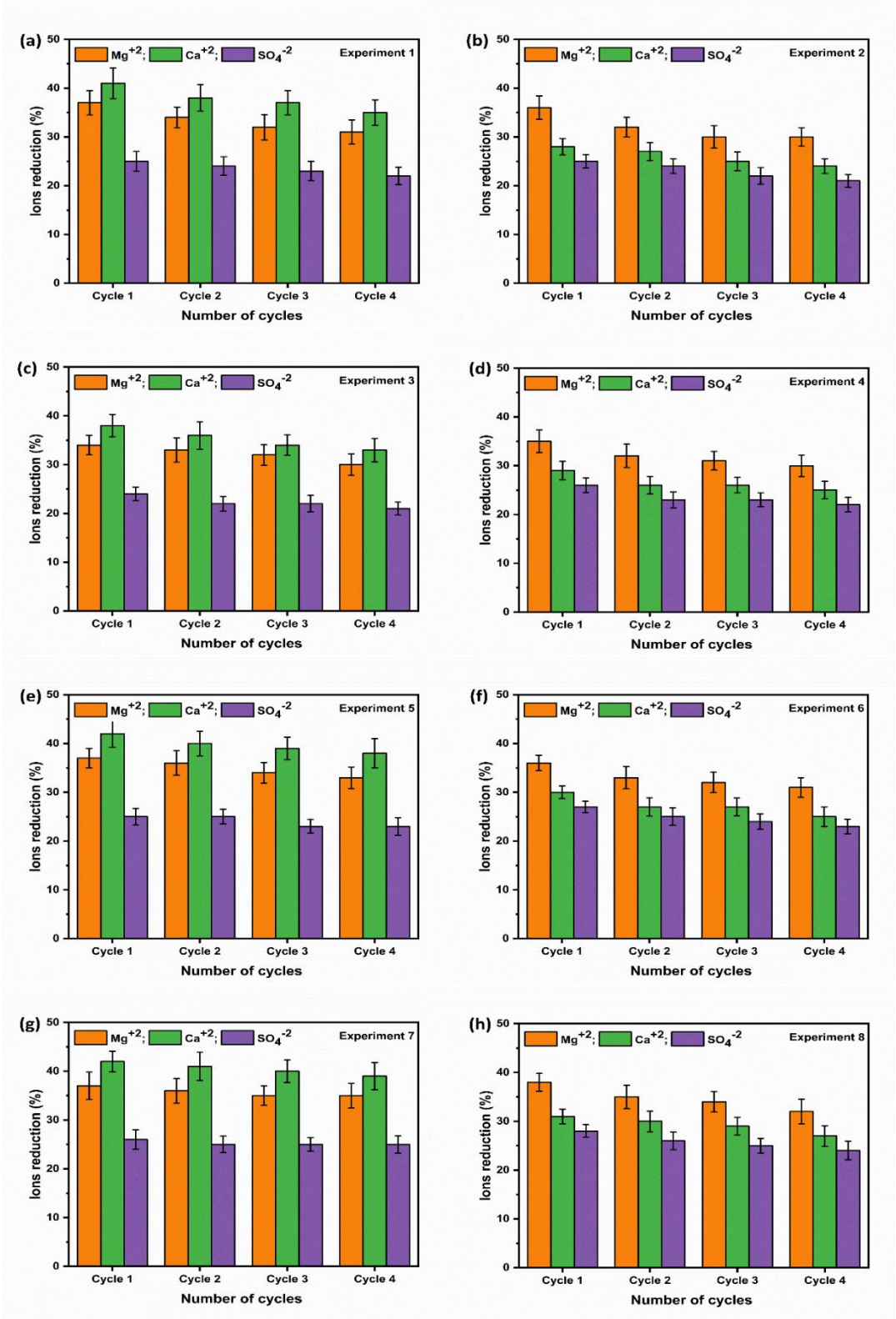

Figure 5.11. Reduction of Mg^{2+}, Ca^{2+} and SO_4^{2-} in % in FO experiments, (a-d) without prefiltration and (e-h) with prefiltration.

5.4. Conclusions

In this study, treated wastewater and brine-reject were the FS and the DS in a FO system. The performance of the FO process was correlated to the operating parameters studied. Experimental work showed that the prefiltation of the stream solutions was effective in terms of better water flux and fouling mitigation. The average water flux generated was considerably higher in the AL-FS mode in all cycles following the physical cleaning. The maximum average water flux achieved was 31.1 L/m^{2}h when the prefiltered wastewater was the FS compared to 9.57 L/m^{2}h when real seawater was used as FS. The physical cleaning methods reduced the membrane fouling and restored the water flux to a minimum of 86% at the end of cycle 4 of the FO experiment. SEM/EDS and FTIR analysis revealed that cleaning with 40 °C DI water and NaCl osmotic backwash effectively reduced the fouling that was believed to be reversible and not severe. The dilution of the brine reject solution was successfully achieved, with the reduction of the ions reaching 43%. The proposed FO system consumed maximum energy of 0.007 kWh/m^2, which is a promising economical outcome in competition with 0.020 kWh/m^2 consumed when seawater was used as FS. Overall, the high water flux recorded, the efficiency of the cleaning methods used, and the potential to reduce the divalent ions in the DS are the results that can build up further research. The outcomes of this study revealed the potential of the FO process in the dilution of brine-reject using wastewater and 40 °C DI water with NaCl osmotic backwash for membrane cleaning. There is about a 473% decrease in the number of FO elements and membrane cost when the TSE replaces seawater as the FS in the FO process. The FO process will reduce concentrated brine discharge to seawater and chemicals use and prevent thermal pollution due to brine discharge at 40 °C to seawater. The promising results of this study open more doors for additional research on implementing the FO process in wastewater application for brine reject dilution for reuse in the MSF plant.

Chapter 6: Performance of Nanofiltration membranes in a lab-scale forward osmosis system for brine recycling

Abstract

This chapter investigated the feasibility of using commercial nanofiltration (NF) membranes in the FO process for seawater pretreatment in the MSF plant. The NF membrane is usually more permeable than the FO membrane and is designed to reject divalent ions. These divalent ions, such as sulfate, magnesium and calcium, are the main reason for scale formation and deposition in the MSF plant. Economically, NF membranes are much cheaper than FO membranes when used in the FO process, reducing the pretreatment cost. Antifouling commercial NF membranes are available for wastewater treatment and were tested in the FO process. Three flat sheet NF membranes were acquired from Microdyn-Nadir Company (Australia), TS80, XN45 and UA60. The main obstacle in using commercial flat sheet NF membranes in the FO process is the structure of these membranes with a large structure parameter (S) that would promote the internal concentration polarization phenomenon. This chapter will apply the FO and the pressure-assisted FO (PAFO) processes for seawater pretreatment using commercial NF membranes in the FO process. Since commercial NF membranes were designed to tolerate pressure when applied in the direction of the selective membrane layer only, the PAFO experiments were conducted in the FO mode

(active membrane layer facing the feed solution) to avoid the delamination of the selective membrane layer when the applied pressure is on the support layer. The MSF brine reject and seawater at 40 °C, and 20 °C were the draw and feed solutions in the FO process.

6.1. Introduction

The deposition of scales on the surface of the heat exchangers in the thermal desalination plant is a very common operating issue (Budhiraja and Fares, 2008). This is one of the technical limitations that can affect the desalination process's performance and efficiency (Hassan et al., 1998). Non-alkaline scale formation is usually developed in the multi-stage flashing (MSF) desalination technology, the main thermal desalination technology in the Middle East. The deposited non-alkaline scales in the MSF plants, operating at high temperatures, are mostly of calcium sulphate ($CaSO_4$) and magnesium sulphate ($MgSO_4$) (Hassan et al., 1998). This kind of scaling cannot be removed by chemical cleaning and is only responsive to physical cleaning that requires periodic shutdown of the desalination plant (Warsinger et al., 2015). Recently, pre-treating the feed seawater to thermal plants has been investigated in the literature as an alternative to adding antiscalants and to regular physical cleaning. Altaee et al. (2014) introduced the FO process as a pretreatment step to produce high-quality feed seawater with lower ions count for a stable and efficient thermal desalination process **(Figure 6.1)**. The reduction in scaling ions will minimise scale formation for more reliable MSF plant performance in the thermal stage. Experiments in this field have shown promising outcomes in divalent ions removal using commercially available FO membranes such as cellulose triacetate (CTA) and thin-film composite (TFC). The main features of the FO technology are the low operating cost and ability to treat wide range of feed salinities. However, there are some concerns related to the application of the FO technology such as limited water flux and the cost of the FO membrane, which is several times more than reverse osmosis (RO) and Nanofiltartion (NF) membranes.

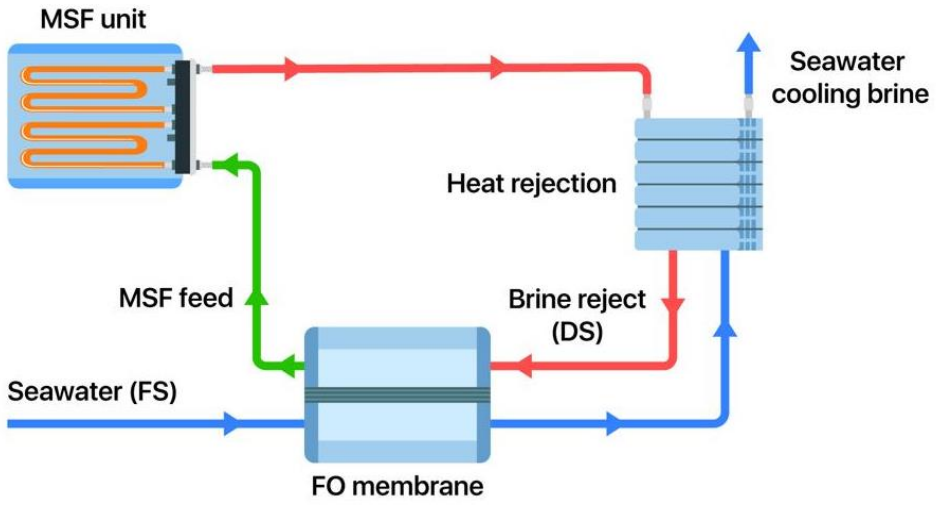

Figure 6.1. Fundamental demonstration of the FO-MSF hybrid system using the MSF brine reject as DS in the FO process.

Simulation results showed that divalent ions concentration decreased alongside the scale layer thickness when the FO process was used for seawater pretreatment (Altaee et al., 2013). The removal of divalent ions from seawater allowed the thermal plant to operate at elevated top brine temperature (TBT), achieving a higher recovery rate (Altaee et al., 2014a). The main limitation recorded in applying the FO process is the limited permeation flux and membrane fouling that led to a decline in the water flux over the operation time (Ibrar et al., 2019; Ly et al., 2019). A theoretical FO-MSF hybrid system model revealed that the FO process could minimise the MSF plant scaling problem by recycling the brine reject. In the simulation study, the MSF plant brine-reject was used as a DS and fresh seawater as FS, resulting in a 62% reduction in the divalent ions (Altaee and Zaragoza, 2014). The conceptual design was experimentally investigated for the first time in 2019 by Thabit et al. (Thabit et al., 2019). The team studied the feasibility of the FO process as a pretreatment of seawater in an MSF desalination plant. MSF brine solution at 40 °C was the draw solution, and seawater at 25°C was the FS in the FO process, which achieved a maximum average membrane flux of 22.3 L/m^{2}h and 8.5% dilution of the DS.

NF membranes attracted worldwide attention for their advantages in providing high permeability and high divalent ions rejection (Abdelkader et al., 2018). It was proposed and investigated for the pretreatment of feed entering the thermal plants, and results revealed its capability to decrease the concentration of scaling species in seawater, specifically Ca^{2+}, Mg^{2+} and SO_4^{2-}. The NF process could remove 30% of the monovalent ions and up to 98% of the divalent ions in the feed water (Hassan, 2006; Hassan et al., 1998). Despite the wealthy literature that has discussed and evaluated NF membrane use for pretreatment in various desalination techniques and under various parameters (Kaya et al., 2015; Zhou et al., 2015), it is still considered impractical due to the high operating cost and the membranes selection and effectiveness (Abdelkader et al., 2018; Hassan et al., 1998; Kaya et al., 2015). In the FO process, Torlon® polyamide-imide (PAI) NF-like FO membrane fabricated in the laboratory for the FO applications achieved 29.64 L/m^2h water flux when the active layer faced a 0.5M $MgCl_2$ DS and DI water FS(Qiu et al., 2012). Water flux decreased to 19.2 L/m^2h when the FS faced the active membrane layer interpreted as a result of the severe concentration polarisation. Due to concentrative concentration polarisation, lower water flux is expected in the PAI NF-like FO membrane at increased FS salinity (Arjmandi et al., 2020; Tan and Ng, 2008). In another study, NF-like FO membrane performance was ~27 L/m^2h using 47 mmol/L sodium polyacrylate (equivalent to 1M NaCl) DS and DI water FS (Okamoto and Lienhard, 2019). In effect, NF-like FO membranes are still developing and could be more expensive than FO membranes because of their limited applications.

In the FO-thermal plant hybrid system, the FO process is designed for divalent ions rejection only since monovalent ions are not affecting scale formation in the thermal plant. The commercially available NF membranes were shown promise in terms of ionic rejection ratios that vary among the NF membrane brands as well as the unexpansive cost compared to the FO membrane; however, they require higher energy and applied pressure for operation (Kaya et al., 2015). However, no study investigated the application of commercial NF membranes in seawater softening using the FO system.

In this study, commercial NF membranes were utilised in the FO process system for seawater softening using brine reject as the draw solution for the first time. The study aimed to determine the performance of the three TRISEP® NF membranes to compare with the CTA and TFC FO membranes for seawater pretreatment to the MSF process. Commercial NF membranes are believed to exhibit high water permeability and are significantly cheaper than the FO membrane. However, NF membranes are designed to operate under hydraulic pressure and have a different structure from the FO membranes. Hence, they should operate in a pressure-assisted process to induce water flux across the membrane. Moreover, the FS is to face the active layer of the membrane to prevent SL delamination under the applied hydraulic pressure (Jamil et al., 2016). A range of hydraulic pressures from 1 to 4 bar was applied on the NF membrane feed side operated in the FO mode (AL-FS) (Qiu et al., 2012). Three commercially available TRISEP® NF membranes (TS80, XN45 and UA60) were tested to determine the NF potential in seawater pretreatment to the MSF plant. The DS was a brine reject solution at 40 °C, and the FS was fresh seawater at 25°C. The influence of each NF membrane's morphology on its performance was examined by measuring the three membranes' water flux and recovery rate. In addition, the study evaluated divalent ions (Ca^{2+}, Mg^{2+} and SO_4^{2-}) concentration in the draw solution, calculated the operational energy consumption, and presented a cost analysis of the FO process using NF membrane in the FO process.

6.2. Materials and methods

6.2.1. **NF membranes**

Three commercial NF membranes, TS80, XN45 and UA60 from TRISEP®, were used in this study. TRISEP® TS80 membrane is a flat sheet thin-film Polyamide membrane considered a softening membrane in various water purification applications. XN45 and UA60 membranes are made of a thin-film Polypiperazine with a pore size of 300-500 Daltons and 1000 Daltons, respectively. The characteristics of each membrane under the following conditions: 7.6 bar, 25 °C and 30 min operation are presented in **Table 3.3**, **Chapter 3**. Notably, the water permeability coefficients of the selected NF membrane are 4 to 6.7 times higher

than the Porifera TFC FO membrane (**Table 3.2**, **Chapter 3**) and 12.5 to 20 times higher than the FTSH_2O CTA FO membrane. The water permeability of NF membranes offers significantly higher water flux compared to TFC and CTA FO membranes.

6.2.2.**Feed and draw solutions**

The FS used in the experiments was fresh seawater collected from the Sydney area (Australia) and stored at room temperature (20 °C ±2). The DS was the brine reject solution similar to the MSF desalination plant in the Middle East. This study referenced the concentration of seawater and MSF brine reject in Qatar. In all the experiments, the concentration of the FS was 45g/L at 25°C with 80g/L for the DS concentration at 40 °C. These concentrations were obtained by heating seawater until the desired concentrations were reached. The constitutions of the stream solutions are summarised in **Table 3.1, Chapter 3**.

6.2.3. **Experimental set-up**

The lab-scale installation was presented in **Chapter 3, Section 3.2.4**. A schematic diagram of the FO system used in the experiments is presented in **Figure 6.2**. The NF membrane is incorporated in the FO cell. The FO system contained two flow meters, F-550 (Blue-White Industries Ltd) and two pressure gauges (USG U.S. Gauge on both sides of the cell. In addition, two pumps manufactured by Cole-Parmer maintain the water circulation in the system. The turbidity of the solutions was measured using a turbidity meter, HACH 2100P. The conductivity of solutions, the TDS, and the salinity were measured using HQ 14d portable conductivity and TDS meter (HACH, Australia). A digital scale balance connected to a computerized system was used to detect the stream solution's weight variations.

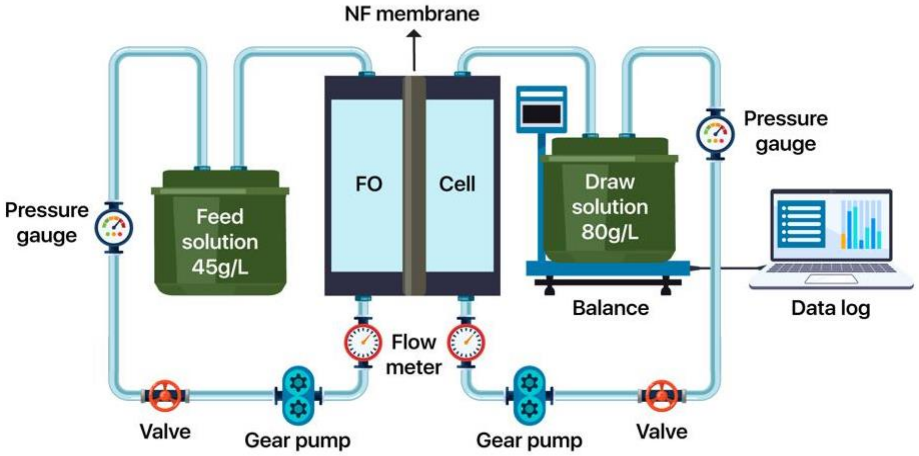

Figure 6.2. Schematic diagram of the laboratory FO system set up using NF membranes in the FO Cell.

6.2.4.**Test design**

In this study, each FO process using one NF membrane module was operated for 3 hours in a set of three consecutive runs where the membrane was washed in between with DI water for 30 min. The applied hydraulic pressure on the feed side changed from 0 bar in the first run to 2 and 4 bar in the second and third runs, respectively. A new NF membrane was used in each test, operated for 3 hours, washed and reused in the other two consecutive runs under the same operational parameters. Fouled and washed membranes at 0, 2 and 4 bar tests were imaged, and SEM images were taken when necessary.

6.2.5. **Analytical methods**

The conductivity and the pH of the feed and draw solutions were measured by HQ 14d portable conductivity meter from HACH, Australia. Feed and draw solutions samples were taken and stored for further analysis at the beginning and end of each NF process. The variation in the volume of the FS weight was recorded and used to calculate the water flux during the NF process according to **Equation 3.4 (Chapter 3)**. The recovery rate was also calculated using **Equation**

3.7 (Chapter 3). In addition, the specific energy consumption of each FO process was obtained using **Equation 3.8 (Chapter 3)**.

To study the FO process efficiency when NF membranes were used, the concentrations of divalent ions in the brine solution were measured before and after the FO process using an ion chromatography machine at the beginning and after each set of experiments. 7900 ICP-MS provided by Agilent technologies was used to measure Ca^{2+} and Mg^{2+} concentrations, whereas SO_4^{2-} was measured using Dionex VWDIC manufactured by HPIC. It is desirable to study the membrane surface morphology using scanning Electron Microscopy (SEM) to better analyse and understand water flux through the FO process. The cost of the NF membranes was also analysed and compared to the commercially available FO membranes (Porifera TFC and FTSH_2O CTA).

6.3. Results and discussions

6.3.1. **Membranes characterizations**

6.3.1.1. *Water permeability of the NF membranes in the FO process*

The NF membranes were tested in the FO process, and the effect of feed-applied hydraulic pressure on the water flux was obtained using a 2 LPM flow rate for both FS and DS (**Figure 6.3)**. The feed and draw solutions temperature was 25 °C and 40 °C, respectively. The water flux for the three NF membranes increased when the hydraulic pressure was applied. For the TS80 membrane, 5.7, 18, and 21.8 L/m^{2}h were the initials water flux at 0, 2 and 4 bar, respectively. Water flux reached 2.8, 8.8 and 10.6 L/m^{2}h, respectively, after 180min of operation (**Figure 6.3a**) due to DS dilution and possible membrane fouling. XN45 membrane water flux was 3.2, 14.3 and 15.6 L/m^{2}h at 0, 2, and 4 bar feed hydraulic pressures (**Figure 6.3b**). The lowest initial water flux was recorded by the UA60 membrane and was 3.1, 8.6 and 13.1 L/m^{2}h under 0, 2 and 4 bar hydraulic pressure (**Figure 6.3c**). Overall, the TS80 membrane achieved the highest water flux, followed by the XN45 membrane, followed by the UA60 membrane. TS80 membrane exhibited better water performance because of its high water flux and rejection rate to retain the DS from diffusion to the feed side. The UA60 membrane

exhibited the lowest water flux among the NF membranes because of its low rejection rate, which promoted DS loss through diffusion and compromised the osmotic driving force. As shown in the graphs in **Figure 6.3a**, in the PAFO process at 4bar, the TS80 membrane recorded the highest water flux (22 L/m^{2}h) compared to the XN45 membrane (16 L/m^{2}h) and the UA60 membrane (13 L/m^{2}h) (**Figure 6.3b&c,** respectively). Water flux in the TS80 membrane operating at 4 bar was 1.4 times higher than in the XN45 membrane and 1.7 times higher than in the UA60 membrane. Figure 6.3 shows that water flux at the end of the FO experiment using the TS80 membrane at all feed pressures was higher than in XN45 and UA60 membranes.

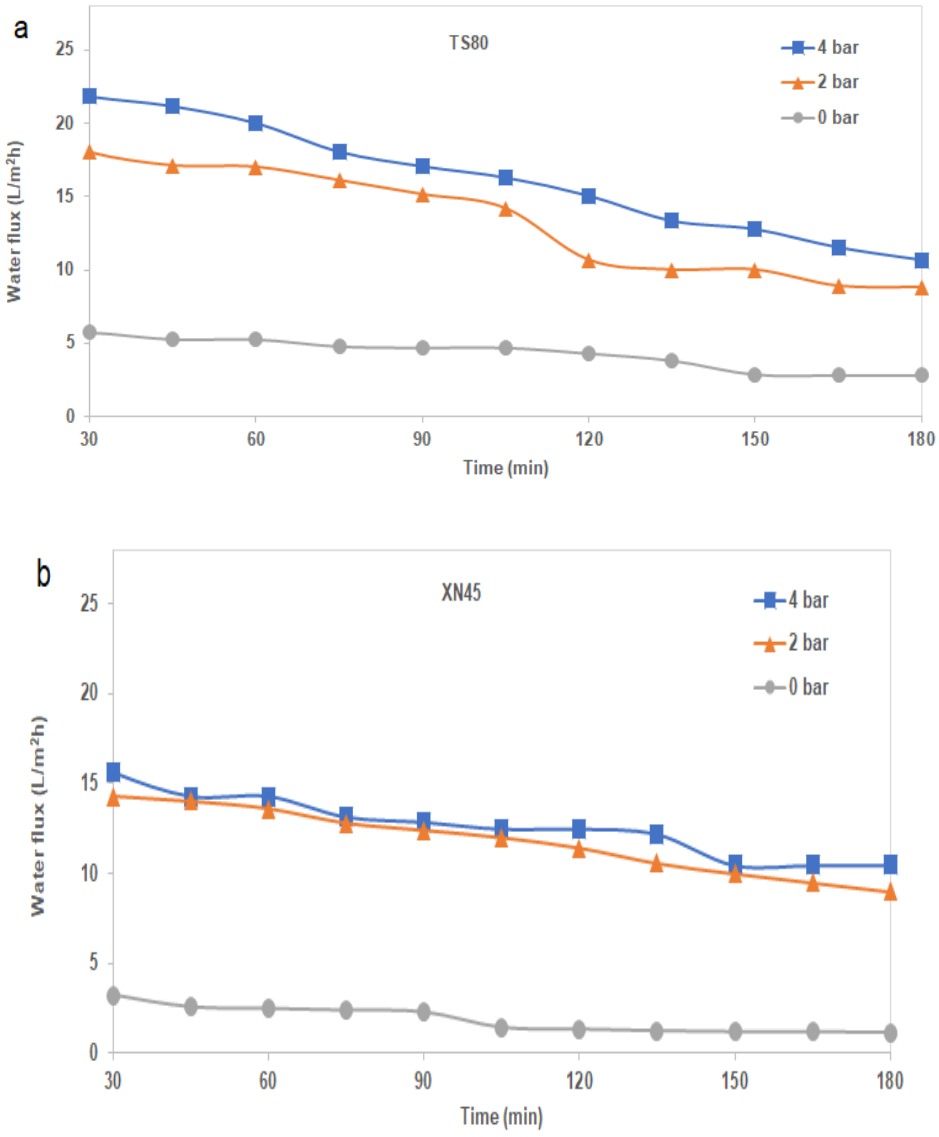

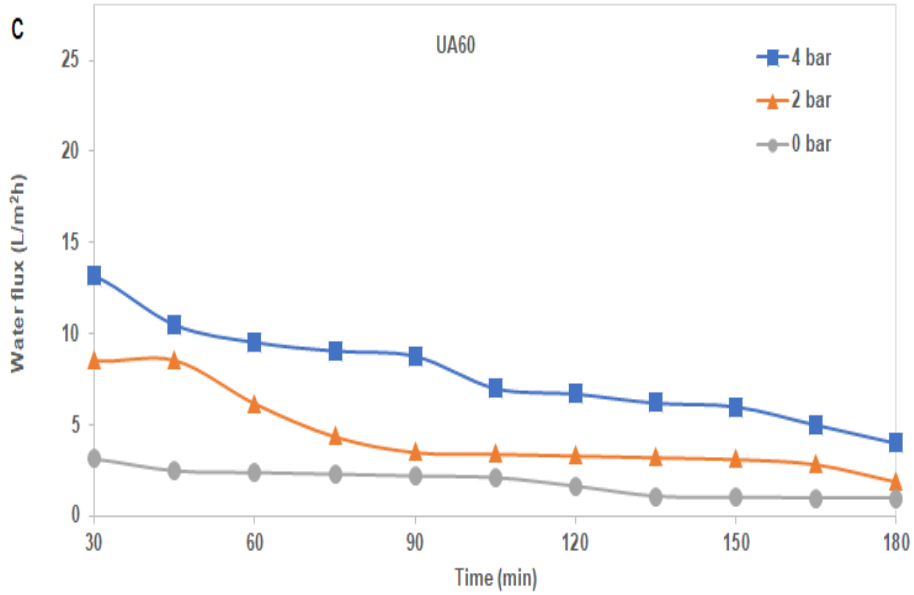

Figure 6.3. Water flux was calculated following the use of the three NF membranes, (a) TS80, (b) XN45 and (c) UA60, in the FO process at 0, 2, and 4 bar applied pressure in the Al-FS mode and 2LPM flow rate. (FS= seawater, 45g/L, 25°C; DS=brine solution, 80g/L, 40°C).

The difference in membrane structures and characteristics is clearly shown in the FTIR spectra of each membrane (**Figure 6.4**), as well as the values of the zeta potentials. Basically, the zeta potential impacts the rejection rate and the fouling performance of the membrane (Back et al., 2017; Zazouli et al., 2010). As highlighted in the FTIR spectra, the surface functional groups differ among the membranes, and the changes in spectra between pristine and used membranes were clearly shown. The peak height variations and distributions were observed, confirming that all three membranes underwent significant fouling.

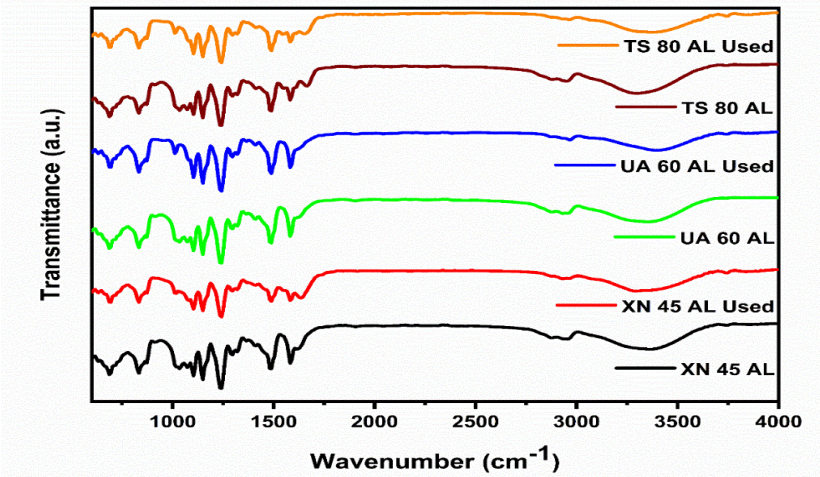

Figure 6.4. FTIR spectra of the new and used NF membranes.

The drop in the membrane flux over the 3 hours of operational time can be related to the reduction in the pressure gradient between the FS and the DS in the FO process, in addition to the membrane fouling (Jamil et al., 2016). Since the hydraulic pressure was maintained constant in the PAFO process, the water flux decline can be explained due to the foulant matter accumulation during the filtration process. **Figure 6.5** shows the average water flux of each NF membrane at different applied pressure; the average water flux in the TS80 membrane was 16.7 L/m^{2}h at 4 bar, 13.8 L/m^{2}h at 2 bar, and 4.4 L/m^{2}h at 0 bar. Indeed, applying 4 bar enhanced the process performance, showing a 21% improvement in the average water flux compared to the FO process at 2 bar. The average water flux reported in the XN45 membrane was 2, 12 and 13 L/m^{2}h at 0, 2, and 4 bar feed pressure compared to 1.9, 4.8 and 8.3 L/m^{2}h when the UA60 membrane was used, respectively. As expected, the average water flux in the NF membranes was in the following order TS80> XN45> UA60.

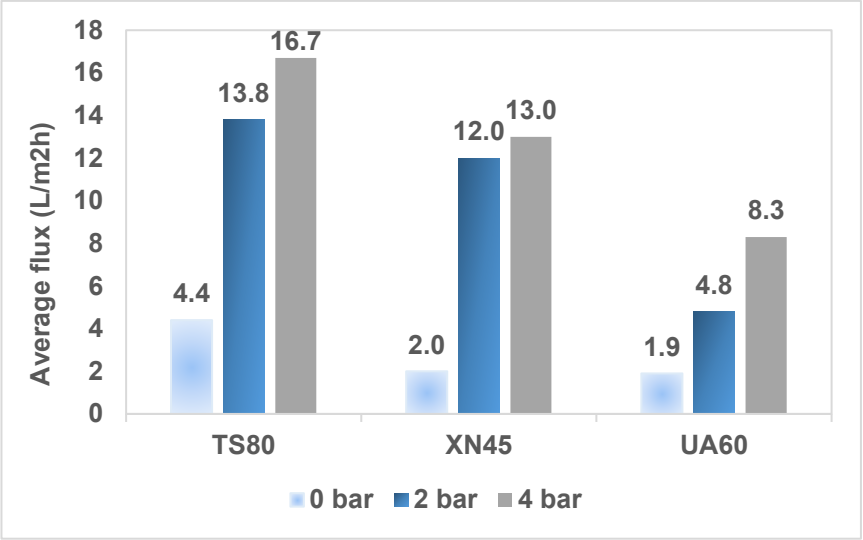

Figure 6.5. The average flux was recorded when NF membranes were used in the FO processes at 0, 2 and 4 bar applied pressure. FS= seawater, 45g/L, 25 °C; DS=brine solution, 80g/L, 40 °C; 2LPM flow rate.

It was reported that the membrane's surface properties and materials would affect the separation performance and, therefore, the water flux (Back et al., 2017). In the experiments mentioned above, the difference in structure between the membranes is clearly shown in SEM images of pristine membranes presented in **Figure 6.6**. The new and fouled TS80 membrane images are presented and compared with those of the XN45 and UA60**.** The fouling materials are clearly observed in **Figure 6.6 (d, e &f)**. The results correspond with other studies where the NF membrane that achieved the highest water permeability showed the greatest fouling and quicker flux decline (Parveen and Hankins, 2019). Also, in correlation with the manufacturer manual where TS80 membranes are mentioned in their characteristics, including the reject of divalent ions and organic solutes.

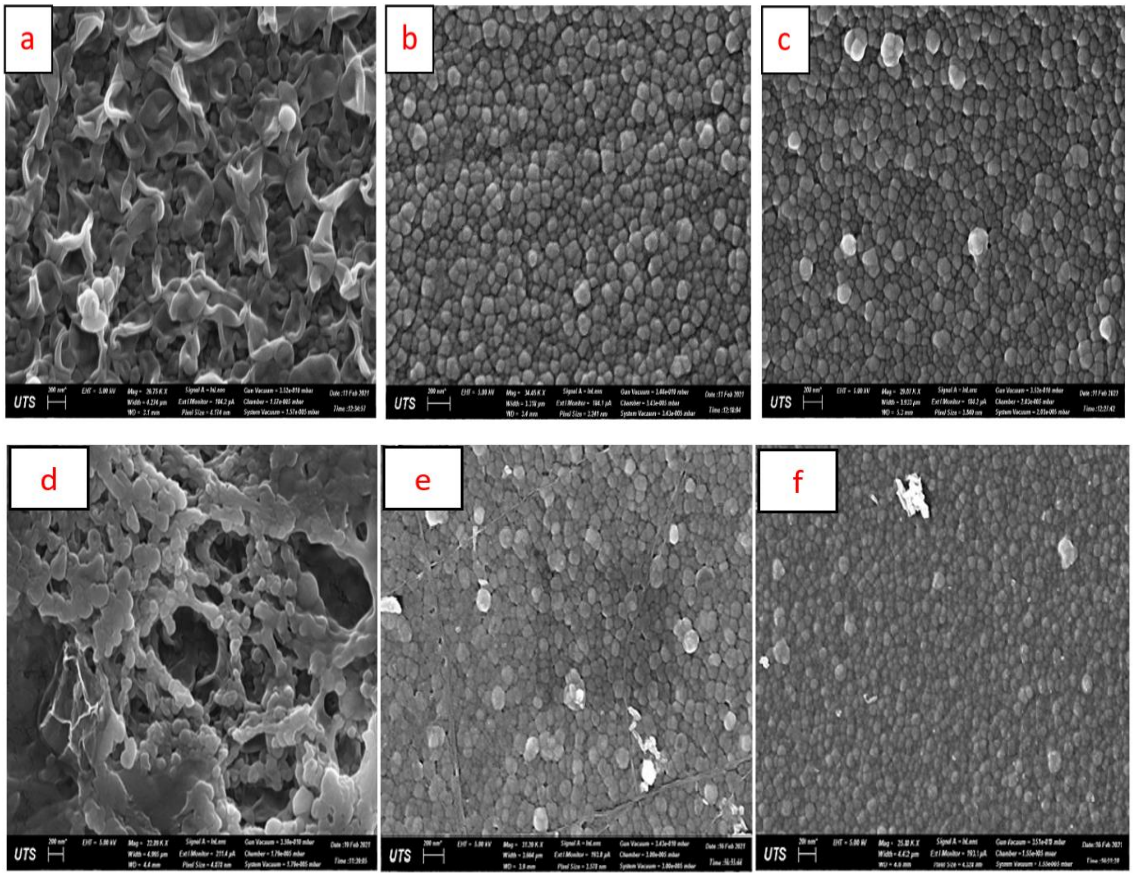

Figure 6.6. SEM images of pristine NF membranes. (a) TS80, (b) XN45 and (c) UA60 and fouled membrane at 4 bar, (d) TS80, (e) XN45 and UA60.

6.3.2. **Divalent ions rejection**

TS80, XN45 and UA60 NF membranes were used in the FO system in order to treat the MSF brine reject. Seawater (45g/L) at 25 °C was used as the FS, and 80g/L total dissolved solids concentration brine at 40 °C was the draw solution at a 2 LPM flow rate for both solutions. To study the effectiveness of the NF membranes, the latter were tested for calcium, magnesium, and sulfate ion concentrations in the brine solution at the end of each experiment. As mentioned earlier, these three ions were specifically studied as they are responsible for the scale deposition in the MSF plants. Data are presented in the percentage of ions dilutions for each membrane at different applied feed hydraulic pressures (**Figure 6.7)**. It is shown that the ions rejection increased when the applied feed pressure increased; therefore, higher dilution of the draw solution was achieved. The

dilution of Mg, Ca, and SO_4 ions using XN45 NF membrane at 4 bar was 16%, 20%, and 17%, respectively (**Figure 6.7b**). The corresponding percentages for the UA60 NF membrane under the same operating conditions were 22%, 23%, and 20%, respectively (**Figure 6.7c**). For an MSF desalination plant that operates at 110 °C top brine temperature and 8 gain output ratio (GOR), the target multivalent reduction percentage is 14% (Morin, 1993). It is clear in **Figure 6.7a** that the highest divalent ions reduction percentage was recorded for the TS80 NF membrane operated at 4 bar feed pressure. The TS80 NF membrane achieved 25%, 27%, and 28% dilution of Mg^{2+}, $Ca^{2+}$and SO_4^{2-}, respectively. The diluted brine solutions were previously analysed for the divalent ions reductions under the same operational parameters, using Porifera TFC and FTSH_2O CTA FO membranes. The analytical test revealed that the dilution of the divalent ions at 4 bar for THF FO was 17%, 17% and 22% and 15%, 22% and 21% for Mg, Ca and SO_4, respectively (**Figures 6.7d and 6.7e**). When comparing the performance of NF and FO membranes, the TS80 NF membrane showed the best performance compared to the TFC FO membrane, which achieved 22% to 66% lower dilution of the brine than the TS80 NF membrane when PAFO in the FO system operates at 4 bar.

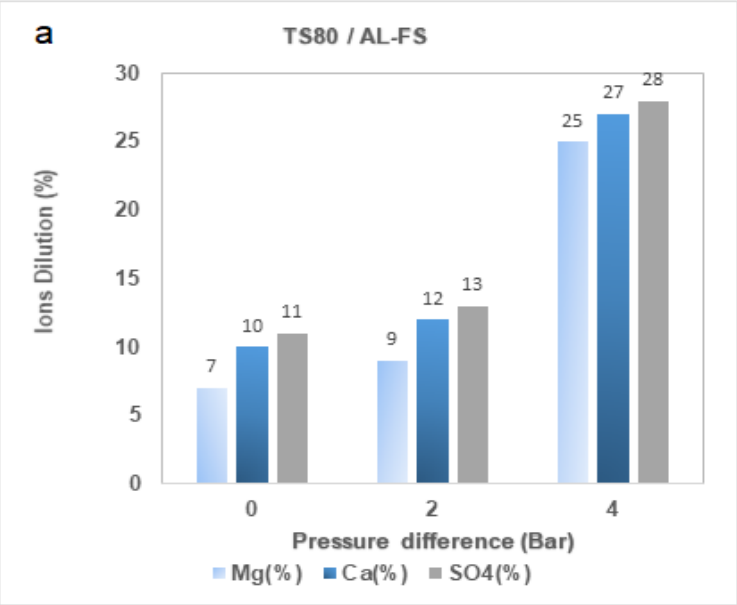

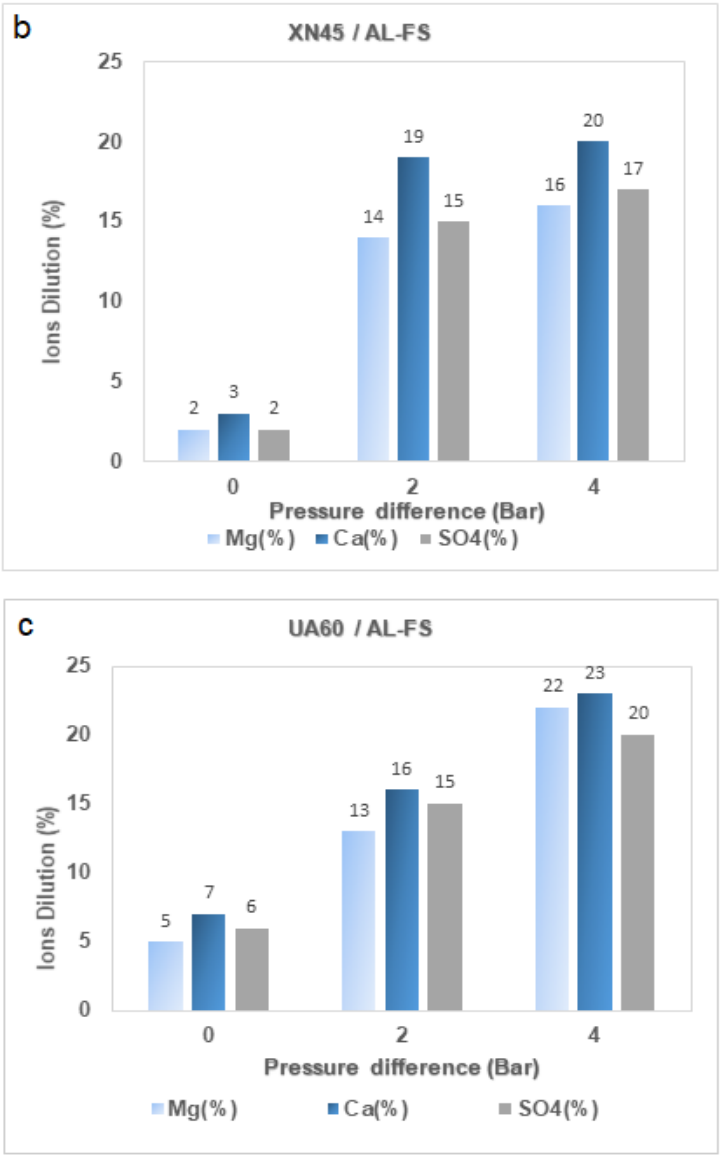

Figure 6.7. The percentage of ions dilution in the DS following the FO process (PAFO) using (a) TS80, (b) XN45 and (c) UA60 NF membranes, respectively. (FS= seawater, 45g/L, 25 °C; DS=brine solution, 80g/L, 40 °C; 2LPM flow rate; AL-FS orientation).

6.3.3. **Effect of applied pressure on the water recovery rate**

The water flux in the FO experiments using the XN45 membrane at 4 bar was 16 L/m^{2}h which is around 1.5 times higher than the flux achieved in the CTA FO membrane and under the same experimental conditions (**Figure 4.4A, Chapter 4**) but in a similar range of the water flux of the TFC/FO membrane (**Figure 4.3A, Chapter 4**). What is remarkable is that the water flux of TS80 at 4 bar, 22 L/m^{2}h

counted as double the water flux of the CTA FO membrane and around 1.4 times of the TFC Porifera FO membrane. Hence, the recovery rate when the FO experiments used the TS80 NF membrane was the highest on a large scale. Analysing the data (**Figure 6.8**) revealed that when no pressure was applied (0 bar), the recovery rate was 2.6%, increased to 8.3% at 2 bar and reached 10% when 4 bar feed hydraulic pressure was applied. XN45 NF membrane, in its turns, recorded a 7.8% recovery rate at 4 bar and 7 % at 2 bar, with only 1.2% at 0 bar. The lowest water recovery was 1.1% when UA60 operated at 0 bar, 2.9% and 5% at 2 and 4 bar, respectively. The recovery rate in all three membranes was the highest at 4 bar; this could be explained due to the pressure added to the same direction of the FS that promotes further water penetration throughout the membrane. A previously collected data on the TFC and CTA FO membranes recovery rate is incorporated in **Figure 6.8**. The maximum recovery rates of CTA and TFC FO membranes in the AL-FS orientation at 4 bar were 7.6% and 6.6% for TFC and CTA, respectively, where values were closer to the XN45 NF values. According to **Figure 6.8**, it is evident that the TS80 NF membrane showed the highest recovery rate compared to the NF and FO membranes.

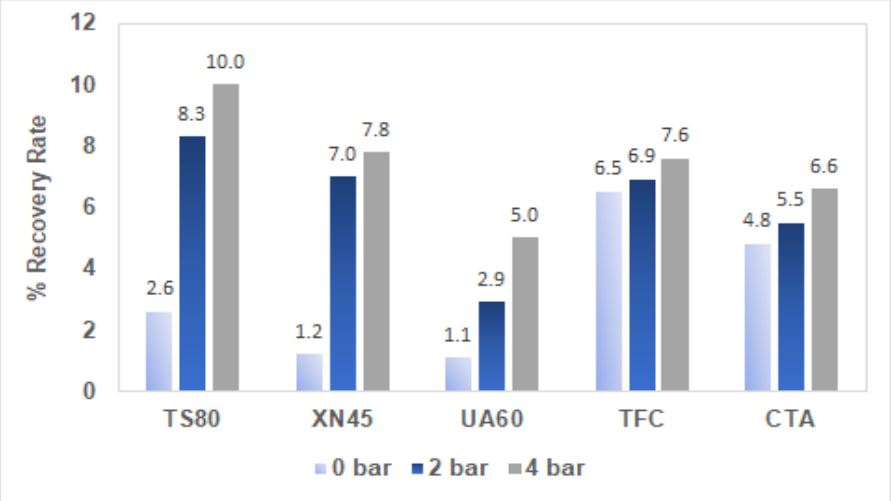

Figure 6.8. Water flux recovery rate of NF membranes (TS80, XN45 and UA60) and FO membranes (TFC and CTA) in PAFO process at 0, 2 and 4 bar. (FS= seawater, 45g/L, 25 °C; DS=brine, 80g/L, 40 °C; 2LPM flow rate).

6.3.4. **Energy consumption**

In this study, the FO process implemented low cost, high permeability and thin support layer (~200μm) NF membranes. The NF membrane operation requires hydraulic pressure (PAFO process) to be competitive with the FO membranes. Experimental work on the PAFO processes using FO membranes (at 4 bar and 2 LPM flow rate) showed that the specific power consumption was only 0.05 and 0.08 kWh/m^3 for the TFC and CTA FO membranes, respectively. Each membrane's energy consumption at different applied pressures is presented in **Figure 6.9**; 0.04, 0.05, and 0.07 kWh/m^3 was the energy consumption calculated at 4 bar for TS80, XN45 and UA60, respectively. It is noticeable that the energy consumed when the TS80 membrane was used in the FO process was lower than the other two NF membranes and the FO membranes due to the higher water flux achieved in the TS80 membrane. **Equation 3.8, Chapter 3** shows that the specific power consumption is inversely proportional to the permeate flow (Q_p) in the FO process. As such, when the permeate flux decrease, specific power consumption increases. This explains why the specific power consumption in the FO process using UA60 and XN45 NF membranes was higher than in the TS80 NF membrane.

Experimental work results showed that PAFO at 4 bar using the TS80 NF membrane consumed the least energy compared to the TFC and CTA FO membranes. Therefore, according to **Figure 6.9** PAFO process using NF membranes is feasible for diluting the brine solution without a significant increase in energy consumption.

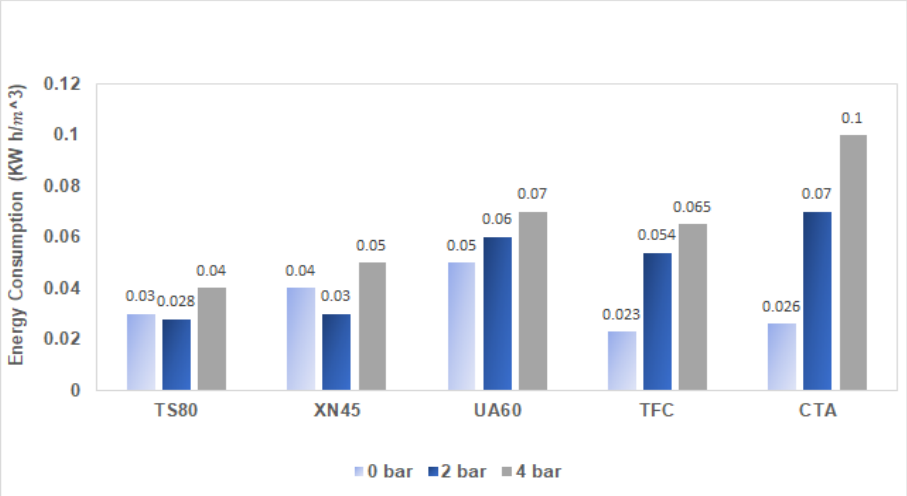

Figure 6.9. Energy consumption of the FO process using TS80, XN45 and UA60 NF membranes in the AL-FS mode at 0, 2 and 4 bar. FS= seawater, 45g/L, 25°C; DS=brine solution, 80g/L, 40°C; 2LPM flow rate.

6.3.5. **Cost analysis**

The membranes' cost was presented based on reported data and quotes for TRISEP®, Porifera, and HTI. The commercially available NF membranes are 10 times cheaper than the FO membranes. A CTA FO membrane costs US$ 1.719 per element for an area of 16.5 m2 compared to US$ 600 for a 40 m^2 TS80 NF membrane. The cost of the CTA FO membrane (model 8040FO-FS-P) required for 10.000 m^3/d FO is US$ 5.426.136, while the cost is remarkably lower when using TS80 NF for the same capacity, US$ 274.582. The CTA FO membrane cost is 20 times more than the TS80 NF membrane for an FO plant of 10.000 m^3/d (**Table 6.1**).

There is a cost-benefit in using the TS80 NF membrane compared to the commercial FO membranes. For example, a 10,000 m^3/d FO plant using a TFS CTA FO membrane will cost US$ 5,426,136 compared to US$ 274,582 using a TS80 NF membrane. The cost is based on 16.5 m^2 CTA FO membrane model 8040FO-FS-P at US$ 1,719 per element, while the cost of 40 m^2 TS80 NF membrane is assumed to be US$ 600 per element (cost per market price of previous HTI FO membrane and commercial NF membranes). The CTA FO

membrane cost is 20 times more than the TS80 NF membrane for a 10,000 m^3/d FO plant. Also, the number of pressure vessels of the CTA FO membrane is more than the TS80 NF membrane.

Table 6.1. cost of CTA FO and TS80 NF membrane required for 10,000 m^3/d capacity plant. The cost of the CTA FO membrane is US$ 1,719 and of the TS80 NF membrane is US$ 600. The membrane area is 16.5 m^2 and 40 m^2 for CTA FO and TS80 NF membranes, respectively.

Membrane	Membrane Area (m^2)	No. Element	Cost US$
TS80 4 bar	18305	458	274,582
CTA	52083	3157	5,426,136

6.4. Conclusions

To investigate their effectiveness in pretreating the feed water prior to the MSF desalination plant, three commercial NF membranes (TS80, XN45, UA60) were tested in a laboratory-scale FO testing unit to determine their potential in brine rejections recycling. The experiments were carried out with applied hydraulic pressure on the feed side (up to 4 bar), seawater salinity of 45 g/L and brine solution of 80 g/L. The results showed that the recovery rate and the membrane permeability increased with the hydraulic pressure applied on the feed side. TS80 NF membrane has the highest water flux of 22 L/m^2h at 4 bar applied pressure achieving 21% improvement in the average flux when 2 bar was applied. The PAFO process at 4 bar using TS80 in the FO system recorded 22% to 66% higher ions reduction compared to the TFC FO membrane. 0.04 kWh/m^3 was the maximum specific power consumption at 4 bar using the TS80 NF membrane, which is remarkably low compared to the CTA FO membrane energy consumption under the same operational parameters. It is thus concluded that NF membranes have the potential to be implemented in the FO system to dilute the MSF brine solution.

Chapter 7: Nanofiltration membranes Application in the Forward Osmosis process for MSF brine dilution with Tertiary Sewage Effluent

Abstract

In this chapter, treated wastewater and Multi-Stage Flash (MSF) brine was integrated into the Forward Osmosis (FO) system using commercial Nanofiltration (NF) membranes to dilute the MSF plant brine reject. The latter solution is usually concentrated with divalent ions such as magnesium, calcium, and sulfate that precipitate in the heat exchanger tubes at high operating temperatures. The deposition of magnesium sulfate and calcium sulfate in the MSF plants is one of the main issues affecting the performance and efficiency of the thermal desalination process. Reducing the concentration of the divalent ions can minimize the scale formation and deposition to a level that the MSF plant can operate at higher temperatures. The NF membranes were chosen to be used in the FO system as they are cheaper than the FO membranes and are able to reject various divalent ions. Pressure-assisted FO (PAFO) experiments were conducted in the FO mode using three NF membranes (TS80, XN45 and UA60). The maximum hydraulic pressure of 4 bar was applied on the active layer of the NF membranes since they are designed to tolerate pressure. The only noticed

issue with the NF membrane structure is the larger structural parameter compared to the FO membranes, which might lead to serious internal concentration polarization. In all the experiments, the wastewater temperature remained 25 °C while 40 °C was the brine operational temperature. A maximum water flux of 39.5 L/m^2h was recorded at 4 bar feed pressure when the TS80 NF membrane was used for the brine dilution, achieving up to 42% divalent ions dilution.

7.1. Introduction

Despite the advantages of thermal desalination, it suffers from various drawbacks that can affect the overall process. MSF, one of the leading thermal-based desalination techniques, faces the problem of non-alkaline scale formation on the heat exchanger tube at high operating temperatures. The ionic species responsible for the non-alkaline scaling are mainly Ca^{2+}, Mg^{2+}, and SO_4^{2-}. The scale deposition results in augmenting the power consumption and increasing the overall cost. Currently, different techniques are used to mitigate fouling, such as Antiscalants and periodic physical cleaning of the MSF plant tubes. As an alternative to these techniques, feed water pretreatment using the membrane process was proposed. Ata initially proposed the NF separation process to remove the ions responsible for scaling (Hassan, 2006). It is a membrane technology intermediate between reverse osmosis (RO) and ultrafiltration in terms of pore size. The NF membranes have selectivity for various organic and inorganic microorganisms and divalent and multivalent ions. The NF technique is widely used in filtration applications, including industrial wastewater treatment to remove compounds and ions from water, the textile industry to remove colour, the food industry for concentration and recovery, and the water industry as a pretreatment for other desalination techniques (Mulyanti and Susanto, 2018). NF pilot plants were used for seawater filtration to the MSF plants in Saudi Arabia; this implementation successfully increased the top brine temperature (TBT) in the MSF to 120 °C without scaling issues (Hamed et al., 2005). In a study conducted by Wafi et al. (2018) in Qatar, the three years performance of standalone RO and NF pilot plants for seawater desalination was recorded and analysed. The results demonstrated the dominance of the NF desalination process, where NF recorded

29% less energy consumption and 29% less cost. The major drawback was the problem of fouling which was explained to be related to the membrane quality (Wafi et al., 2019). Despite the NF technique characteristics of low energy consumption compared to the RO and the high rejection rate of a wide range of commercial NF membranes, the NF process is not yet commercialized in seawater treatment. Data collection based on studies and pilot-scale operations showed the feasibility of the NF technique in wastewater treatment if fouling, poor durability, instability and low flux can be controlled (Abdel-Fatah, 2018). To determine the suitability of the NF process as a pretreatment prior to desalination plants, Hilal et al. studied the performance of three commercially available membranes (NF90, N30F, NF270) in treating high salinity salt solutions similar to the seawater salinity. The results showed that NF90 achieved salt rejection of 95% at high salinity at a pressure of 9 bar (Hilal et al., 2005). In another study, an NF polypiperazine membrane was used for brackish groundwater treatment at a 6-10 bar pressure range. The NF membrane was able to remove 70-76% of hardness; however, it only achieved 44-66% salinity removal.

In this study, TSE was proposed to be used as the feed solution (FS) in the FO system with three commercially available NF membranes (TS80, XN45 and UA60) for diluting the MSF brine solution, i.e. the DS. The FO system was designed to reduce the divalent ions responsible for scale deposition in the MSF plants. The tertiary sewage effluent (TSE) temperature was maintained at 25 °C, and the brine was 40 °C. Since the NF process is pressure-driven, hydraulic pressures up to 4 bar were applied on the TSE side to promote water flux. The AL-FS orientation was the operational mode in the FO experiments to avoid the delamination of the selective membrane layer at the applied feed pressure. The feed and draw solution was filtered using a microfilter of 20 µm to remove the turbidity and the organic matter. The performance of each membrane was represented by the water flux calculation, the flux reduction, the ions concentrations and the energy consumption.

7.2. Materials and Methods

7.2.1. **NF membranes**

TS80, XN45, and UA60 were the three commercially available NF membranes used in this study. The characteristics of each membrane are presented in **Table 3.3, Chapter 3**.

7.2.2. **Stream solutions**

In this study, treated wastewater (TSE) was the FS and brine solution was the DS. The Blacktown wastewater treatment plant in Sydney (Australia) provided the TSE samples. The brine concentration was 80 g/L and maintained at 40 °C temperature during the experiments. The TSE TDS was 0.9 g/L and maintained 25 °C temperature during the FO experiments. The osmotic pressure of the DS was about 70.4, whereas the FS osmotic pressure was about 0.804 bar; the osmotic gradient between the two streams was remarkably high for promoting a considerable water flux. The characteristics of the TSE are presented in **Table 3.1, Chapter 3.** The turbidity and the TOC of the stream solutions before and after prefiltration were summarized in **Table 5.1, Chapter 5**.

7.2.3. **Lab-scale setup**

A detailed demonstration of the bench-scale FO system setup used in this study is presented in **Chapter 3, section 3.2.4**. **Figure 7.1** illustrates the FO system used in the experiments.

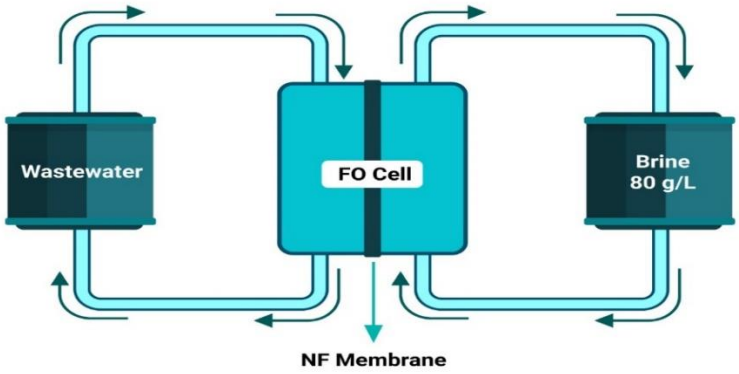

Figure 7.1. Illustration of the experimental lab-scale setup.

7.2.4.**Experimental work**

The first task was the prefiltration of the stream solution. The TSE and brine solution were filtered using HP4750 dead-end stirred cell (Sterlitech, USA). The 20 micron Whatman membrane was placed perfectly against the porous disc to avoid leakage, and filtration was run at 1 bar and 20 °C. The active membrane area is 17.3 cm^3 and 47-48 mm is the diameter.

The MSF brine solution was prepared by seawater concentration to reach the salinity of the real brine reject of the MSF plants. Each FO experiment was operated at a 2 LPM flow rate for 180 min, repeated three times on the same membrane with physical cleaning of the membrane after each cycle. The cleaning was performed with DI water for 30 min and at 40 °C. All the experiments were operated in the FO mode, where membrane AL faces FS. For the TS80 NF membrane, each set of experiments was conducted at 0, 2 and 4 bar, respectively. For XN45 and UA60, the four cycles of the FO process were operated at 4 bar.

7.2.5.**Analytical methods**

Section 3.3.2, chapter 3 presents the methods to determine the water flux, the flux reduction, and the reverse solute flux. The specific energy consumption of the FO process was detailed in **section 3.3.3**, **chapter 3**.

7.3. Results and Discussion

7.3.1. **Flux patterns with applied pressures and membrane modules**

Commercial NF membranes require hydraulic pressure to operate. Since the FO system is based on a naturally driven separation process, a PAFO of a maximum pressure of 1 to 4 bar was applied for ion filtration. This feed pressure is to overcome the membrane resistance, much lower than the hydraulic pressure required in the NF membrane filtration of MSF brine, 15 to 25 bar (Hassan, 2006). The TS80 membrane was tested at 0, 2, and 4 bar; **Figure 7.2** displays the variation of the water flux with time and the applied pressure. The water flux was calculated according to **Equation 3.4, chapter 3**. Results show that the highest flux recorded for the first cycle at 0 bar was 8.5 L/m^{2}h but increased to 14.8 L/m^{2}h and 45 L/m^{2}h at 2 and 4 bar, respectively. The water flux decreased to 5.4, 10 and 34 L/m^{2}h at the end of 180 min cycle one at 0, 2 and 4 bar, respectively. Following three consecutive 30 min cleanings with 40 °C DI water, cycle 4 showed that the initial flux was 6.5, 12.5 and 40 L/m^{2}h at 0, 2 and 4 bar, respectively. According to Figure 7.2, in all cases, the water flux decreased over time with a remarkable slight decrease at 4 bar (**Figure 7.2c**) compared to 0 and 2 bar. The reduction flux was 19, 24 and 15% for the TS80 at 0, 2 and 4 bar, respectively. This behavior might be related to the structure and the characteristics of TS80 compared to XN45 and UA60. Chemical or more sophisticated pretreatment could be applied for membrane cleaning and fouling reduction.

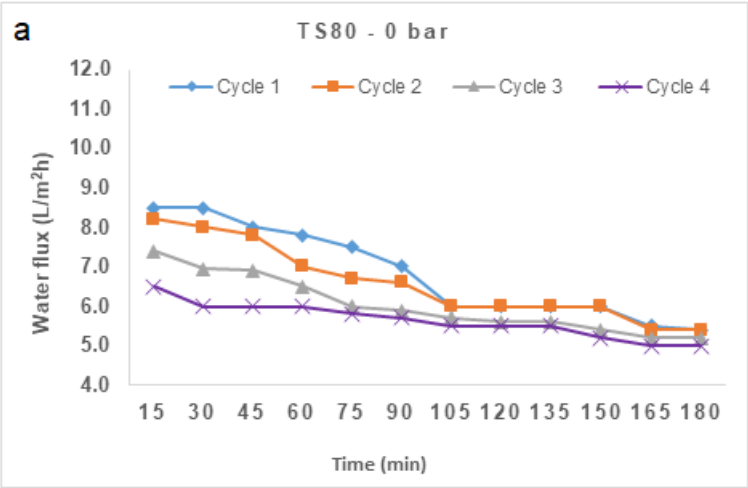

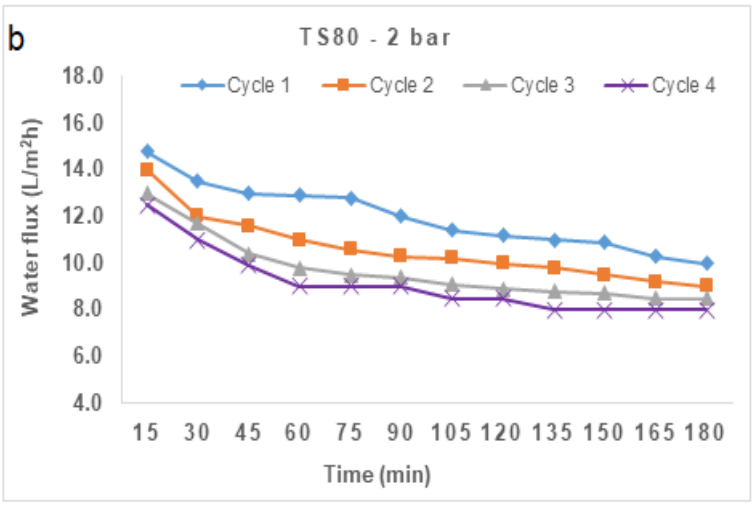

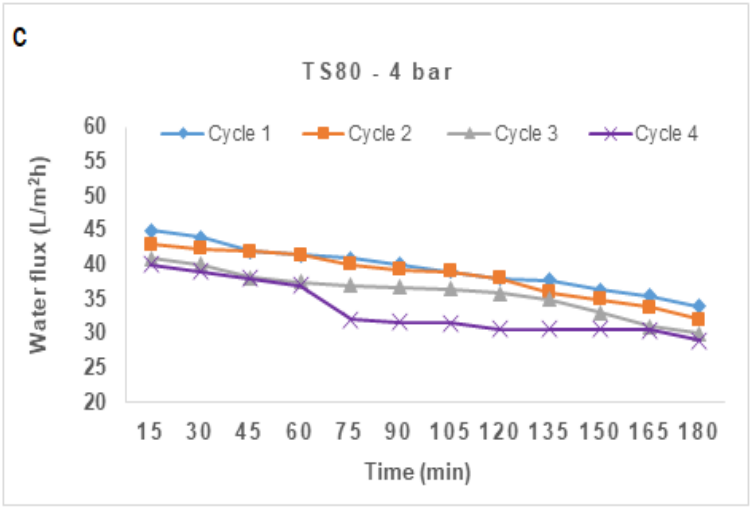

Figure 7.2. The water flux of the FO system using TS80 membrane at 0, 2 and 4 bar for the 4 FO process cycles.

The other two NF membranes were used in the FO system operated at 4 bar only since water flux at 0 and 2 bar feed pressure was insignificantly less than at 4 bar. As shown in **Figure 7.3**, the membrane XN45 recorded a maximum water flux of 42 L/m^{2}h for the first cycle that decreased to 33.2 L/m^{2}h at the end of the cycle. The initial water flux using XN45 in cycle 4 was 38 L/m^{2}h (**Figure 7.3a**), indicating a 9.5% reduction in water flux compared to the first cycle. 35 L/m^{2}h was the initial flux in cycle 1 for the membrane UA60 and decreased to 27 L/m^{2}h after 180 min filtration time. Following three consecutive cleaning with DI water, 30 L/m^{2}h was the initial water flux for cycle 4 (**Figure 7.3b**). For filtration cycle 4,

the water flux reduction was 14.3% compared to cycle 1. The graphs clearly demonstrate that the performance of the TS80 NF membrane in terms of water permeability outstands the other two NF membrane modules.

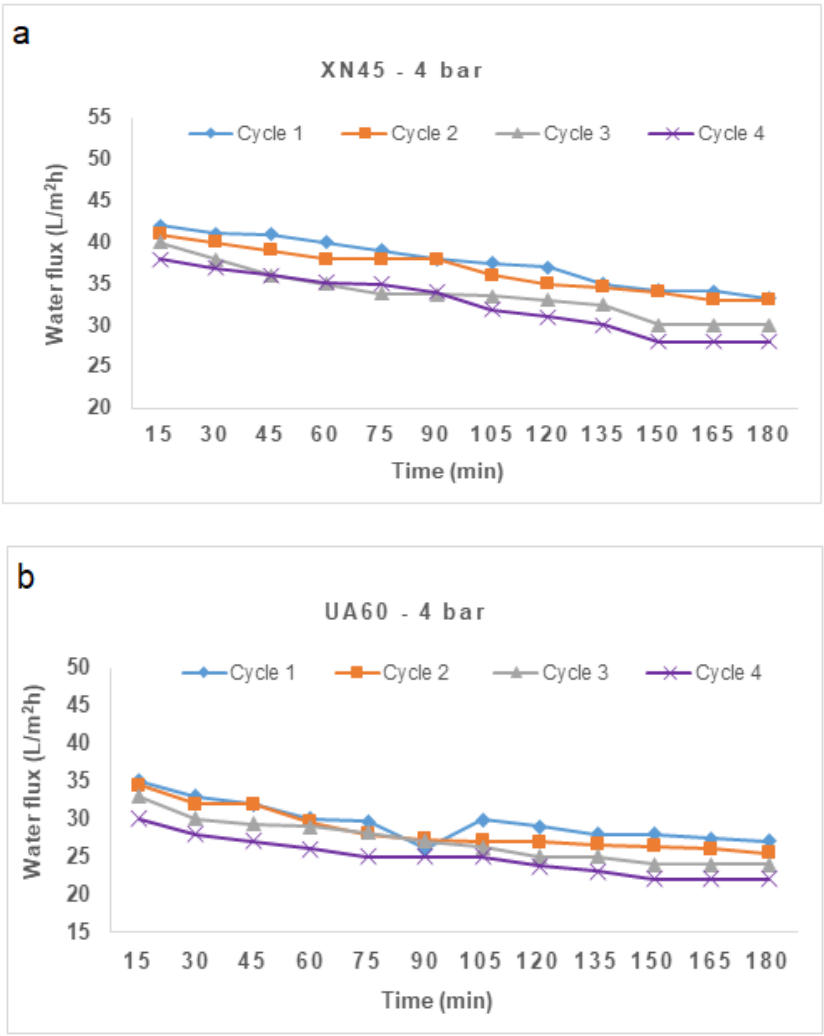

Figure 7.3. Water flux pattern with the time in the FO system at 4 bar when a) XN45 and b) UA60 membranes were used.

To yield a better understanding on the behavior of the NF membranes in the FO system with TSE the FS, the values were compared with data previously collected when seawater FS was used under the same operational parameters using NF membranes (**Chapter 6**). The average water flux at 4 bar using the NF membranes in the FO system recorded 39.5 L/m^{2}h for the membrane TS80, 37.6 L/m^{2}h for the membrane XN45 and 29.5 L/m^{2}h for the membrane UA60 (Figure 7.4). For the FO tests with seawater feed solution, the average water flux for the

TS80 NF membrane was 16.7 L/m^{2}h, 13 L/m^{2}h for the XN45 NF membrane and 8.3 L/m^{2}h for the UA60 NF membrane. The water flux in the membrane TS80 at 4 bar when TSE was used as the FS was 2.3 times higher than when the FS was 45 g/L seawater. In addition, the water flux using TS80 and TSE NF membranes at 4 bar feed pressure is 6.3 and 5.8 times higher than the water flux recorded in the FO process using TFC and CTA FO membrane in the AL-FS mode and seawater (45g/L) feed stream, respectively (**Chapter 4**). The water flux recorded when TSE FS and TS80 NF membrane were integrated into the FO system at 4 bar is promising, knowing that the higher permeation flux and the slight decrease in the water flux during the FO process might result in higher dilution of the brine solution.

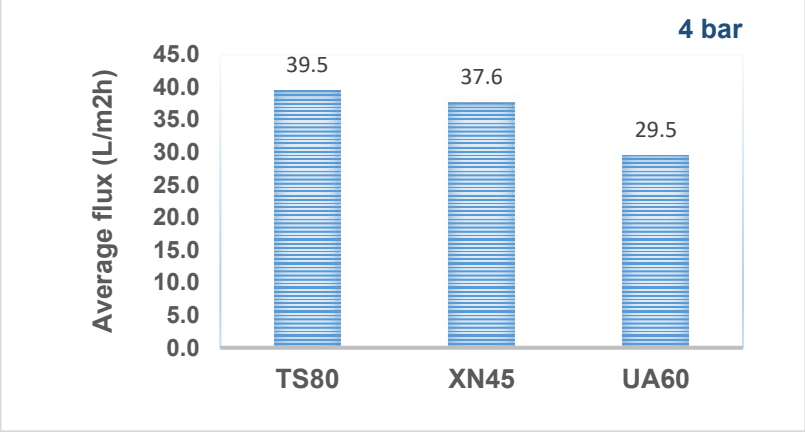

Figure 7.4. Comparison of the average water flux of the NF membranes (TS80, XN45, UA60) operating at 4 bar for four cycles.

Alongside the water flux, another phenomenon known as RSF occurs despite the high solute rejection property of the separation membranes. RSF is an additional issue that might affect the performance of the FO system. An amount of the draw solute can penetrate the membrane from the draw side toward the feed side. RSF was calculated, and results showed that at 0 bar using the TS80 NF membrane, the RSF was 12.7 g/m^{2}h, followed by 22.4 and 25.7 g/m^{2}h when the FO system was operated at 2 and 4 bar, respectively. The RSF values were recorded using TSE FS in the FO system, and brine reject DS is a promising step to achieve

higher flux with no resource loss. When comparing these values with the RSF when TS80 was used in the FO system using DI water FS and 0.5M NaCl DS, the results were 8.1, 10.6 and 24.4 g/m^{2}h at 0, 2 and 4 bar, respectively.

7.3.2. **Cleaning efficiency and fouling reversibility**

In the physical cleaning, DI water at 40 °C was used for 30 min to wash the fouled membrane after each cycle. The washed membrane was then reused in three consecutive cycles. DI water flushing is widely used and is considered adequate in restoring the water flux (Ibrar et al., 2020b). As shown in **Figure 7.5**, the water flux reduction was the lowest after the first wash, with only 2.5, 2.76 and 3.72% reduction for membranes TS80, XN45 and UA60, respectively. After the final wash, these values increased to 18.33, 13.4 and 15.8%. Following three consecutive cleaning with hot water at 40 °C, the percentage of water flux reduction was the highest after the third cleaning. It might be due to the accumulative fouling effect on the membrane surface in the consecutive filtration cycles.

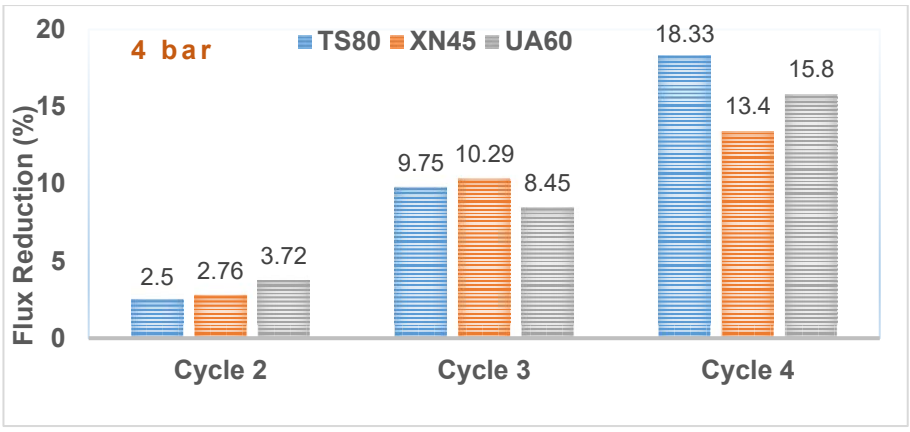

Figure 7.5. Illustration of flux reduction after each cycle for each membrane at 4 bar applied pressure.

The fouled and washed membranes were tested using a scanning Electron Microscope. The fouling materials were clearly shown on the surface of the AL of the NF membranes (**Figure 7.6 a,c&e**). After flushing with hot DI water for 30

min, the foulants were largely removed, explaining the reversibility of the fouling (Figure 7.6 b,d&f). The results of the water flux reduction following the membrane cleaning were in agreement with the SEM images (**Figure 7.6**).

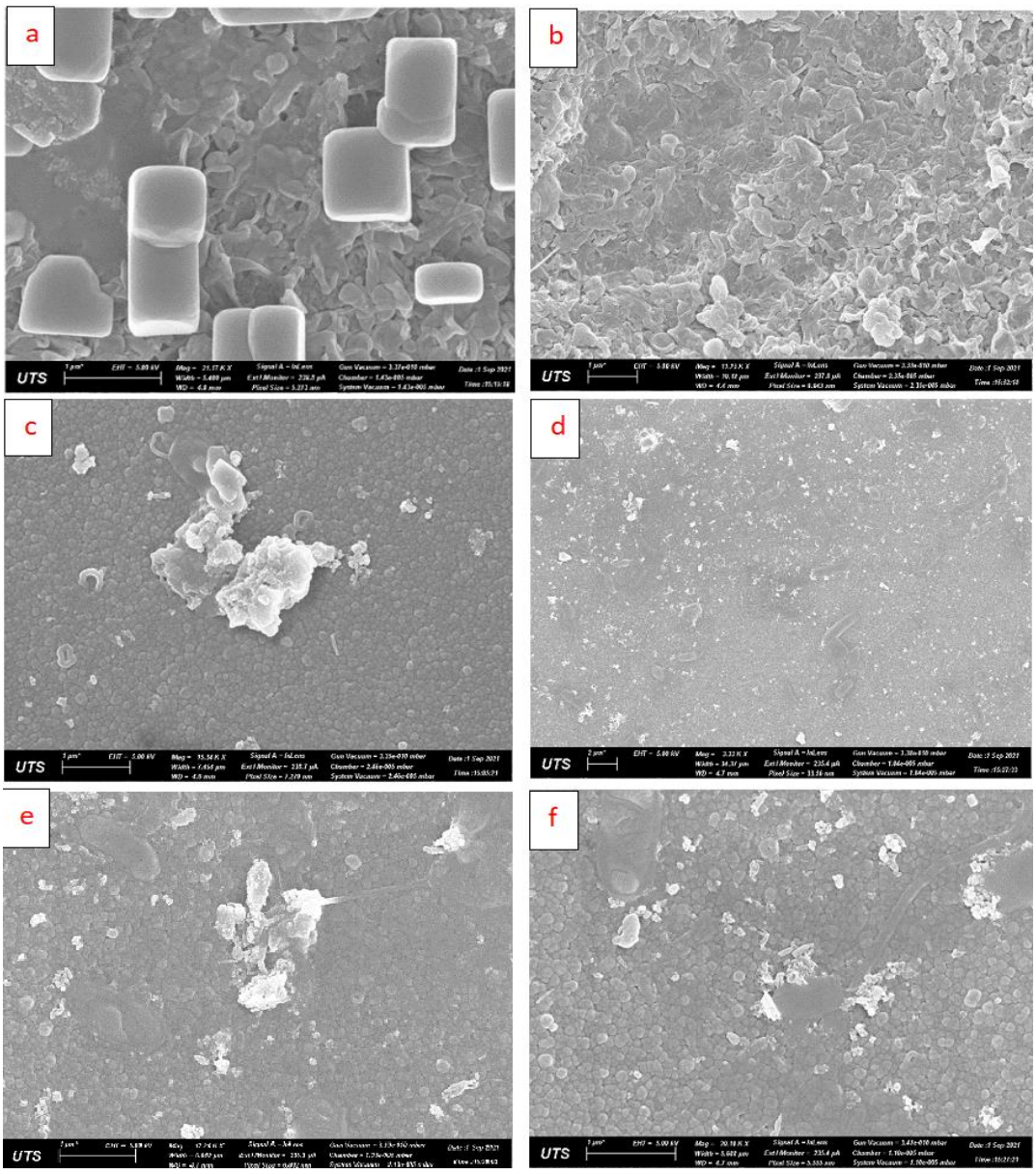

Figure 7.6. SEM images of the fouled and cleaned NF membranes when FO operated at 4 bar: a) TS80 fouled, b) TS80 washed with hot DI water, c) XN45 fouled, d) XN45 washed, e) UA60 fouled, UA60 washed.

Mitigating the fouling matters using physical cleaning is an indication that the NF membranes can be reused without severely affecting the water flux and, therefore, the overall performance of the FO system.

7.3.3. **Removal of ionic species**

The NF membranes were investigated for their potential to remove or reduce the divalent ions from the MSF brine. TS80, XN45 and UA60 NF membranes were tested for rejection of magnesium, calcium, and sulfate ions. The diluted DSs from the experiments were analyzed for these ions at the end of the FO experiments. Ions dilution in percentage at 4 bar for each NF membrane is presented in **Figure 7.7**. The results revealed that the dilution of Mg^{2+}, $Ca^{2+}$and SO_4^{2-} using TS80 membrane was 40, 42 and 32%, respectively. The corresponding percentages for the XN45 membrane were 28, 25 and 27% and for the UA60 membrane were 19, 16 and 23 %, respectively. The highest draw solution dilution achieved when seawater (45g/L) was used as an FS in the FO system with the three NF membranes was 27, 25 and 28% (**Figure 6.7, chapter 6**). These values were obtained with the TS80 membrane under the same operational parameters but seawater feed solution.

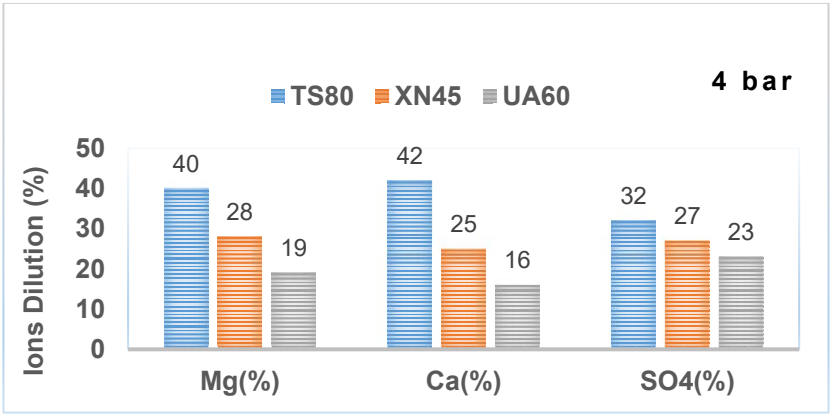

Figure 7.7. The percentage of Mg, Ca and SO_4 ions dilutions at 4 bar using TS80, XN45 and UA60.

The TS80 NF membrane outstands the TFC FO membrane for its capacity of reducing the divalent ions in the brine solution while using treated wastewater as FS. 17, 17, and 22% were the percentage of ions dilutions recorded for TFC membrane for Mg^{2+}, $Ca^{2+}$and SO_4^{2-}, respectively (**Figure 6.7, Chapter 6**). The best performance TS80 NF membrane achieved approximately 2.4 times higher

dilution for Mg^{2+} and Ca^{2+} and ~1.5 times for SO_4^{2-} than the TFC FO membrane when the PAFO process was operated at 4 bar feed pressure.

7.3.4. **Energy consumption**

The energy consumption was calculated using **Equation 3.8** (**Chapter 3**), and the results are presented in **Figure 7.8**. The specific power consumed in the prefiltration process of the solutions was calculated using **Equation 3.9** (**Chapter 3**), and 0.034 kWh/m^2 was the amount of energy consumed for the prefiltration of stream solutions before the FO process. This extra energy is not added to the values presented in **Figure 7.8**. The experimental work at 4 bar using membranes TS80, XN45 and UA60 and TSE pre-filtered FS showed that the specific power consumption was only 0.02, 0.02 and 0.03 kWh/m^3, respectively (**Figure 7.8**). The energy consumed in this study was the lowest compared to the previous experiments with commercial FO membrane or with NF membrane and seawater FS. The energy demand was higher for the same membrane modules with a brine DS but seawater (45g/L) FS instead of the TSE. The values were 0.04, 0.05 and 0.07 kWh/m^3 for membranes TS80, XN45 and UA60, respectively. On the other hand, using FO membrane with seawater (45g/L) FS and brine DS, 0.065 and 0.1 kWh/m^3 were the energy consumed by TFC and CTA FO membrane in the separation process, respectively (**Figure 6.9, Chapter 6**).

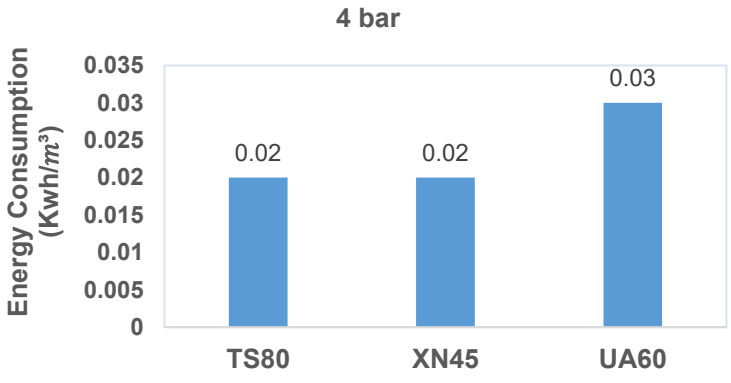

Figure 7.8. TS80, XN45 and UA60 NF membranes energy consumption in the PAFO process at 4 bar.

This study chose NF membranes characterised by high water permeability and low operational energy (Mulyanti and Susanto, 2018) for the PAFO process. The outcome of the experiments confirmed the great potential of the NF membranes, specifically TS80, in treating the brine solution. Commercial NF membranes are inexpensive, exhibit high water flux, and tolerate higher feed pressure compared to FO membranes.

7.4. Conclusions

To further investigate the feasibility of the FO system in the pretreatment of the feed water to the MSF plants, treated wastewater and brine reject solution was the FS and DS, respectively, in the FO system. In this study, three NF membranes, TS80, XN45 and UA60, were evaluated in the FO system instead of the FO membranes. The TS80 membrane achieved the highest water flux of 45 L/m^2h in cycle one at 4 bar. The maximum average flux generated by the TS80 membrane during the four cycles was considerably higher than the TFC FO membrane under the same operational parameters. It was recorded at 39.5 L/m^2h for the TS80 membrane compared to 16.7 L/m^2h for the TFC membrane. The physical cleaning using hot DI water flushing for 30 min effectively reduced the fouling that was concluded to be reversible and not severe. The dilution of the brine draw solution using TS80 reached up to 42%. The proposed PAFO system delivers a promising energy-saving outcome with a maximum of 0.02 and 0.03 kWh/m^3 energy consumed at 4 bar. To sum up, the proposed system provides a high water flux, a steady flux decrease, a considerable decrease in the ions count, and low energy consumption. The potential of the PAFO system in diluting the brine solution by integrating TSE FS with the NF membrane in the FO process is revealed in this study, and additional research is required on a wider spectrum.

Chapter 8: Conclusions and future recommendations

8.1. Conclusions

MSF seawater desalination is reasoned to be the leading desalination technology in offering the daily supply of fresh water in arid areas such as Qatar. After decades of operations, MSF desalination as a practice has witnessed a major drawback of scale deposition on heat exchangers. The scale layer leads to a decrease in the heat transfer and, therefore, in the plant's overall efficiency, which requires extra energy input. The components of the seawater are the main cause of the scale formation, specifically, the divalent ions Ca^{2+}, Mg^{2+} and SO_4^{2-} (Darwish et al., 2016a). In an attempt to unfold this issue, pretreating the feed solution to the MSF plants has been proposed to ameliorate the performance of the MSF desalination. It is believed that the FO technique, as an energy-efficient process, is an attractive process. In this project, FO and PAFO processes were proposed to remove the divalent ions from the brine reject of the MSF plant. The dilute brine was reused as a feed solution in the MSF plants. On the wide spectrum, the findings demonstrated the FO process's potential to dilute the brine solution under different operating parameters.

Chapter 2 reviewed the literature available on the topic of the FO process. It highlights the state of the art of the FO techniques, presenting the FO's advantages and the barriers that face scaling up from laboratory to full-scale applications. The direct usage of the DS after the first filtration step of the FO process is considered the energy-efficient perspective of the FO technique. However, the regeneration step of the DS when the draw solute is not well chosen is a very energy extensive process. The commercialization of the FO process is delayed due to the FO membrane challenges in terms of structure and materials,

as well as fouling mitigations. In addition to the design of the ideal draw solute that can generate the osmotic pressure of the FO system and be easily regenerated. The FO hybrid configurations were studied in specific applications and showed promising results (Awad et al., 2019; Johnson et al., 2018; Ndiaye et al., 2021; Wang and Liu, 2021).

Chapter 3 presented the FO membrane used in the FO experiments, the feed and draw solutions characteristics, analytical methods for membrane and feed solution, the mathematical equations used to deliver the intrinsic parameters and the performance measurement values. The experimental methods were designed in clear, detailed steps in an attempt to eliminate confusion and minimise ambiguity.

Chapter 4 introduced the novel approach of integrating seawater (45 g/L) and brine solution (80 g/L) in a PAFO process using TFC and CTA membranes. Operating the FO process at 40 °C DS (80 g/L) and 25 °C FS temperatures at 2 LPM flow rates showed promising results. Results recorded a 50% amelioration in the water flux by increasing the applied pressure from 1 to 4 bar on the feed side. The commercial TFC FO membrane achieved 16.7 L/m^2h in the PAFO process, with the AL of the membrane facing the DS. The TFC membrane experienced a 15% reduction in the permeation flux following the cleaning with DI water. A maximum of 28% ions dilutions and 0.065 kWh/m^3 energy consumption were recorded using a TFC membrane at 4 bar and seawater feed solution.

In chapter 5, treated wastewater was used as FS, and TFC membrane in both orientations was studied. The fouled membranes were physically cleaned, and various cleaning methods were investigated. Introducing treated wastewater as FS under the same operational parameters in the FO process (0 bar) using a TFC membrane delivered higher water flux. 35 L/m^2h was the highest water flux generated when the stream solution was prefiltered. The water flux of the fouled TFC membrane was highly recovered using an osmotic backwash at 3 LPM flow rate cleaning. Interestingly the maximum power consumption was 0.007 kWh/m^3 with a dilution of brine solution to up to 40% for some ions. The AL-DS operational

orientation of the membrane has recorded the highest water flux; however, it is the operational mode with the more fouling propensity.

In Chapter 6, since the FO membrane cost is considered expensive compared to the commercially available NF membranes, NF membranes were proposed to be used in the FO system. Integrating NF membranes (TS80, XN45, UA60) with seawater (45g/L) FS in the PAFO system delivered promising results. The water flux of the XN45 NF membrane at 4 bar was 1.5 times higher than the CTA FO membrane. Accordingly, the TS80 NF membrane achieved 1.4 times higher flux than the TFC FO membrane. The recovery rate at 4 bar was 10% for membrane TS80 compared to 7.6 % for the TFC FO membrane. The recorded ions dilutions percentage of the TS80 membrane was 28% higher than the TFC FO membrane operated in the same mode. The maximum energy consumed at 4 bar for the NF membranes was in the range of 0.04-0.07 kWh/m^3. Figure 8.1 shows the water flux, recovery rate, specific power consumption, and ions dilution of the FO process using seawater feed solution and brine reject draw solution.

Table 8.1. Comparison of the outcome of the seawater-brine FO process using TFC and CTA FO membranes and TS80, XN45 & UA60 NF membranes at 4 bar applied pressure.

Membrane	**TFC**		**CTA**		**TS80**	**XN45**	**UA60**
Orientation	AL-FS	AL-DS	AL-FS	AL-DS	AL-FS	AL-FS	AL-FS
Maximum water flux (L/m^2h)	14.8	16.7	8	11.1	21.8	15.6	13.1
Maximum Average flux (L/m^2h)	6.26	9.57	6.8	8.4	16.5	13	8.3
Recovery rate (%)	7.6	11.5	6.6	10.1	10	7.8	5
Ions dilution (%)	23	28	21.5	25	28	20	23
Energy (kWh/m^3)	0.053	0.065	0.08	0.1	0.04	0.05	0.07

In Chapter 7, TSE and NF membranes were coupled in the FO system. Interestingly, a maximum water flux of 45 L/m^{2}h was generated at 4 bar. The flux was recovered using hot DI water flushing for 30 minutes, explaining the reversible type of fouling matter. The suggested PAFO process at 4 with wastewater FS and TS80 NF membrane could dilute the brine solution up to 42% for specific species with a maximum energy consumption of 0.02 kWh/m^3. Figure 8.2 presents water flux, ions dilution, and specific power consumption using TSE feed solution and brine reject draw solution in the FO process.

Table 8.2. TSE-brine FO system outcome. TFC FO membrane and TS80, XN45 and UA60 NF membranes. Fouled membranes are cleaned with 3LPM DI water at 40 °C for 30 min; AL-FS is the operational mode. FS and DS prefiltered with a microfilter of 20 µm.

Membrane	TFC	TS80	XN45	UA60
Pressure (bar)	0	4	4	4
Maximum water flux (L/m^{2}h)	35	45	42	35
Maximum Average flux (L/m^{2}h)	31	39.5	37.6	29.5
Flux Reduction (%)	8	2.5	2.76	3.72
Ions dilution (%)	35	42	28	23
Energy (kWh/m^3)	0.005	0.02	0.02	0.03

To sum up, the TSE-NF configuration in the FO system at 4 bar applied pressure demonstrated its potential to dilute the MSF. TS80 NF membrane recorded the highest water flux with a slight steady increase throughout the process. The flux was recovered following the physical cleaning, which explains the reversible quality of the fouling matters. The energy consumed by the FO system when the membrane TS80 was used with the TSE FD was considerably low compared to any other membrane-based separation technology. The benefits of FO and PAFO processes were added to the NF membranes to establish a real system that can fit into the existing MSF units with minimum requirements. The

laboratory-scale experimental activities and results explain and support the viability of the FO technique for brine recycling.

8.2. Recommendations for future work

Despite the advancements in the thermal desalination systems that have recorded an increase in the flow of desalinated water, the intensive energy requirement is still a massive load on the production cost. Generally, thermal desalination techniques consume more energy when compared to pressure-driven membrane technology. The MSF and MED are the leading thermal desalination mainly located in the Middle East, specifically the GCC region. In its turn, the RO process is the worldwide membrane desalination technique. Pretreatment of the feed solution to thermal desalination using membrane-based techniques was proposed to reduce the thermal plants' operational and overall energy. FO, the emerging low-energy process, was proposed and investigated for its potential to treat the feed water to the MSF plant in Qatar by using the MSF brine as DS in the FO process. Diluting the concentrated brine will reduce the divalent ions responsible for the non-alkaline deposition on the heat exchangers. Therefore, the TBT of the MSF plants will increase, leading to better MSF plant performance and a high recovery rate. Besides this, brine recycling can save the marine ecosystem from the consequences of the continuous discharge of hot, concentrated brine into the sea. Preliminary experimental work was conducted regarding this proposal and showed promising results. This project examined the potential of applying the PAFO technique to remove divalent ions in an energy-efficient process. FO and NF membranes performance were studied under similar operational conditions when seawater or treated wastewater was used as FS. However, the conducted experimental processes are insufficient to be implemented in a full-scale system. Further research is required to determine the optimal FO and PAFO configurations and parameters for MSF brine dilution. Following are the recommendations for future work:

- Pilot-scale trials and the practical realization of the proposed FO systems at pilot-scale studies can deliver more detailed results.

- Study the performance of other commercially available FO and NF membranes as well as in-house membranes. Transitioning from laboratory research to full-scale application requires developing the ideal membrane.
- More research work is needed to tackle membrane fouling in an energy-efficient technique.
- Investigate the potential of various feed solutions with low TDS other than seawater and treated wastewater.

Future research developments in the hybrid FO-MSF for brine recycling might deliver a more energy-efficient and environmentally friendly desalination system.

References

Abdel-Fatah, M.A. 2018. Nanofiltration systems and applications in wastewater treatment. Ain Shams Engineering Journal 9(4), 3077-3092.

Abdelkader, B.A., Antar, M.A. and Khan, Z. 2018. Nanofiltration as a pretreatment step in seawater desalination: A review. Arabian Journal for Science and Engineering 43(9), 4413-4432.

Abou El-Nour, F. 2016. Water desalination studies using forward osmosis technology, A Review. Arab Journal of Nuclear Sciences and Applications 49(4), 167-176.

Achilli, A., Cath, T.Y. and Childress, A.E. 2010. Selection of inorganic-based draw solutions for forward osmosis applications. Journal of membrane science 364(1-2), 233-241.

Aende, A., Gardy, J. and Hassanpour, A. 2020. Seawater desalination: A review of forward osmosis technique, its challenges, and future prospects. Processes 8(8), 901.

Ahmed, F.E., Hashaikeh, R. and Hilal, N. 2020. Hybrid technologies: The future of energy efficient desalination–A review. Desalination 495, 114659.

Al-Karaghouli, A. and Kazmerski, L.L. 2013. Energy consumption and water production cost of conventional and renewable-energy-powered desalination processes. Renewable and Sustainable Energy Reviews 24, 343-356.

Al-Mutaz, I.S. and Al-Namlah, A.M. 2004. Characteristics of dual purpose MSF desalination plants. Desalination 166, 287-294.

Al-Rawajfeh, A.E., Glade, H. and Ulrich, J. 2005. Scaling in multiple-effect distillers: the role of CO2 release. Desalination 182(1-3), 209-219.

Al-Rawajfeh, A.E., Ihm, S., Varshney, H. and Mabrouk, A.N. 2014. Scale formation model for high top brine temperature multi-stage flash (MSF) desalination plants. Desalination 350, 53-60.

Al-Sofi, M.A.-K. 1999. Fouling phenomena in multi stage flash (MSF) distillers. Desalination 126(1-3), 61-76.

Al-Zuhairi, A., Merdaw, A.A., Al-Aibi, S., Hamdan, M., Nicoll, P., Monjezi, A.A., Al-ASwad, S., Mahood, H.B., Aryafar, M. and Sharif, A.O. 2015. Forward osmosis desalination from laboratory to market. Water Science and Technology: Water Supply 15(4), 834-844.

Al Bloushi, A., Giwa, A., Mezher, T. and Hasan, S.W. 2018. Environmental Impact and Technoeconomic Analysis of Hybrid MSF/RO Desalination: The Case Study of Al Taweelah A2 Plant. Sustainable Desalination Handbook, 55-97.

Altaee, A., Mabrouk, A. and Bourouni, K. 2013. A novel forward osmosis membrane pretreatment of seawater for thermal desalination processes. Desalination 326, 19-29.

Altaee, A., Mabrouk, A., Bourouni, K. and Palenzuela, P. 2014a. Forward osmosis pretreatment of seawater to thermal desalination: high temperature FO-MSF/MED hybrid system. Desalination 339, 18-25.

Altaee, A., Millar, G.J., Zaragoza, G. and Sharif, A. 2017. Energy efficiency of RO and FO–RO system for high-salinity seawater treatment. Clean technologies and Environmental policy 19(1), 77-91.
Altaee, A., Sharif, A. and Zaragoza, G. 2016. Forward Osmosis Pretreatment of Seawater for Thermal Desalination. Water Filtration Systems: Processes, Uses and Importance.
Altaee, A. and Zaragoza, G. 2014. A conceptual design of low fouling and high recovery FO–MSF desalination plant. Desalination 343, 2-7.
Altaee, A., Zaragoza, G. and Sharif, A. 2014b. Pressure retarded osmosis for power generation and seawater desalination: Performance analysis. Desalination 344, 108-115.
Altaee, A., Zaragoza, G. and van Tonningen, H.R. 2014c. Comparison between forward osmosis-reverse osmosis and reverse osmosis processes for seawater desalination. Desalination 336, 50-57.
Ang, W.L., Mohammad, A.W., Johnson, D. and Hilal, N. 2019. Forward osmosis research trends in desalination and wastewater treatment: A review of research trends over the past decade. Journal of Water Process Engineering 31, 100886.
Anis, S.F., Hashaikeh, R. and Hilal, N. 2019. Reverse osmosis pretreatment technologies and future trends: A comprehensive review. Desalination 452, 159-195.
Ansari, A.J., Hai, F.I., Price, W.E., Drewes, J.E. and Nghiem, L.D. 2017. Forward osmosis as a platform for resource recovery from municipal wastewater-A critical assessment of the literature. Journal of membrane science 529, 195-206.
Arjmandi, M., Peyravi, M., Altaee, A., Arjmandi, A., Chenar, M.P., Jahanshahi, M. and Binaeian, E. 2020. A state-of-the-art protocol to minimize the internal concentration polarization in forward osmosis membranes. Desalination 480, 114355.
Attarde, D., Jain, M., Singh, P.K. and Gupta, S.K. 2017. Energy-efficient seawater desalination and wastewater treatment using osmotically driven membrane processes. Desalination 413, 86-100.
Australia, U. 2002. Introduction to desalination technologies in Australia. Report for Agriculture, Fisheries and Forestry–Australia.
Awad, A.M., Jalab, R., Minier-Matar, J., Adham, S., Nasser, M.S. and Judd, S. 2019. The status of forward osmosis technology implementation. Desalination 461, 10-21.
Back, J.O., Spruck, M., Koch, M., Mayr, L., Penner, S. and Rupprich, M. 2017. Poly (piperazine-amide)/PES composite multi-channel capillary membranes for low-pressure nanofiltration. Polymers 9(12), 654.
Baig, H., Antar, M.A. and Zubair, S.M. 2011. Performance evaluation of a once-through multi-stage flash distillation system: Impact of brine heater fouling. Energy conversion and management 52(2), 1414-1425.
Bennett, A., Awerbuch, L., Pankratz, T., Rothaermel, J. and Sharma, M. 2016. Desalination technology in power generation. Filtration+ Separation 53(6), 30-35.
Blandin, G., Verliefde, A.R., Comas, J., Rodriguez-Roda, I. and Le-Clech, P. 2016a. Efficiently combining water reuse and desalination through forward osmosis—reverse osmosis (FO-RO) hybrids: a critical review. Membranes 6(3), 37.

Blandin, G., Verliefde, A.R., Tang, C.Y., Childress, A.E. and Le-Clech, P. 2013. Validation of assisted forward osmosis (AFO) process: Impact of hydraulic pressure. Journal of membrane science 447, 1-11.
Blandin, G., Vervoort, H., Le-Clech, P. and Verliefde, A.R. 2016b. Fouling and cleaning of high permeability forward osmosis membranes. Journal of Water Process Engineering 9, 161-169.
Borsani, R. and Rebagliati, S. 2005. Fundamentals and costing of MSF desalination plants and comparison with other technologies. Desalination 182(1-3), 29-37.
Budhiraja, P. and Fares, A.A. 2008. Studies of scale formation and optimization of antiscalant dosing in multi-effect thermal desalination units. Desalination 220(1-3), 313-325.
Buros, O. (2000) The ABCs of desalting, International Desalination Association Topsfield, MA.
Cath, T.Y., Childress, A.E. and Elimelech, M. 2006. Forward osmosis: principles, applications, and recent developments. Journal of membrane science 281(1-2), 70-87.
Cath, T.Y., Hancock, N.T., Lundin, C.D., Hoppe-Jones, C. and Drewes, J.E. 2010. A multi-barrier osmotic dilution process for simultaneous desalination and purification of impaired water. Journal of membrane science 362(1-2), 417-426.
Chadwick, R., Good, P., Andrews, T. and Martin, G. 2014. Surface warming patterns drive tropical rainfall pattern responses to CO2 forcing on all timescales. Geophysical Research Letters 41(2), 610-615.
Chekli, L., Phuntsho, S., Kim, J.E., Kim, J., Choi, J.Y., Choi, J.-S., Kim, S., Kim, J.H., Hong, S. and Sohn, J. 2016. A comprehensive review of hybrid forward osmosis systems: Performance, applications and future prospects. Journal of Membrane Science 497, 430-449.
Choi, H.-g., Son, M. and Choi, H. 2017. Integrating seawater desalination and wastewater reclamation forward osmosis process using thin-film composite mixed matrix membrane with functionalized carbon nanotube blended polyethersulfone support layer. Chemosphere 185, 1181-1188.
Chun, Y., Kim, S.-J., Millar, G.J., Mulcahy, D., Kim, I.S. and Zou, L. 2017. Forward osmosis as a pre-treatment for treating coal seam gas associated water: Flux and fouling behaviour. Desalination 403, 144-152.
Chung, T.-S., Zhang, S., Wang, K.Y., Su, J. and Ling, M.M. 2012. Forward osmosis processes: yesterday, today and tomorrow. Desalination 287, 78-81.
Coday, B.D., Heil, D.M., Xu, P. and Cath, T.Y. 2013. Effects of transmembrane hydraulic pressure on performance of forward osmosis membranes. Environ. Sci. Technol. 47(5), 2386-2393.
Cosgrove, W.J. and Loucks, D.P. 2015. Water management: Current and future challenges and research directions. Water Resources Research 51(6), 4823-4839.
Darwish, M., Abdulrahim, H., Hassan, A., Mabrouk, A. and Sharif, A. 2016a. The forward osmosis and desalination. Desalination and Water Treatment 57(10), 4269-4295.
Darwish, M., Hassan, A., Mabrouk, A.N., Abdulrahim, H. and Sharif, A. 2016b. Viability of integrating forward osmosis (FO) as pretreatment for existing

MSF desalting unit. Desalination and Water Treatment 57(31), 14336-14346.
El-Ghonemy, A. 2018. Performance test of a sea water multi-stage flash distillation plant: Case study. Alexandria engineering journal 57(4), 2401-2413.
El Din, A.S., El-Dahshan, M. and Mohammed, R. 2002. Inhibition of the thermal decomposition of HCO3− A novel approach to the problem of alkaline scale formation in seawater desalination plants. Desalination 142(2), 151-159.
Emadzadeh, D., Lau, W., Matsuura, T., Hilal, N. and Ismail, A. 2014. The potential of thin film nanocomposite membrane in reducing organic fouling in forward osmosis process. Desalination 348, 82-88.
Energy, D.U.R. 2011. MENA Regional Water Outlook.
Ettouney, H.M., El-Dessouky, H.T. and Alatiqi, I. 1999. Understand thermal desalination. Chemical engineering progress 95(9), 43-54.
Feria-Díaz, J.J., López-Méndez, M.C., Rodríguez-Miranda, J.P., Sandoval-Herazo, L.C. and Correa-Mahecha, F. 2021. Commercial Thermal Technologies for Desalination of Water from Renewable Energies: A State of the Art Review. Processes 9(2), 262.
Ge, Q., Ling, M. and Chung, T.-S. 2013. Draw solutions for forward osmosis processes: developments, challenges, and prospects for the future. Journal of membrane science 442, 225-237.
Ge, Q., Su, J., Chung, T.-S. and Amy, G. 2011. Hydrophilic superparamagnetic nanoparticles: synthesis, characterization, and performance in forward osmosis processes. Industrial & Engineering Chemistry Research 50(1), 382-388.
Gilron, J. 2014. Water-energy nexus: matching sources and uses. Clean Technologies and Environmental Policy 16(8), 1471-1479.
Hamed, O.A., Al-Shail, K., Ba-Mardouf, K., Al-Otaibi, H., Hassan, A.M., Farooque, A., Al-Sulami, S. and Al-Hamza, A. 2005. Nanofiltration (NF) membrane pretreatment of SWRO feed & MSF make up. Saline Water Desalination Research Institute, Saline Water Conversion Corporation (SWCC), Saudi Arabia, Research Activities and Studies Book, Volume No fifteen-1425-1426 H.
Hassan, A. 2006 Fully integrated NF-thermal seawater desalination process and equipment, Google Patents.
Hassan, A., Al-Sofi, M., Al-Amoudi, A., Jamaluddin, A., Farooque, A., Rowaili, A., Dalvi, A., Kither, N., Mustafa, G. and Al-Tisan, I. 1998. A new approach to membrane and thermal seawater desalination processes using nanofiltration membranes (Part 1). Desalination 118(1-3), 35-51.
Haupt, A. and Lerch, A. 2018. Forward osmosis application in manufacturing industries: A short review. Membranes 8(3), 47.
Hawari, A.H., Al-Qahoumi, A., Ltaief, A., Zaidi, S. and Altaee, A. 2018. Dilution of seawater using dewatered construction water in a hybrid forward osmosis system. Journal of Cleaner Production 195, 365-373.
Hawari, A.H., Kamal, N. and Altaee, A. 2016. Combined influence of temperature and flow rate of feeds on the performance of forward osmosis. Desalination 398, 98-105.

Hilal, N., Al-Zoubi, H., Mohammad, A. and Darwish, N. 2005. Nanofiltration of highly concentrated salt solutions up to seawater salinity. Desalination 184(1-3), 315-326.
Ibrar, I., Altaee, A., Zhou, J.L., Naji, O. and Khanafer, D. 2020a. Challenges and potentials of forward osmosis process in the treatment of wastewater. Critical Reviews in Environmental Science and Technology 50(13), 1339-1383.
Ibrar, I., Naji, O., Sharif, A., Malekizadeh, A., Alhawari, A., Alanezi, A.A. and Altaee, A. 2019. A review of fouling mechanisms, control strategies and real-time fouling monitoring techniques in forward osmosis. Water 11(4), 695.
Ibrar, I., Yadav, S., Altaee, A., Samal, A.K., Zhou, J.L., Nguyen, T.V. and Ganbat, N. 2020b. Treatment of biologically treated landfill leachate with forward osmosis: Investigating membrane performance and cleaning protocols. Science of The Total Environment 744, 140901.
IDA 2014 Desalination Yearbook, Global Data Report DesalData 2013–2014, International Desalination Association.
Intelligence, G.W., Yearbook, I.D., Summit, G.W. and Card, R. 2011. Global Water Intelligence. Global Water Intelligence 12(10), 1-72.
Jamil, S., Jeong, S. and Vigneswaran, S. 2016. Application of pressure assisted forward osmosis for water purification and reuse of reverse osmosis concentrate from a water reclamation plant. Separation and Purification Technology 171, 182-190.
Johnson, D.J., Suwaileh, W.A., Mohammed, A.W. and Hilal, N. 2018. Osmotic's potential: An overview of draw solutes for forward osmosis. Desalination 434, 100-120.
Kaya, C., Sert, G., Kabay, N., Arda, M., Yüksel, M. and Egemen, Ö. 2015. Pre-treatment with nanofiltration (NF) in seawater desalination—Preliminary integrated membrane tests in Urla, Turkey. Desalination 369, 10-17.
Khan, J.A., Shon, H.K. and Nghiem, L.D. 2019. From the laboratory to full-scale applications of forward osmosis: research challenges and opportunities. Current Pollution Reports 5(4), 337-352.
Khanafer, D., Yadav, S., Ganbat, N., Altaee, A., Zhou, J. and Hawari, A.H. 2021. Performance of the Pressure Assisted Forward Osmosis-MSF Hybrid Desalination Plant. Water 13(9), 1245.
Khawaji, A.D., Kutubkhanah, I.K. and Wie, J.-M. 2008. Advances in seawater desalination technologies. Desalination 221(1-3), 47-69.
Kim, B., Gwak, G. and Hong, S. 2017a. Analysis of enhancing water flux and reducing reverse solute flux in pressure assisted forward osmosis process. Desalination 421, 61-71.
Kim, B., Gwak, G. and Hong, S. 2017b. Review on methodology for determining forward osmosis (FO) membrane characteristics: Water permeability (A), solute permeability (B), and structural parameter (S). Desalination 422, 5-16.
Kim, Y., Elimelech, M., Shon, H.K. and Hong, S. 2014. Combined organic and colloidal fouling in forward osmosis: Fouling reversibility and the role of applied pressure. Journal of Membrane Science 460, 206-212.
Korenak, J., Basu, S., Balakrishnan, M., Hélix-Nielsen, C. and Petrinic, I. 2017. Forward osmosis in wastewater treatment processes. Acta chimica slovenica 64(1), 83-94.

Kucera, J. (2014) Desalination: water from water, John Wiley & Sons.
Lattemann, S. and Höpner, T. 2008. Environmental impact and impact assessment of seawater desalination. Desalination 220(1-3), 1-15.
Lee, S. 2020. Performance Comparison of Spiral-Wound and Plate-and-Frame Forward Osmosis Membrane Module. Membranes 10(11), 318.
Li, D., Yan, Y. and Wang, H. 2016. Recent advances in polymer and polymer composite membranes for reverse and forward osmosis processes. Progress in polymer science 61, 104-155.
Li, L., Liu, X.-p. and Li, H.-q. 2017a. A review of forward osmosis membrane fouling: Types, research methods and future prospects. Environmental technology reviews 6(1), 26-46.
Li, L., Shi, W. and Yu, S. 2020. Research on forward osmosis membrane technology still needs improvement in water recovery and wastewater treatment. Water 12(1), 107.
Li, X., Loh, C.H., Wang, R., Widjajanti, W. and Torres, J. 2017b. Fabrication of a robust high-performance FO membrane by optimizing substrate structure and incorporating aquaporin into selective layer. Journal of membrane science 525, 257-268.
Li, Z.-Y., Yangali-Quintanilla, V., Valladares-Linares, R., Li, Q., Zhan, T. and Amy, G. 2012. Flux patterns and membrane fouling propensity during desalination of seawater by forward osmosis. Water research 46(1), 195-204.
Li, Z., Siddiqi, A., Anadon, L.D. and Narayanamurti, V. 2018. Towards sustainability in water-energy nexus: Ocean energy for seawater desalination. Renewable and Sustainable Energy Reviews 82, 3833-3847.
Linares, R.V., Li, Z., Sarp, S., Bucs, S.S., Amy, G. and Vrouwenvelder, J.S. 2014. Forward osmosis niches in seawater desalination and wastewater reuse. Water research 66, 122-139.
Long, Q., Jia, Y., Li, J., Yang, J., Liu, F., Zheng, J. and Yu, B. 2018. Recent Advance on Draw Solutes Development in Forward Osmosis. Processes 6(9), 165.
Luo, H., Wang, Q., Zhang, T.C., Tao, T., Zhou, A., Chen, L. and Bie, X. 2014. A review on the recovery methods of draw solutes in forward osmosis. Journal of Water Process Engineering 4, 212-223.
Lutchmiah, K., Verliefde, A., Roest, K., Rietveld, L.C. and Cornelissen, E. 2014a. Forward osmosis for application in wastewater treatment: A review. Water research 58, 179-197.
Lutchmiah, K., Verliefde, A., Roest, K., Rietveld, L.C. and Cornelissen, E.R. 2014b. Forward osmosis for application in wastewater treatment: a review. Water research 58, 179-197.
Lyster, E., Kim, M.-m., Au, J. and Cohen, Y. 2010. A method for evaluating antiscalant retardation of crystal nucleation and growth on RO membranes. Journal of Membrane Science 364(1-2), 122-131.
Mabrouk, A.N., Fath, H., Darwish, M. and Abdulrahim, H. (2015) Desalination Updates, InTech.
Mabrouk, A.N.A. 2013. Technoeconomic analysis of once through long tube MSF process for high capacity desalination plants. Desalination 317, 84-94.

Madsen, H.T., Nissen, S.S., Muff, J. and Søgaard, E.G. 2017. Pressure retarded osmosis from hypersaline solutions: investigating commercial FO membranes at high pressures. Desalination 420, 183-190.
Mannan, M., Alhaj, M., Mabrouk, A.N. and Al-Ghamdi, S.G. 2019. Examining the life-cycle environmental impacts of desalination: A case study in the State of Qatar. Desalination 452, 238-246.
Mazlan, N.M., Marchetti, P., Maples, H., Gu, B., Karan, S., Bismarck, A. and Livingston, A.G. 2016. Organic fouling behaviour of structurally and chemically different forward osmosis membranes–a study of cellulose triacetate and thin film composite membranes. J. Membr. Sci. 520, 247-261.
McGovern, R.K. 2014. On the potential of forward osmosis to energetically outperform reverse osmosis desalination. J. Membr. Sci. 469, 245-250.
Mekonnen, M.M. and Hoekstra, A.Y. 2016. Four billion people facing severe water scarcity. Science advances 2(2), e1500323.
Micale, G., Cipollina, A. and Rizzuti, L. (2009) Seawater desalination, pp. 1-15, Springer.
Morin, O. 1993. Design and operating comparison of MSF and MED systems. Desalination 93(1-3), 69-109.
Mulyanti, R. and Susanto, H. 2018 Wastewater treatment by nanofiltration membranes, p. 012017, IOP Publishing.
Nassrullah, H., Anis, S.F., Hashaikeh, R. and Hilal, N. 2020. Energy for desalination: A state-of-the-art review. Desalination 491, 114569.
Ndiaye, I., Vaudreuil, S. and Bounahmidi, T. 2021. Forward osmosis process: state-of-the-art of membranes. Separation & Purification Reviews 50(1), 53-73.
Oh, Y., Lee, S., Elimelech, M., Lee, S. and Hong, S. 2014. Effect of hydraulic pressure and membrane orientation on water flux and reverse solute flux in pressure assisted osmosis. Journal of membrane science 465, 159-166.
Okamoto, Y. and Lienhard, J.H. 2019. How RO membrane permeability and other performance factors affect process cost and energy use: A review. Desalination 470, 114064.
Organization, W.H., Supply, W.U.J.W. and Programme, S.M. (2015) Progress on sanitation and drinking water: 2015 update and MDG assessment, World Health Organization.
Panagopoulos, A. and Haralambous, K.-J. 2020. Environmental impacts of desalination and brine treatment-Challenges and mitigation measures. Marine Pollution Bulletin 161, 111773.
Park, K., Kim, J., Yang, D.R. and Hong, S. 2019. Towards a low-energy seawater reverse osmosis desalination plant: A review and theoretical analysis for future directions. Journal of Membrane Science, 117607.
Parveen, F. and Hankins, N. 2019. Comparative performance of nanofiltration and forward osmosis membranes in a lab-scale forward osmosis membrane bioreactor. Journal of Water Process Engineering 28, 1-9.
Pimentel, D., Berger, B., David, F., Newton, M., Wolfe, B., Karabinakis, E., Clark, S., Poon, E., Abbett, E. and Nandagopal, S. 2004 Water resources, agriculture and the environment.

Ping Chu, H. and Li, X.y. 2005. Membrane fouling in a membrane bioreactor (MBR): sludge cake formation and fouling characteristics. Biotechnology and bioengineering 90(3), 323-331.
Qasim, M., Badrelzaman, M., Darwish, N.N., Darwish, N.A. and Hilal, N. 2019. Reverse osmosis desalination: A state-of-the-art review. Desalination 459, 59-104.
Qasim, M., Darwish, N.A., Sarp, S. and Hilal, N. 2015. Water desalination by forward (direct) osmosis phenomenon: A comprehensive review. Desalination 374, 47-69.
Qiu, C., Setiawan, L., Wang, R., Tang, C.Y. and Fane, A.G. 2012. High performance flat sheet forward osmosis membrane with an NF-like selective layer on a woven fabric embedded substrate. Desalination 287, 266-270.
Qureshi, A.S. 2020. Challenges and prospects of using treated wastewater to manage water scarcity crises in the Gulf Cooperation Council (GCC) countries. Water 12(7), 1971.
Rao, P., Morrow, W.R., Aghajanzadeh, A., Sheaffer, P., Dollinger, C., Brueske, S. and Cresko, J. 2018. Energy considerations associated with increased adoption of seawater desalination in the United States. Desalination 445, 213-224.
Salgot, M. and Folch, M. 2018. Wastewater treatment and water reuse. Current Opinion in Environmental Science & Health 2, 64-74.
Sanaye, S. and Asgari, S. 2013. Four E analysis and multi-objective optimization of combined cycle power plants integrated with Multi-stage Flash (MSF) desalination unit. Desalination 320, 105-117.
Shahzad, M.W., Burhan, M., Ang, L. and Ng, K.C. 2017. Energy-water-environment nexus underpinning future desalination sustainability. Desalination 413, 52-64.
Shatat, M. and Riffat, S.B. 2012. Water desalination technologies utilizing conventional and renewable energy sources. International Journal of Low-Carbon Technologies 9(1), 1-19.
Shomar, B. and Dare, A. 2015. Ten key research issues for integrated and sustainable wastewater reuse in the Middle East. Environmental Science and Pollution Research 22(8), 5699-5710.
Shukla, N., Harbola, M., Sanjay, K. and Shekhar, R. 2017. Electrochemical Fencing of Cr (VI) from Industrial Wastes to Mitigate Ground Water Contamination. Transactions of the Indian Institute of Metals 70(2), 511-518.
Singh, V.P. 2017. Challenges in meeting water security and resilience. Water International 42(4), 349-359.
Suwaileh, W., Pathak, N., Shon, H. and Hilal, N. 2020. Forward osmosis membranes and processes: A comprehensive review of research trends and future outlook. Desalination 485, 114455.
Suwaileh, W.A., Johnson, D.J., Sarp, S. and Hilal, N. 2018. Advances in forward osmosis membranes: Altering the sub-layer structure via recent fabrication and chemical modification approaches. Desalination 436, 176-201.
Tan, C.H. and Ng, H.Y. 2008. Modified models to predict flux behavior in forward osmosis in consideration of external and internal concentration polarizations. Journal of Membrane science 324(1-2), 209-219.

Tang, C.Y., She, Q., Lay, W.C., Wang, R. and Fane, A.G. 2010. Coupled effects of internal concentration polarization and fouling on flux behavior of forward osmosis membranes during humic acid filtration. J. Membr. Sci. 354(1-2), 123-133.
Thabit, M.S., Hawari, A.H., Ammar, M.H., Zaidi, S., Zaragoza, G. and Altaee, A. 2019. Evaluation of forward osmosis as a pretreatment process for multi stage flash seawater desalination. Desalination 461, 22-29.
Tiraferri, A., Yip, N.Y., Phillip, W.A., Schiffman, J.D. and Elimelech, M. 2011. Relating performance of thin-film composite forward osmosis membranes to support layer formation and structure. Journal of membrane science 367(1-2), 340-352.
Van der Bruggen, B. and Luis, P. 2015. Forward osmosis: understanding the hype. Reviews in Chemical Engineering 31(1), 1-12.
Vu, M.T., Ansari, A.J., Hai, F.I. and Nghiem, L.D. 2018. Performance of a seawater-driven forward osmosis process for pre-concentrating digested sludge centrate: Organic enrichment and membrane fouling. Environmental Science: Water Research & Technology 4(7), 1047-1056.
Wafi, M.K., Hussain, N., Abdalla, O.E.-S., Al-Far, M.D., Al-Hajaj, N.A. and Alzonnikah, K.F. 2019. Nanofiltration as a cost-saving desalination process. SN Applied Sciences 1(7), 1-9.
Wang, J. and Liu, X. 2021. Forward osmosis technology for water treatment: Recent advances and future perspectives. Journal of Cleaner Production 280, 124354.
Wang, Y.-N., Goh, K., Li, X., Setiawan, L. and Wang, R. 2018. Membranes and processes for forward osmosis-based desalination: Recent advances and future prospects. Desalination 434, 81-99.
Wang, Z., Tang, J., Zhu, C., Dong, Y., Wang, Q. and Wu, Z. 2015. Chemical cleaning protocols for thin film composite (TFC) polyamide forward osmosis membranes used for municipal wastewater treatment. Journal of Membrane Science 475, 184-192.
Warsinger, D.M., Swaminathan, J., Guillen-Burrieza, E. and Arafat, H.A. 2015. Scaling and fouling in membrane distillation for desalination applications: a review. Desalination 356, 294-313.
Xu, Y., Peng, X., Tang, C.Y., Fu, Q.S. and Nie, S. 2010. Effect of draw solution concentration and operating conditions on forward osmosis and pressure retarded osmosis performance in a spiral wound module. J. Membr. Sci. 348(1-2), 298-309.
Yadav, S., Ibrar, I., Altaee, A., Déon, S. and Zhou, J. 2020a. Preparation of novel high permeability and antifouling polysulfone-vanillin membrane. Desalination 496, 114759.
Yadav, S., Ibrar, I., Bakly, S., Khanafer, D., Altaee, A., Padmanaban, V., Samal, A.K. and Hawari, A.H. 2020b. Organic fouling in forward osmosis: A comprehensive review. Water 12(5), 1505.
Yadav, S., Saleem, H., Ibrar, I., Naji, O., Hawari, A.A., Alanezi, A.A., Zaidi, S.J., Altaee, A. and Zhou, J. 2020c. Recent developments in forward osmosis membranes using carbon-based nanomaterials. Desalination 482, 114375.
Yangali-Quintanilla, V., Li, Z., Valladares, R., Li, Q. and Amy, G. 2011. Indirect desalination of Red Sea water with forward osmosis and low pressure reverse osmosis for water reuse. Desalination 280(1-3), 160-166.

Yu, Y., Lee, S. and Maeng, S.K. 2017. Forward osmosis membrane fouling and cleaning for wastewater reuse. Journal of Water Reuse and Desalination 7(2), 111-120.
Zazouli, M.A., Nasseri, S. and Ulbricht, M. 2010. Fouling effects of humic and alginic acids in nanofiltration and influence of solution composition. Desalination 250(2), 688-692.
Zhang, S., Wang, P., Fu, X. and Chung, T.-S. 2014a. Sustainable water recovery from oily wastewater via forward osmosis-membrane distillation (FO-MD). water research 52, 112-121.
Zhang, X., Ning, Z., Wang, D.K. and da Costa, J.C.D. 2014b. Processing municipal wastewaters by forward osmosis using CTA membrane. Journal of Membrane Science 468, 269-275.
Zhao, J., Wang, M., Lababidi, H.M., Al-Adwani, H. and Gleason, K.K. 2018. A review of heterogeneous nucleation of calcium carbonate and control strategies for scale formation in multi-stage flash (MSF) desalination plants. Desalination 442, 75-88.
Zhao, P., Gao, B., Yue, Q., Liu, P. and Shon, H.K. 2016. Fatty acid fouling of forward osmosis membrane: Effects of pH, calcium, membrane orientation, initial permeate flux and foulant composition. Journal of Environmental Sciences 46, 55-62.
Zhao, S., Zou, L., Tang, C.Y. and Mulcahy, D. 2012. Recent developments in forward osmosis: opportunities and challenges. Journal of membrane science 396, 1-21.
Zhou, D., Zhu, L., Fu, Y., Zhu, M. and Xue, L. 2015. Development of lower cost seawater desalination processes using nanofiltration technologies—A review. Desalination 376, 109-116.
Zou, S., Qin, M. and He, Z. 2019. Tackle reverse solute flux in forward osmosis towards sustainable water recovery: reduction and perspectives. Water research 149, 362-374.